7-2011

Delayed Composite Action Coupled with Post-tensioning for Cast in Place Bridge Deck Systems

Nathanael J. Toenies
University of Nebraska-Lincoln, ntoenies@unomaha.edu

Delayed Composite Action Coupled with Post-tensioning for Cast in Place Bridge Deck Systems

By

Nathan J Toenies

A Thesis

Presented to the Faculty of

The Graduate College at the University of Nebraska

In Partial Fulfillment of Requirements

For the Degree of Master of Science

Major: Civil Engineering

Under the Supervision of Professor Maher Tadros

Lincoln, NE

July 2011

Delayed Composite Action Coupled with Post-tensioning for
Cast in Place Bridge Deck Systems

Nathan J Toenies, M.S.

University of Nebraska, 2011

Advisors: Maher K Tadros

Cast-in-place bridge decks are known to have transverse cracking early in the life of the bridge due to shrinkage and temperature effects. The cracks result from immediate composite behavior between the girder and the deck. For steel bridges, this bond is caused by shear studs welded to the steel beams and embedded in the cast-in-place deck. Prevention or closure of these cracks could greatly increase the durability of the bridge.

The following research focuses on introducing a system that will have delayed composite action, allowing strain in the concrete before it becomes composite with the girder. The system is meant to reduce or eliminate transverse cracks before behaving as a fully composite section. Additionally, post-tensioning is used to put compressive strain on the concrete deck before bonding to the shear studs in order to prevent cracking once composite behavior is achieved.

The results of this research prove to be promising. In addition to small scale development and testing of the delayed composite action (DCA) with post-tensioning (PT) system, a full scale system was constructed and tested. The DCA beam showed no cracks due to shrinkage or temperature effects, in addition to more movement relative to the girder before bond to the shear studs. The moment capacity of the DCA with PT

system equaled the specimen with identical parameters minus the DCA and PT. This shows that full composite behavior was achieved in addition to reduced cracking due to immediate composite behavior.

Acknowledgements

I would like to thank my professors and advisors Dr. Kromel Hanna and Dr Maher Tadros. They provided valuable insight on this project and with all of my other work in obtaining my masters degree. It was a privilege to work under these professors.

I would also like to express appreciation to some of my fellow graduate students who offered their time to assist me in my work: Eliya Henin, Jenna Hansen, Ibrahim Lofty, Afshin Hatami, and Jimmy Deng. Their assistance was very valuable in the completion of my research. Thanks also to Kelvin Lein and Jeff Svatora who provided assistance in the lab.

I would like to acknowledge the Strategic Highway Research Project (SHRP) for sponsoring the research. Thanks also to Coreslab and BASF Corporation for their donation of materials to the project. I would also like to thank Drake Williams for supplying numerous small orders throughout the project.

Table of contents

List of Figures

List of Tables

Chapter 1. Introduction

1.1. Problem Statement

The majority of bridge decks for beam-slab type bridges are constructed using field cast concrete. While accelerated construction and rapid renewal is one of the foci of the Strategic Highway Research Program (SHRP), addressing the durability of this commonly used bridge deck construction method is extremely important.

Cast-in-place bridge deck systems are known to exhibit transverse cracking before bridges are opened to traffic. This cracking is partly contributed to restraining forces that are provided by shear studs which prevent fresh concrete from being able to shrink. Closure of these cracks through the introduction of compression from post-tensioning should greatly enhance the durability of these bridge decks. This compression can be maximized by utilizing the Delayed Composite Action (DCA) System.

One of the principal causes of CIP bridge deck deterioration is rapid chloride intrusion through transverse cracks, which in turn initiates corrosion of the reinforcement at an early age. Control of these cracks should reduce this potential for reinforcement corrosion. It would also reduce the potential for concrete deterioration in freeze-thaw cycling. Concrete is subjected to early shrinkage and to shortening caused by a drop in temperature in the hydration cycle. These two effects combine to create demand for deck concrete shortening. When concrete sets, it becomes anchored to the supporting girders through immediate composite action with studs (steel girders) or shear bars (concrete

girders). This interaction restrains free shortening of the deck and creates tensile stresses beyond the tensile capacity of the young, weak concrete. As a result, cracking occurs within the first few days of deck life. Furthermore, the problem is compounded by construction done in cold weather where the underside of the deck is not heated, while the top is covered with insulated blankets to avoid freezing of the deck within the first 24 hours of its life.

1.2. Research Objectives

The main objective of this research is to determine the viability of the Delayed Composite Action (DCA) system for cast-in-place systems. Allowing the deck to slide relative to the girders with very little frictional effects would allow for shrinkage and temperature shortening to take place freely in the deck before it is "locked in" with the girders. Adding post-tensioning (PT) in this state allows for the frictional forces to be offset and for the concrete to have a residual compression for future shortening due to volume change effects. It is important to have a system that will allow for low friction before composite action takes effect. Thus, this project focuses on methods to achieve delayed composite action as effectively as possible.

The fundamental concept of this research is to provide open channels over the girders where shear connectors are located. These channels isolate the shear connectors while fresh concrete is placed and allowed to hydrate, undergoing volume changes due to a temperature drop in the hydration cycle as well as shrinkage. The next step in the process is to post-tension the deck. The amount of post-tensioning needed to eliminate crack inducing tension in the deck is considerably reduced due to two effects: (a) the

deck is free to slide relative to the girders through means of low friction bearing and (b) the deck is post-tensioned before development of the composite action, thus the entire PT force is taken up by the deck and not the deck-girder system. Also, the much stiffer girders do not share in a prestressing force which is unnecessary and possibly harmful to their behavior. The final step is to develop the composite action through grouting of the channels.

The proposed research builds on previous pilot studies by Dr Azizinamini (2006). This research will be discussed in detail in the literature review in Chapter 2.

1.3. Report Organization

The report is divided into six chapters. Chapter 1 is the introduction, listing the problem statement, research objectives and report organization. Chapter 2 presents the literature review providing background information for the research. Chapter 3 discusses the system development, including introduction of the basic system, research of materials for low friction bearing, and development of a small scale model and small scale test specimens. Chapter 4 is the experimental program which includes push-off testing of small scale specimens before development and testing of two full scale specimens. These tests are described in detail. Chapter 5 presents a bridge design which uses the delayed composite action with post-tensioning bridge system. Chapter 6 is a summary of the conclusions drawn from the research.

Chapter 2.

Literature Review

Use of a bridge system with delayed composite action and post tensioning is a recent idea. Very little research has been conducted on this type of a system. This did not allow for extensive literature review. Dr. Maher Tadros did some research on rapid construction of bridge decks in 1998. This is not directly related to DCA, but does have some relation to reduction or elimination of deck cracks, the main objective of the research. The Skyline Bridge near Omaha NE was constructed in 2003 and uses precast panels which reduce cracking due to creep, shrinkage, and temperature effects through a reduction in the amount of cast in place concrete.

Some testing was done on potential systems for DCA at the University of Nebraska Lincoln under Dr. Atorod Azizinamini, sponsored by the Nebraska Department of Roads. This research studied and tested several systems which delayed composite action between a concrete deck and a steel beam. Much of the research studied use of an epoxy in place of shear connectors. Other systems were studied and tested with small beam specimens. These systems and the results of the testing will be discussed in more detail. Lastly, the Japanese developed a system for DCA called the post rigid system, which will also be discussed.

2.1. Rapid Replacement of Bridge Decks (Tadros)

Dr. Maher Tadros oversaw research sponsored by the National Cooperative Highways Research Project (NCHRP) for rapid replacement of bridge decks. The primary objective of the research was to develop systems that would decrease the replacement times of bridge decks. Several systems were developed and tested at the University of Nebraska Lincoln. The system that relates most to the objectives of the DCA with PT system is the continuous stay in place subpanel bridge deck system shown in Figure 1.

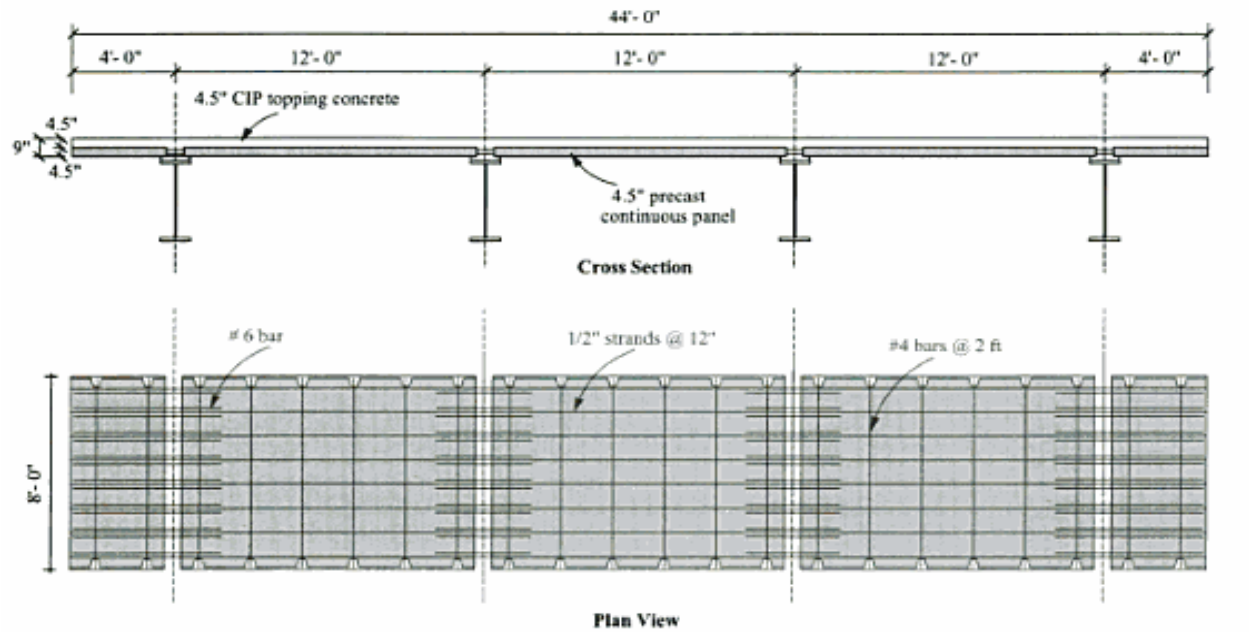

Figure 1: Continuous SIP Subpanel Bridge Deck System (Tadros, 1998)

The system replaces much of the typical cast in place deck with precast panels that are supported on the edge of the top flange with a gap where the shear studs are located. A shallower deck is then placed over the shear studs and above the precast panels. Because of the reduction in volume of cast in place concrete, the amount of cracks due to

shrinkage and temperature effects is diminished. This, though not done through delayed composite action, is the main objective of the research for the DCA coupled with PT bridge deck system.

2.2. Skyline Bridge Construction

A bridge was constructed near Omaha Nebraska that implemented a high performance precast concrete bridge deck system. One of the advantages of the system is that most temperature, creep, and shrinkage effects are eliminated from the deck due to precast deck panels, which are placed on the girders. This is the type of system described in 2.1. Figure 2 shows the cross section of the Skyline Bridge.

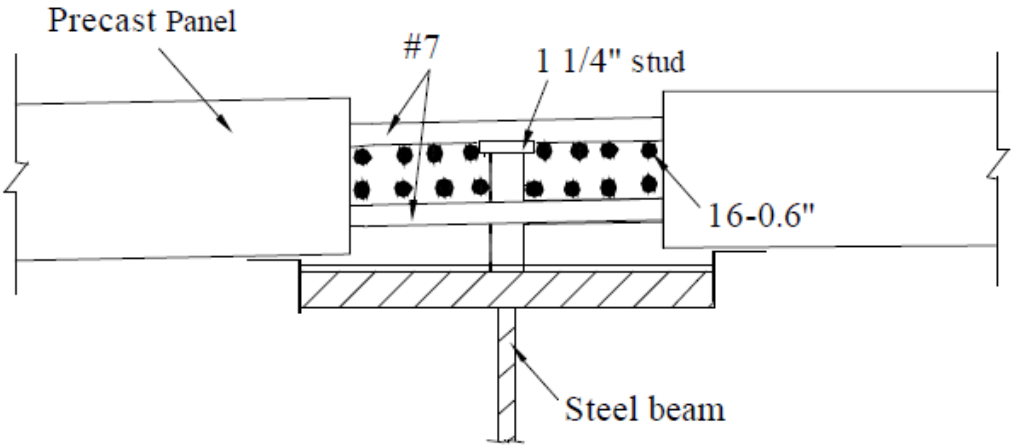

Figure 2: Skyline Bridge Cross Section (Sun, 2004)

The precast panels supply most of the thickness of the deck with a shallow concrete overlay on top with grout to fill above the shear studs. Figure 3 shows the bridge after placement of the precast panels.

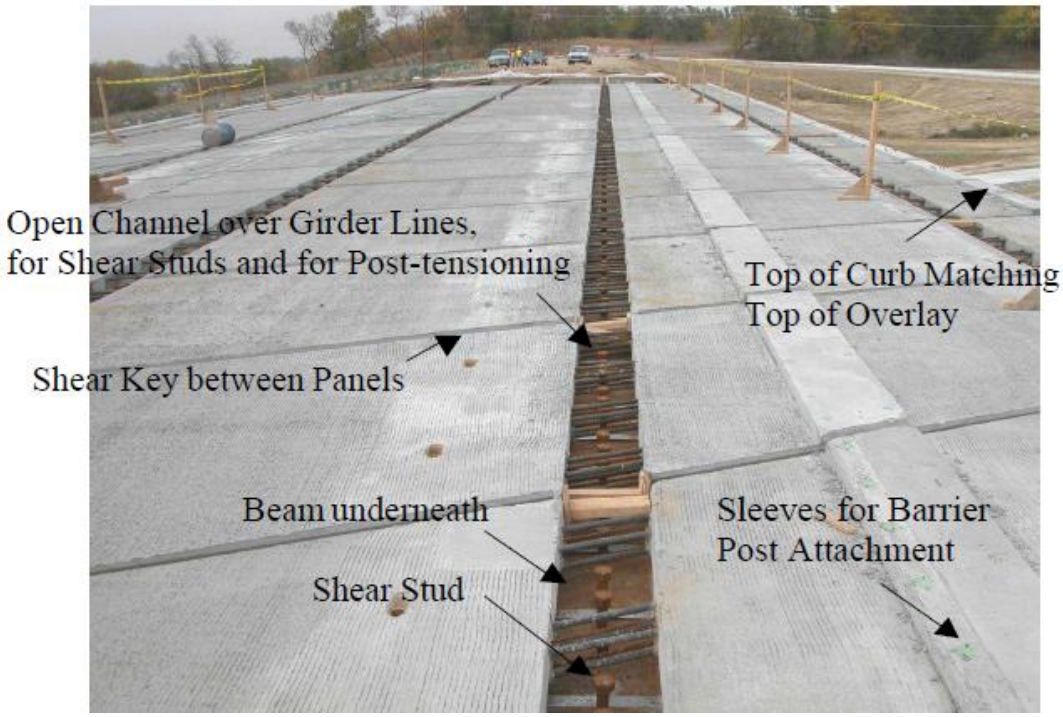

Figure 3: Skyline Bridge after Placement of Precast Panels **(**Sun, 2004)

Though this bridge is not specifically related to DCA, it does achieve one of the main goals of reducing cracks in the deck due to creep, shrinkage, and temperature effects. This is achieved by the significant reduction in cast in place concrete.

2.3. DCA Systems Researched at the University of Nebraska Lincoln (Azizinamini)

All of the following methods discussed were researched by the University of Nebraska Lincoln under Dr Azizinamini. The research attempted to meet two primary objectives:

- Develop a system for delayed composite action.

- Develop a system that eliminated shear studs which were considered a tripping hazard to construction workers.

Systems that met one or both of these objectives were researched and tested. Only the systems that had delayed composite action are discussed in this literature review. The objective of eliminating shear connecters is not one of the objectives for the delayed composite action coupled with post tensioning research.

2.3.1. Epoxy Injection

This method attempts to delay composite action by using an epoxy rather than shear studs. The concrete deck is poured on the steel girders and later epoxy is pumped in between the deck and the top flange to provide a bond for composite action. The epoxy is pumped through a vertical conduit extending from the top flange through the top of the deck.

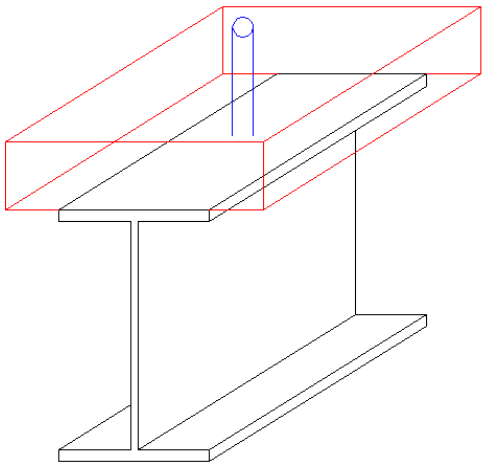

Figure 4: Epoxy Injection for DCA

After initial curing and shrinkage have been allowed, a pressurized pump places epoxy between the deck and the steel beam to develop composite action. The pressure

breaks any initial bond of concrete and steel allowing for a layer of epoxy to flow over the entire surface. Several tubes are needed over the length of a beam to provide necessary flow of epoxy over the entire surface.

The epoxy injection system has several weaknesses. Specimens tested demonstrated a very low strength in shear. Required capacities were not reached. In order for full composite behavior, some sort of mechanism, such as a fastened shear stud was necessary. In addition to this significant problem, failure occurred very suddenly in a non-ductile failure. This is not desirable in structural applications.

2.3.2. Mechanical Alternatives

Mechanical alternatives were considered for the purpose of delayed composite action. The concept of this method is having some device embedded in the deck, but not fastened to the girder right away. After initial shrinkage, the device is then somehow fastened to the girder. Figure 5 shows one possible mechanical system for delayed composite action.

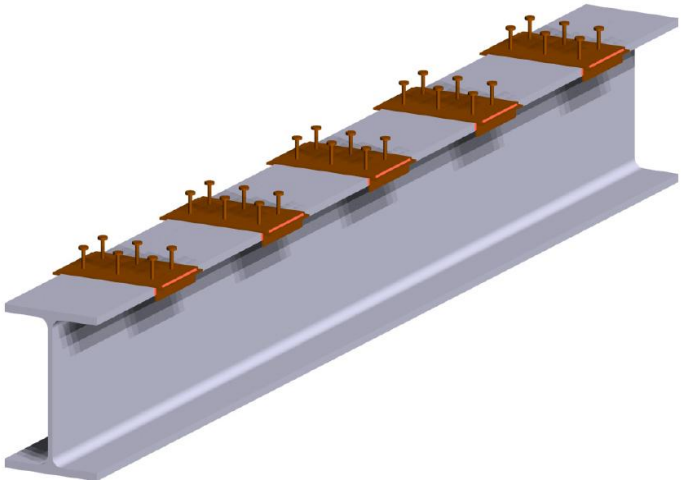

Figure 5: Mechanical Alternative for DCA (Azizinamini, 2003)

The devices which consist of thin plates with welded shear studs are free to move relative to the girder after embedment in the deck. These devices are then welded to the girder after initial curing providing composite action.

This option does successfully delay composite action and can be designed to transfer any force. The system does have several drawbacks. The mechanical devices would be expensive to design and use of them would require labor intensive processes. An additional problem is the exposed weld of the device to the girder. Use of typical shear studs allows for a weld surrounded by concrete, sealed from the elements. This weld would be subject to deterioration, which would require ongoing inspection over the life of the bridge.

2.3.3. Precast Option

Another option studied at the University of Nebraska Lincoln was a precast option. A precast deck would be set on top of the girder and fastened with a previously applied high strength epoxy. The epoxy, which would be applied directly to the top flange surface, would be a much more viscous epoxy with higher strength than the injected epoxy method discussed earlier.

Although this method did provide higher strength than injected epoxy methods, full composite action was not achieved. An additional mechanism was required for vertical shear. Additionally, failure was non-ductile as in other applications using epoxy in place of shear studs.

2.3.4. Stud Strip Method

The stud strip method is similar to the mechanical alternative method. Rather than studs which are embedded in concrete and then later welded, studs are placed with a base below a strip which is later fastened to the top flange by injected epoxy. Figure 6 shows the stud strip method for delayed composite action.

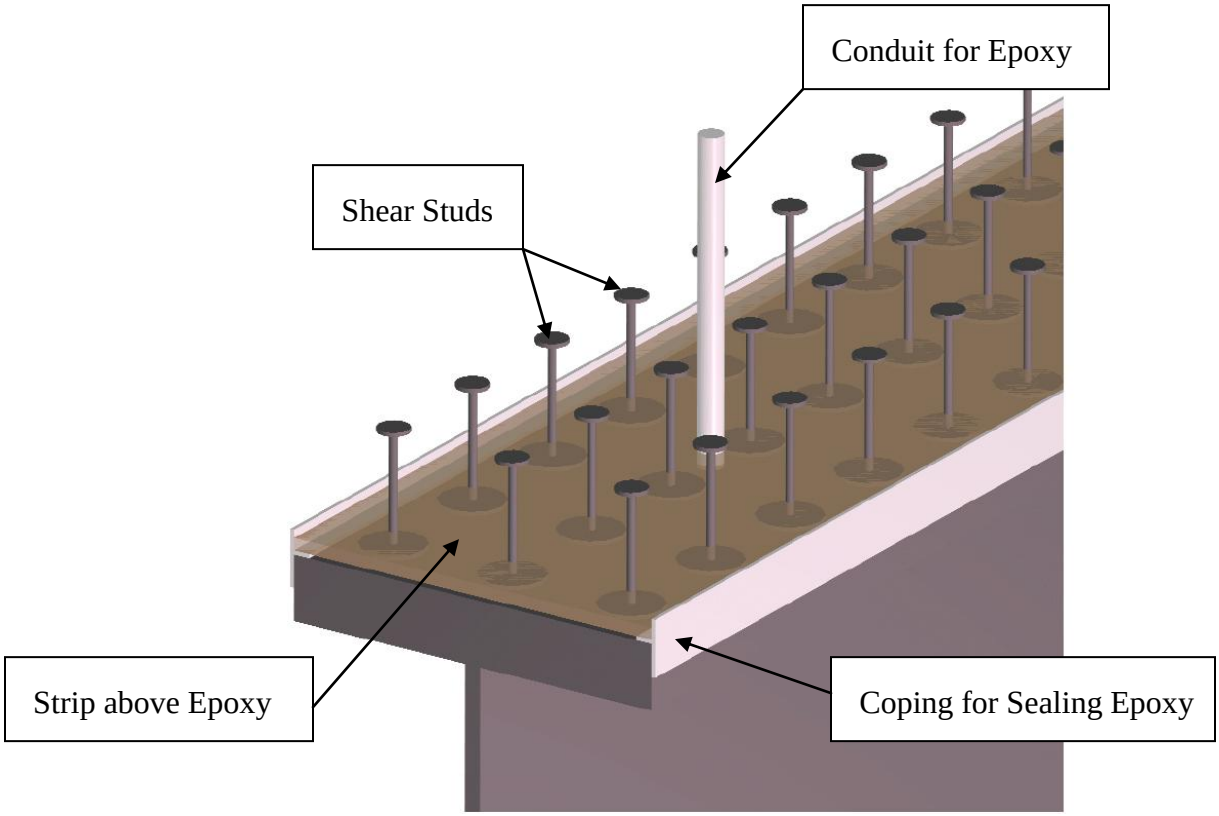

Figure 6: Stud Strip Method (Azizinamini, 2003)

After the deck has been poured and initial curing has been allowed as a non-composite system, the epoxy is pumped through the conduit to provide composite action. Coping along the edge of the top flange provides a seal for the epoxy as it is pumped below the strip.

The system does still require the use of epoxy, which consistently produced less than desirable behavior. Though this method does have potential advantages, no actual testing

of specimens was conducted on the stud strip method at the University of Nebraska Lincoln.

2.3.5. Mixed Aggregate Method

Another idea developed for delayed composite action was the mixed aggregate method. This method involves placing sand on top of the girder before pouring of the deck to create air voids for pumping of epoxy after initial curing has taken place. This provides more surface area for the epoxy compared to the epoxy injection method. Similar to the stud strip method, coping is used to seal the epoxy flow when it is pumped through conduit in between the deck and the top flange of the girder. The mixed aggregate method is demonstrated in Figure 7.

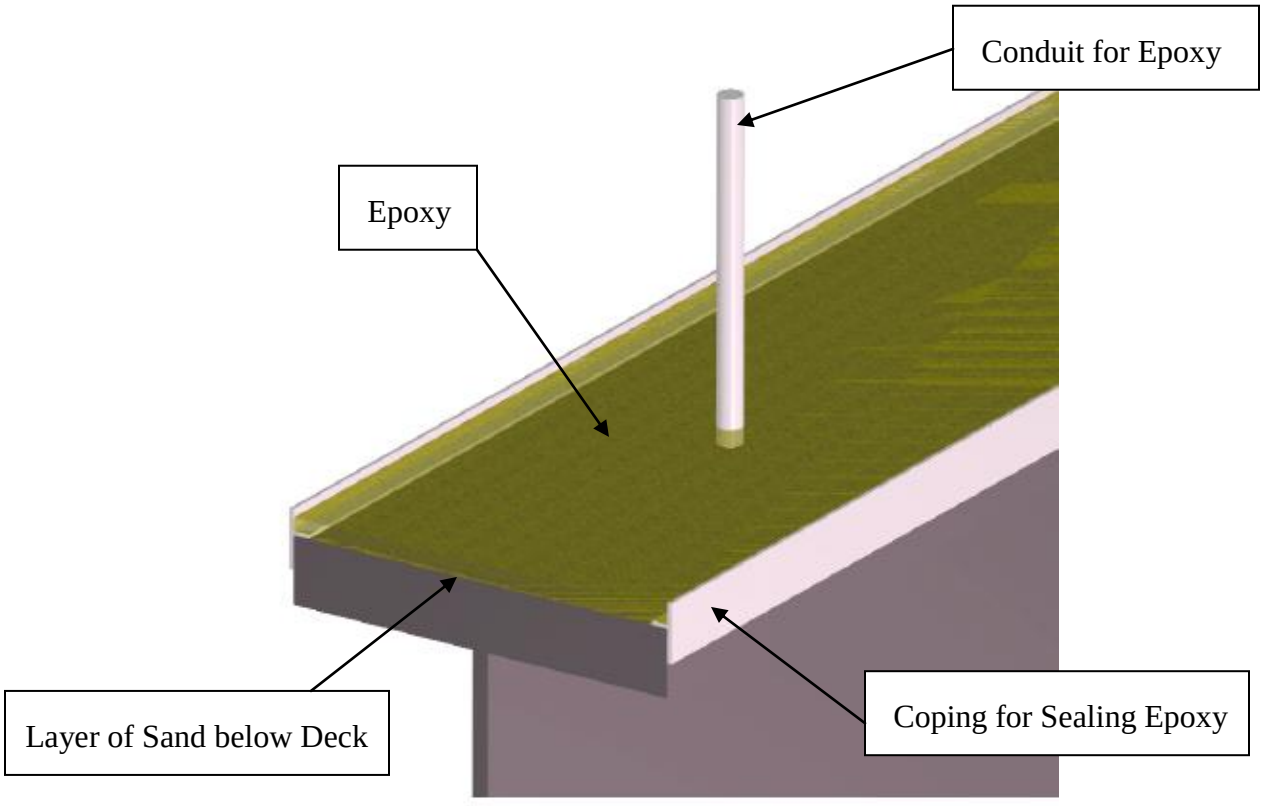

Figure 7: Mixed Aggregate Method (Azizinamini, 2003)

Use of larger aggregate instead of sand allows for even more surface area for the epoxy. The larger aggregates would be glued to the top flange as shown in Figure 8.

Figure 8: Larger Aggregate (Azizinamini, 2003)

This method had similar weaknesses to the other methods that used epoxy in place of shear studs. The tested strengths were not adequate and failure would occur in a non-ductile manner.

2.3.6. Epoxy Embedded Studs

According to the research under Dr Azizinamini, the epoxy embedded studs method provided the most desirable option for delayed composite action. This method uses typical shear studs which are welded to the top flange. A plastic enclosure is then placed over the studs to isolate them from bonding with the deck. Figure 9 shows the basic concept of the epoxy embedded studs method.

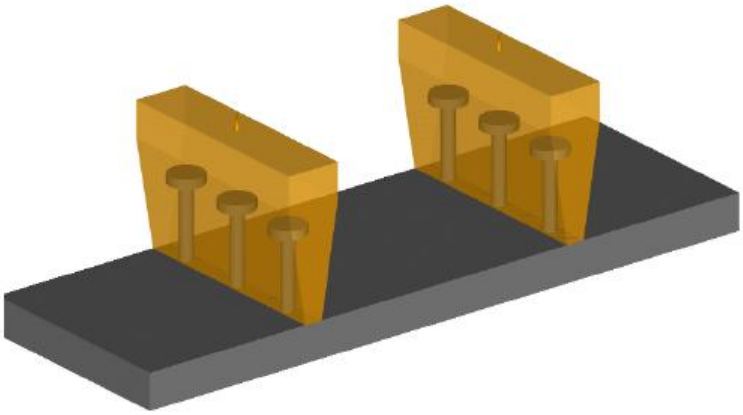

Figure 9: Epoxy Embedded Studs Method (Azizinamini, 2003)

After pouring of the concrete deck, the initial curing occurs without be constrained by the shear studs. The enclosures can then be pierced and have compressed air used to remove it leaving a hole around the shear studs all the way to the top of the girder as shown in Figure 10.

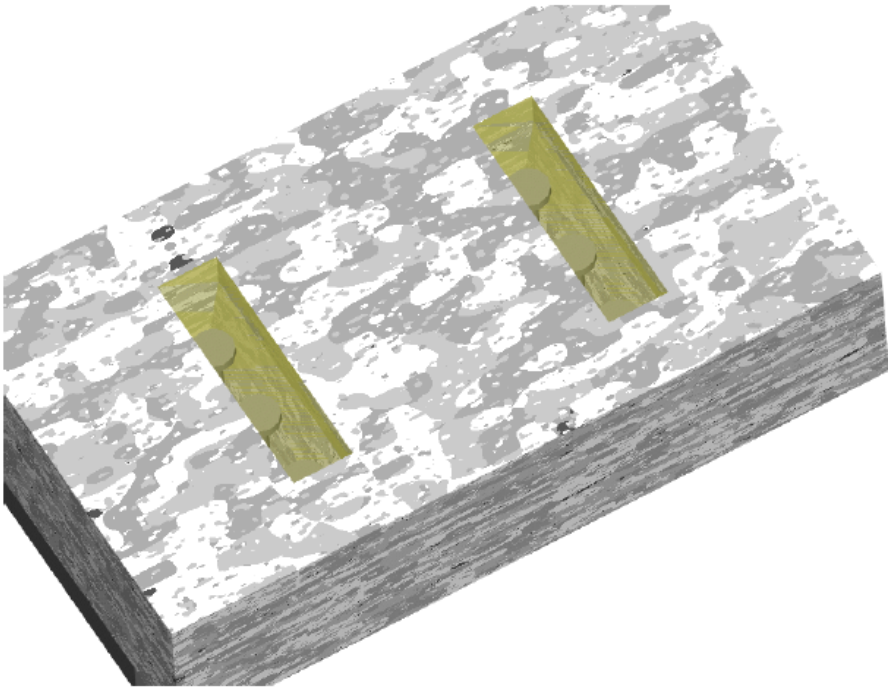

Figure 10: Deck after Removal of Boot (Azizinamini, 2003)

The hole is then filled with epoxy or grout to provide for composite behavior between the deck and the girder. Creating a wedge shaped hole further added to the performance of the system. Another possibility with the epoxy embedded studs method is simply filling the boot with epoxy or grout rather than removing it. This would potentially be easier in the field.

This method does achieve delayed composite action as well as providing adequate strength, making it the most attractive option of those researched by Dr Azizinamini at the University of Nebraska Lincoln. It does have the weakness of exposed block outs. This is a problem for a variety of reason including appearance and potential cracks right at the location of the filled hole. Additionally, the epoxy could be a concern with creep and the high cost of epoxy. A second weakness of the epoxy embedded studs method is bond between the deck and girder between the shear studs. This bond and friction could cause cracks due to shrinkage and temperatures effects within the first few days of curing.

2.4. Japanese Post Rigid System

A system for delayed composite action was developed in Japan called the post rigid system. This system (shown if Figure 11) involves using slow curing mortar resins around the shear studs and on the surface of the top flange for the purpose of delaying composite action.

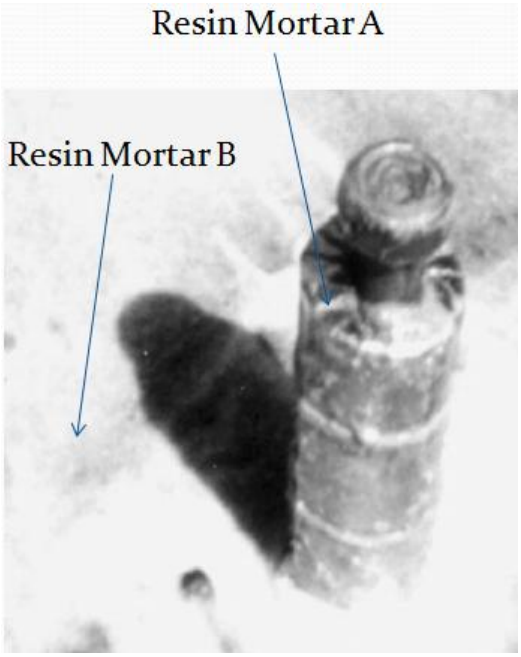

Figure 11: Post Rigid System (Tachibana, 2000)

Mortar A is applied around the shear studs and mortar B is applied to the surface of the top flange. Mortar A is a very slow curing resin which can be designed to cure over a period of months if desired. Mortar B is a faster curing resin which delays composite action between the top flange and the placed concrete deck. The system is post tensioned soon after deck placement. Because the deck and the girder are not a composite section due to the slow curing mortars, all of the prestressing force is applied to the deck rather than much of the force applying the much stiffer steel girder.

The post rigid system does successfully delay composite action. The system was implemented in the Shiratori pedestrian bridge in Japan. One of the main drawbacks of the system is its high cost.

2.5. Conclusions

Methods that use epoxy in place of shear studs proved to be ineffective. The systems that achieved delayed composite action and had adequate strength used shear connectors. The best options were systems that isolated the shear studs during initial curing and provided composite action using the shear connectors later on to achieve composite behavior between the bridge and the deck.

The system described in the next chapter seeks to build upon the idea of isolation of the shear studs for delayed composite action. The systems adds post tensioning as well as a low friction bearing material to further reduce cracks caused by creep and shrinkage early in the curing process.

Chapter 3.

System Development

3.1. Introduction

This chapter discusses the development of a system for delayed composite action. The purpose of the system is to allow the concrete deck to move relative to the girder in order to prevent cracks due to shrinkage and temperature effects shortly after the deck is poured. This is done by isolating the top flange of the steel girder with an enclosed apparatus that rests on a low friction bearing, allowing for movement relative to the steel girder. The channel is eventually filled with SCC grout after initial curing has occurred. Figure 12 shows a cross section of the general system.

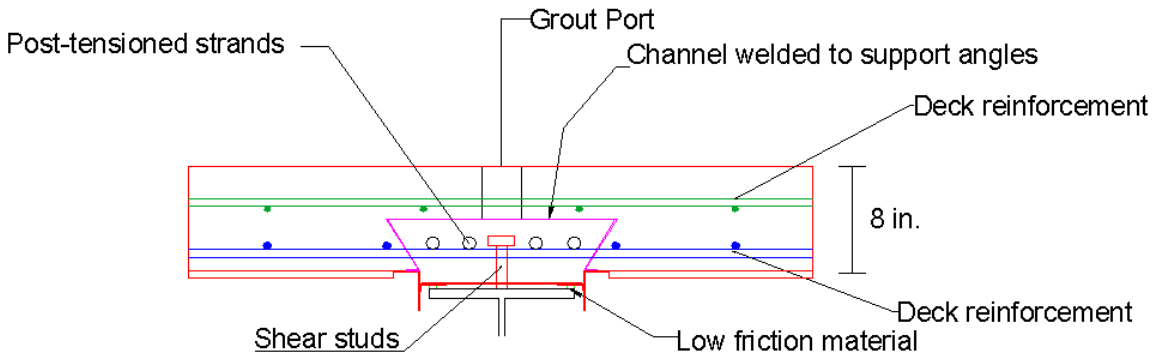

Figure 12: Cross Section of General System

3.2. *Initial Strain and Movement Calculations*

Before development of the system, calculations of the strain and movement of the deck due to creep, shrinkage and temperature effects were done on a full scale bridge. The bridge, discussed in Chapter 5, is a 2 span bridge with equal 120 ft spans. Calculations of strain and movement on the deck were done according to AASHTO LRFD 5.4.2.3. This method was researched by Dr. Tadros in 2003. See Appendix B for the calculation of creep and shrinkage strain. The strain due to temperature drop was calculated by multiplying the coefficient of thermal expansion (found in AASHTO 5.4) by the temperature drop. A temperature drop of 70 degrees Fahrenheit was assumed for the calculation.

Knowing the total prestressing force assuming 20% prestress losses, strain and movement due to creep and shrinkage were calculated over time. Additionally, the strain due to temperature effects was calculated and added to the strains from creep and shrinkage. These calculations for a single point in time are shown in Appendix B. A spreadsheet was used to calculate the strains over a length of time. The strain was converted to movement of the 120 ft long deck. The movement due to creep, shrinkage, and the total movement including temperature effects is shown in Figure 13 over an extended period of time.

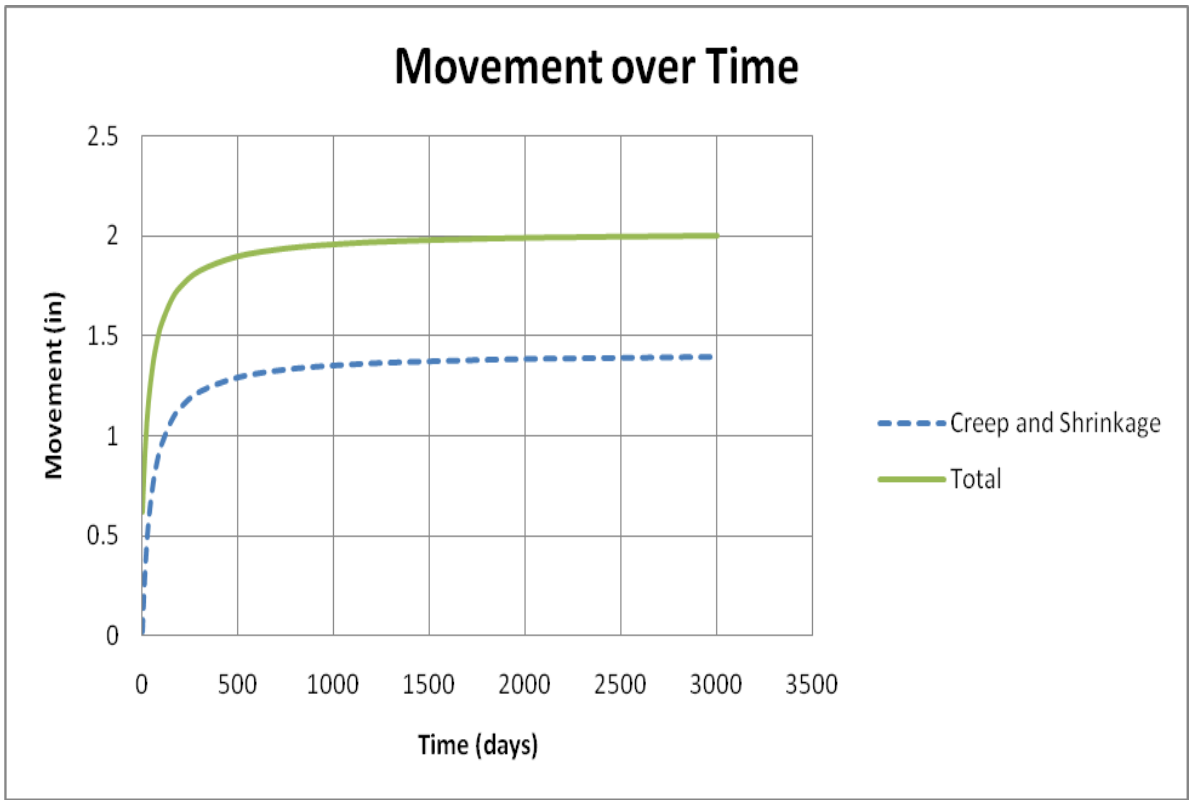

Figure 13: Movement over Long Period of Time

One of the main advantages of the delayed composite action system is that it allows strain and movement in concrete that usually bonds to shear studs early in the curing process, a time in which the concrete is not very strong. The total movement due to creep, shrinkage, and temperature effects for the first few days of the concrete is shown in Figure 14.

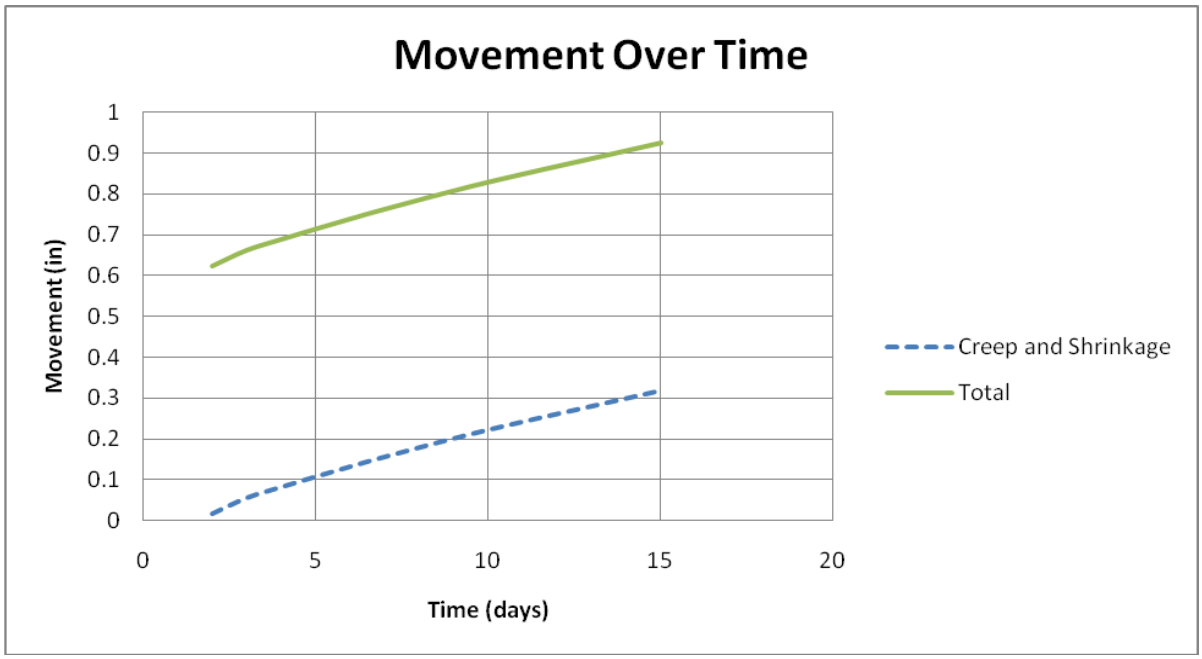

Figure 14: Movement over Short Period of Time

The post-tensioning and placement of the channel concrete would occur shortly after the deck pour. Assuming a time of 2 days between the deck placement and the post-tensioning and channel placement, a total movement of 0.63 in. would be allowed in the young concrete before composite action with the girder. By this time, the deck concrete will be strong enough to resist further strain from creep, shrinkage, and temperature effects. This is the desired effect of DCA coupled with post-tensioning for bridge deck systems.

3.3. Selection of Low Friction Materials

Various materials were researched as possibilities for the low friction bearing material. Most of the products were low friction plastics, which are described in more detail in the following sections.

3.3.1. PFTE Polytetrafluoroethylene

PFTE is also known as Teflon. It is very nonreactive and used in many non-stick applications. It has one of the lowest known coefficients of friction of any solid material with a value of less than 0.1. It is very flexible and can withstand low temperatures. This would be an advantage for bridge deck applications during cold winter temperatures. The dynamic and static friction coefficients are nearly the same so stick/slip behavior is not a concern. The material is typically ordered in rods, tubes, and sheets. It is one of the more expensive options for low friction plastics.

3.3.2. UHMW (Ultra High Molecular Weight Polyethylene)

One of the main advantages of UHMW is that it is a relatively high strength material with high abrasion resistance. It has low stick/slip friction characteristics. It is a self-lubricating material. The product normally comes in sheets in varying thicknesses and prices. It is less expensive than Teflon, but has a higher coefficient of friction.

3.3.3. Slick Strips (UHMW Adhesive Backed)

Slick strip (a specific product with UHMW plastic) is usually applied like a thick tape. It has a high abrasion resistance and very low friction coefficient. It also behaves

acceptably in very low temperatures. It is often used in gaskets and is particularly effective when applied to both top and bottom surfaces or is allowed to slide across another slick strip surface. The price is again less expensive than Teflon, but does have a higher coefficient of friction.

3.3.4. Low Friction Engineering Plastic (Ertalyte)

This product is from a company in Australia. It has similar advantages to the previous products listed, as well as a high strength and low friction coefficient. The exact cost was not listed. The product does include some additional advantages though, such as a high wear resistance.

3.3.5. PMMA Plastic

PMMA has high strength compared to many plastics, but it is also lower than other engineering polymers. It becomes brittle after loading. Common uses include aquariums, helmets, airplane and submarine glass. This is probably a less attractive option. Further price investigation could be done on the price if the other products are not selected. However, other options have better properties even for their price.

3.3.6. HDPE Plastic (High Density Polyethylene)

HDPE has similar characteristics to UHMW. It has a high abrasion resistance and low friction characteristics. The coefficient of friction of HDPE is higher than Teflon and UHMW. It also behaves acceptably in very low temperatures. HDPE is ordered by the sheet and less expensive than UHMW plastic.

3.3.7. Summary

Numerous plastics were researched as possible low friction materials to be used between the supporting straps of the channel and the top flange of the girder. Several businesses in Omaha were contacted to determine possible materials that would be most viable. After investigation, the three most promising options were high density polyethylene (HDPE), ultra high molecular weight (UHMW), and Teflon. Other less expensive options were explored at Home Depot, Menards, and Lowes. Samples and pricing information was obtained for HDPE, UHMW, and Teflon from Midwest Plastics of Omaha. Table 1 shows possible low-friction materials along with friction coefficients (if known) and approximates prices.

Product	Thickness (in.)	Price (ft^2)	Static Friction Coeff.	Dynamic Friction Coeff.	Supplier
HDPE sheet	0.125	1.21	0.31	0.22	Midwest Plastics
HDPE sheet	1	8.19	0.31	0.22	Midwest Plastics
UHMW sheet	0.125	2.85	0.25	0.2	Midwest Plastics
UHMW sheet	1	19.11	0.25	0.2	Midwest Plastics
Teflon sheet	0.25	43.75	0.04	0.04	Midwest Plastics
Optix Acrylic sheet	0.093	0.61	-	-	Home Depot
Optix Acrylic sheet	0.118	2.49	-	-	Home Depot
Optix Acrylic sheet	0.22	4.4	-	-	Home Depot
Tempered Hardboard	0.1875	0.38	-	-	Home Depot
White Panel Board	0.25	0.37	-	-	Home Depot
FRP panels	0.09	0.78	-	-	Home Depot

Table 1: Low Friction Materials

Testing of small scale systems with some of these low friction plastics is presented in Chapter 4.

3.4. Development of Small Scale Model

A small scale model of the delayed composite action system was developed. The model of the proposed system is shown in Figures 15 and 16.

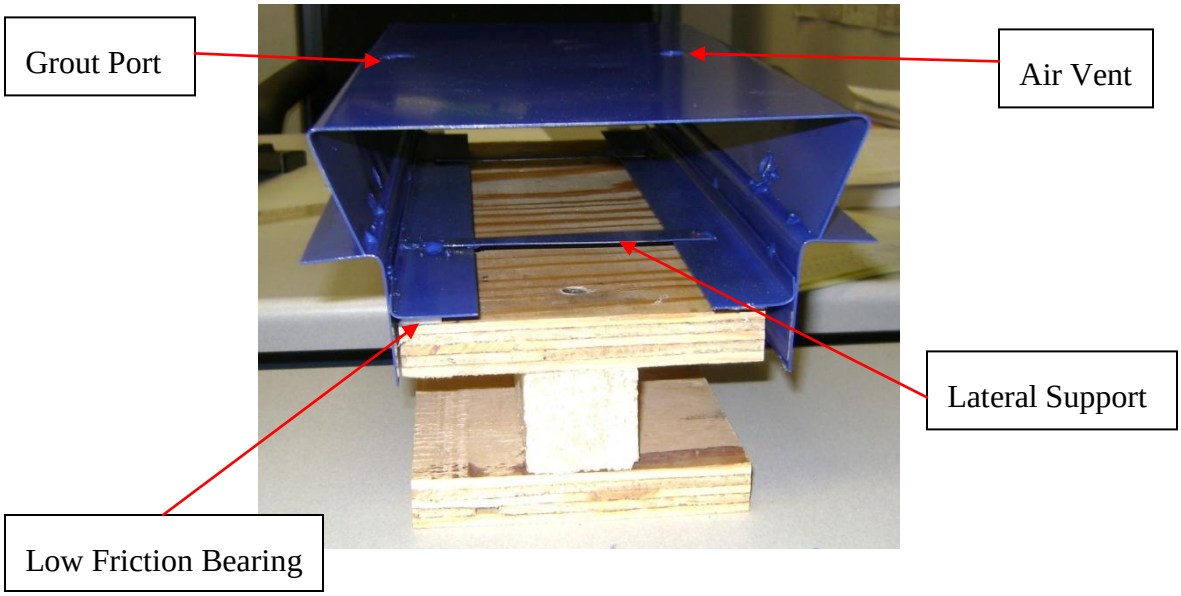

Figure 15: Small Scale Model

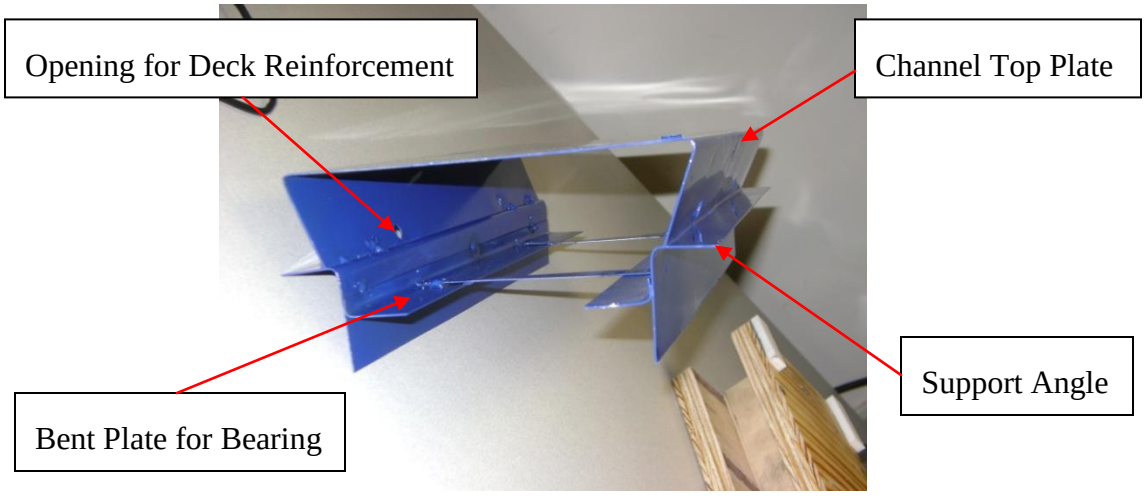

Figure 16: Small Scale Model 2

The model shown is a 1:4 model of the proposed system. An opening between the top flange and the channel allows for the shear studs (not shown in the model) to project up into the channel. Lateral bracing holds the apparatus together at the bottom. Two holes in the top of the channel allow for grout and an air vent when the grout is poured. Holes along the side of the channel allow for deck reinforcement.

The metal formwork is supported by angles which overhang along the side of the top flange. Because the apparatus is not attached to the top flange, friction is reduced. A bent plate is welded to the inside of the support angle to rest on the low friction bearing. A minimum size fillet weld is adequate to support the weight of the system.

The low friction bearing material chosen is Teflon. The model uses ¼ in. thick Teflon strips which are glued to the top flange. Because of the low friction of Teflon, small abrasions were made on the bottom side of the strips to allow them to be glued to the top flange using a high strength epoxy. Another option is using 1/8 in. thick Teflon the full length of the beam. This would reduce the need for sealant to prevent concrete from leaking through the bottom of the channel.

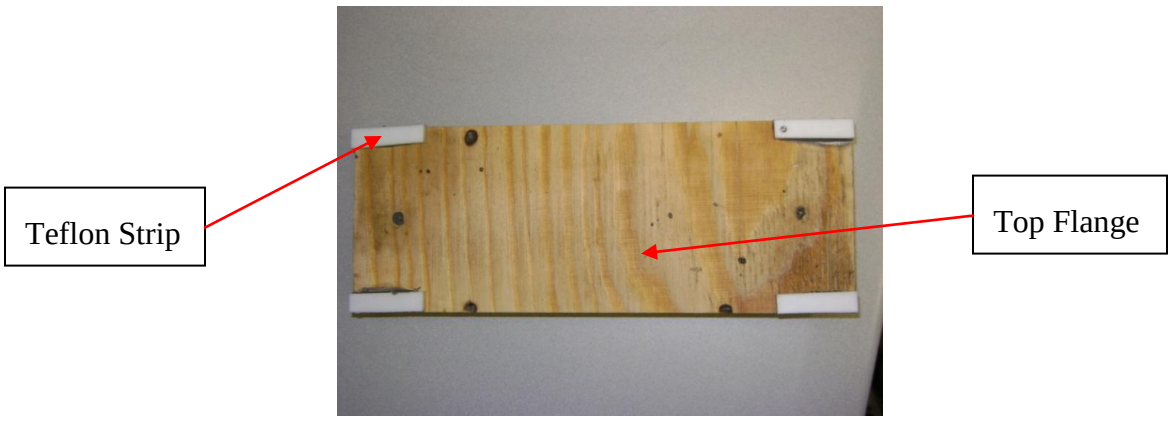

Figure 17: Top Flange with Bearing Strips

The system shown in the model provides several advantages. The low friction bearing allows for movement of the deck relative to the top flange, decreasing cracks shortly after the deck pour. Because the channel is not attached to the top flange, friction is further reduced. The system should also be easy to fabricate since it uses simple angles and bent plates that are welded together.

3.5. *System at Overhang*

System development also included developing the system for exterior girders at the location of overhang. The weight of the overhang would be supported by an adjustable bracket that would be attached to the girder. The deck would rest on a low friction bearing material as shown in Figure 18.

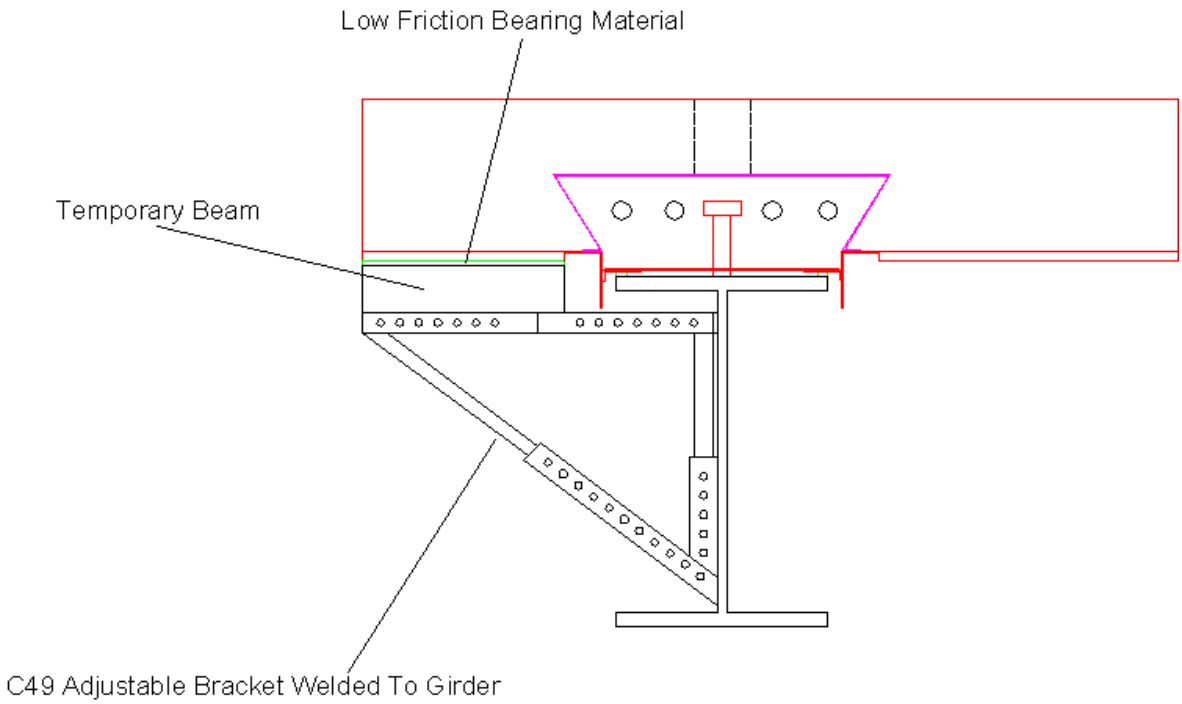

Figure 18: System at Overhang

A temporary beam would rest on top of the brackets with the weight of the deck resting on the beam with the attached low friction bearing material. The entire weight of the deck at overhang would be resting on low friction bearing, just as with an interior girder.

3.6. Development of Test Specimens (1st Round)

Test specimens were fabricated and poured to test the delayed composite action bridge deck system. The test specimens are a continuation of the small scale model explained previously.

Two test specimens were fabricated in the UNO structures lab supporting a 2 ft X 4 ft X 8 in. reinforced concrete deck. The steps for preparing the specimen are as follows:

1) Fabricate the channel top plate, support angles, bent plates, and lateral support strips before installation in the field.
2) Attach the low friction bearing strips to the top flange of the steel beam.
3) Weld the bent plates (connected with lateral support) to the two support angles. The height can be adjusted over the length of the beam for varying haunch.
4) Place the bearing apparatus on the low friction material.
5) Weld the top plate to the bearing apparatus.
6) Attach pipe to the grout and air vent holes
7) Attach the formwork to the support angles.
8) Place the deck reinforcement.

9) Place the concrete.

These steps will be described in more detail in the following sections.

3.6.1. Fabrication of Individual Pieces

The channel top plate, support angles, bent plates for bearing, and lateral support strips were fabricated in the shop of the UNO structures lab. Two 4 ft long specimens were prepared and able to support a 2 ft X 8 in. deck. Figure 19 shows the cross section of the system.

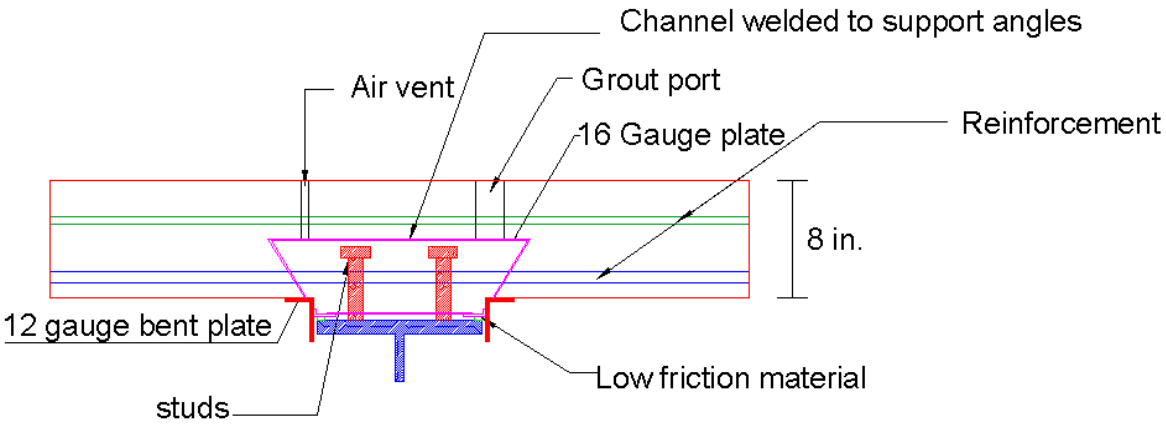

Figure 19: System Cross Section

The support angles were made from bent 12 gauge steel sheet. The channel top plate, bent plate for bearing, and lateral support strips consisted of 16 gauge steel sheet. The top plate was bent and had holes drilled for reinforcement and grout and air holes for pouring of the concrete.

3.6.2. Preparation of Top Flange

The top flange of the steel beam had two shear studs welded every 2 ft. Low friction bearing strips were also attached to the top flange using a high strength two part epoxy. See Figures 20 and 21.

Figure 20: Girder with Teflon Strips

Figure 21: Girder with HDPE Strips

Two low friction materials were used for the test specimens. Teflon strips (2 in X ½ in X ¼ in.) were attached at 12 in. spacing as shown in Figure 15. High Density Polyethylene (HDPE) sheet strips (½ in. wide X 1/8 in. thick) were attached the full

length of the specimen, as shown in Figure 21. Because Teflon is much more expensive and has lower friction than HDPE, small strips spaced at 12 in. were used rather than a full length strip. Both materials had the underside roughened to ensure that the epoxy would bond the materials to the top flange.

3.6.3. Fabrication in the Lab

Once the individual pieces were fabricated and the low bearing materials were fastened to the steel beam, the entire system was fabricated in the lab. The bent plates were welded to the support angles. Because there was no haunch for the test specimens, the height of the bent plates relative to the support angles was constant. The lateral support strips were then welded to hold the apparatus together. Next, the channel top plate was welded to the top of the support angles. The last step of the in-field fabrication was attaching pipes to the holes for grout and air. PVC pipes were attached using high strength two part epoxy. See figures 22 - 24 for the completely fabricated system.

Figure 22: View of Cross Section

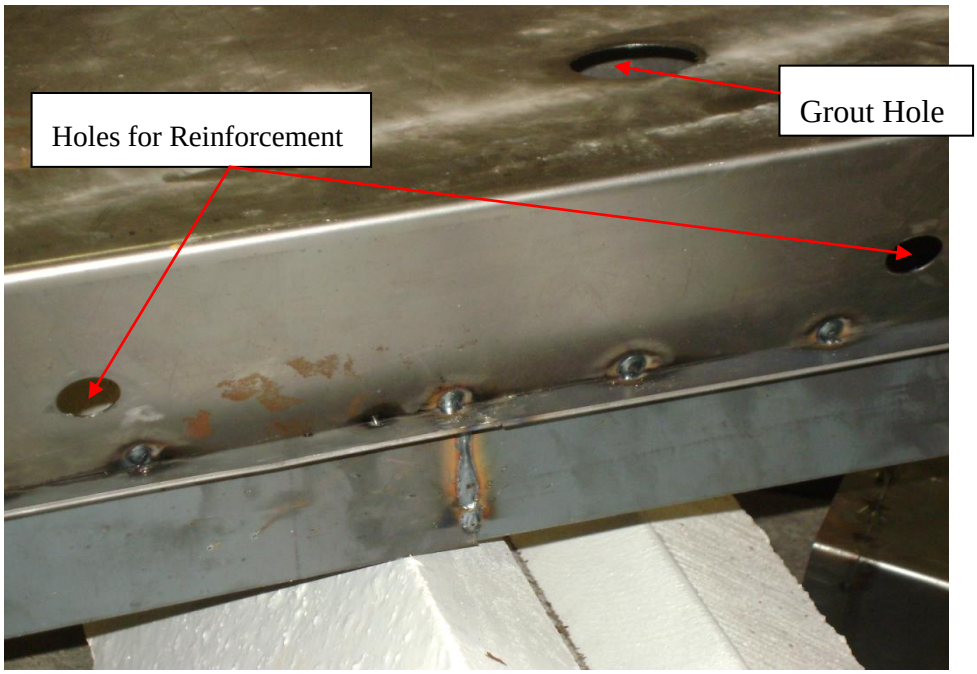

Figure 23: Holes for Grout and Reinforcement

Figure 24: Final Fabricated System

3.6.4. Attachment of Formwork

Wooden formwork was constructed to form a 2 ft X 4 ft X 8 in. slab over the delayed composite action apparatus shown above. This is different from what would happen in the field for a full scale system. Metal formwork would be welded to the support angles and the slab poured over the full width. For the test specimen, the wooden formwork was put flush against the top of the angle.

3.6.5. Placement of Reinforcement

Number 5 bars at 12 in. were used for the positive moment reinforcement (See Figure 25) with number 4 bars at 12 in. for longitudinal reinforcement. The top reinforcement consisted of number 4 bars at 12 in. for primary and longitudinal reinforcement.

Figure 25: Deck Reinforcement

Figure 26 shows the completely fabricated system with formwork and reinforcement just before pouring.

Figure 26: Complete System before Pouring

3.6.6. Placement of the Concrete Deck

The 8 in. deck was then placed over the channel. The grout and air vent holes were covered with duct tape to prevent grout from entering the channel, thus ensuring isolation of the shear studs. Figures 27 - 28 show the specimen right after pouring and curing. The holes in the deck are the grout and air vent holes.

Figure 27: Specimen after Concrete Placement

Figure 28: Specimen after Curing

3.6.7. Proposed Improvements to the System

In order to make the system more efficient and easier to fabricate, two improvements are suggested to the first round of the system described above. The first improvement is rather simple. It involves moving the support angles out further from the top flange. This would also require a wider bent plate to rest on the low friction bearing strips. Figure 29 shows an illustration of this improvement.

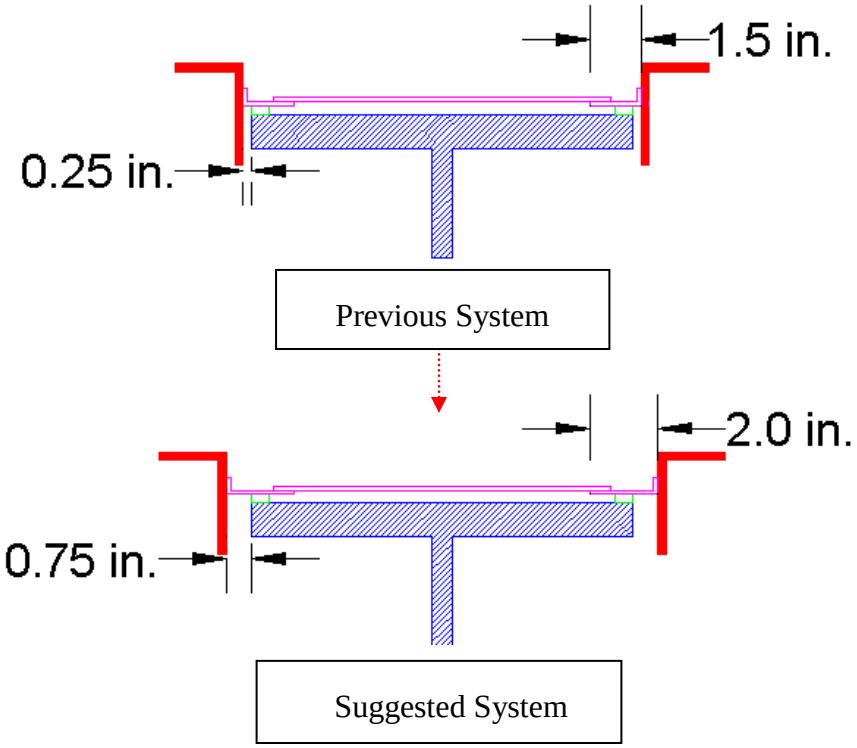

Figure 29: Improvement 1

The purpose of this change is to eliminate friction from the support angle being in contact with the side of the top flange. Weight from the formwork and deck will cause rotation on the support angle toward the side of the top flange. Increasing this gap should

eliminate this concern. This will also allow for creep and shrinkage in the lateral direction of the beam.

The second suggested improvement has to do with the channel top plate. For ease of fabrication and welding, it is suggested that the top plate have a flat bend at the bottom to rest on the support angle. Figure 30 shows an illustration of this improvement.

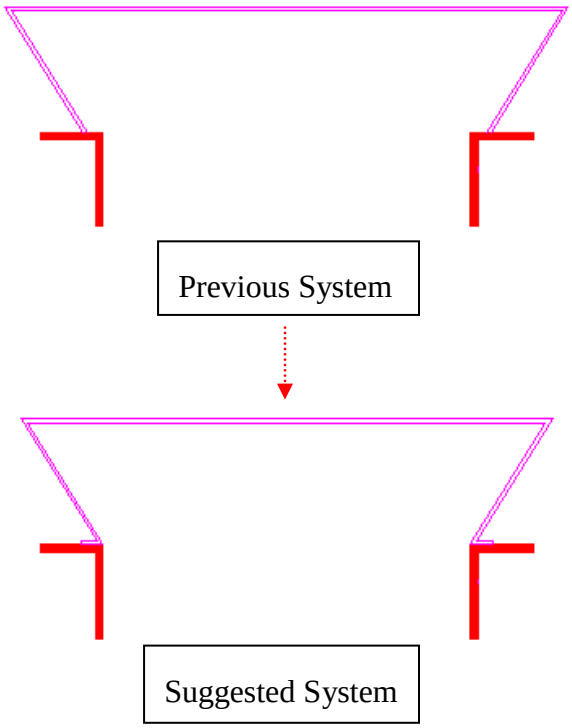

Figure 30: Improvement 2

The top plate would now have a flat surface to rest on the support angle. It would line up flush with the edge of the angle. This would greatly simplify welding the channel top plate to the support angles due to having a straight surface rather than an angle. It

would also make the system less likely to bend downward or not be straight over the length of the beam.

3.7. *Development of Test Specimens (2nd Round)*

Additional test specimens were developed implementing the suggested improvements to the first round of test specimens. The order of fabrication and construction listed in Section 3.6 remained the same. In addition to the two changes illustrated previously, the test specimens were wider and thicker. Instead of 4 ft X 4 ft by 8 in., the 2nd round of test specimens were 4 ft X 4 ft X 16 in. This was to simulate a 4 ft X 8 ft X 8 in. reinforced concrete deck. Figures 31 - 36 illustrate the fabrication and pouring of the 2nd round of test specimens.

Figure 31: Fabricated Pieces before Installation

Figure 32: Welding of Specimen

Figure 33: Specimen with Formwork

Figure 34: Specimen with Reinforcement

Figure 35: Specimen after Placemen of Deck

Figure 36: Specimen after Curing

This 2nd round of test specimens were used in the experimental program to determine the behavior of the system in the field.

Chapter 4.

Experimental program

4.1. Small Laboratory Push-off Testing:

The specimens described in Section 3.7 were tested to determine the friction coefficients for several different low friction materials and thicknesses. Six different cases were tested:

1) ½ in. Slick Strips (UHMW) full length (one side)
2) ½ in. Slick Strips full length (UHMW) (two sides)
3) ½ in. X 2 in. X ¼ in. Teflon strips at 1 ft spacing
4) ¼ in. X ¼ in. Teflon full length
5) ½ in. by 1/8 in HDPE strips full length
6) Metal on metal with no low friction material

This section describes the tests and summarizes the results.

4.1.1. Test Setup

The basic testing setup for the push off specimens is shown in Figure 32. The dead weight of a 4 ft X 8 ft X 8 in. deck was simulated by a 4 ft X 4ft X 16 in. slab. A horizontal load was applied to one side until the slab moved relative to the girder. The movement was measured using a dial gage (or a potentiometer) on the opposite side.

Any small movement signaled that friction had been overcome. The load was measured with a small load cell.

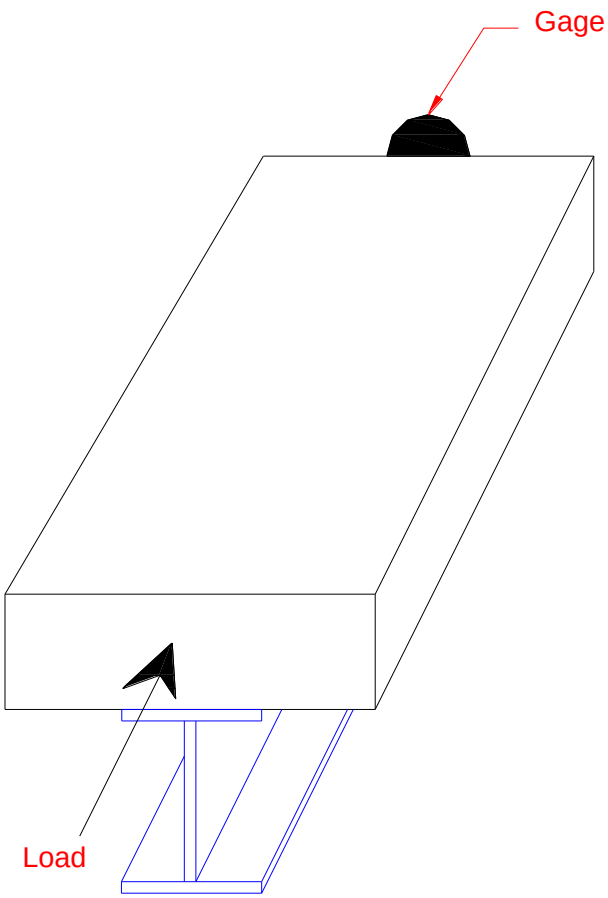

Figure 37: Test setup for Push off Testing

Figures 38 and 39 show the test setup in the lab with the load cell and deflection gauge.

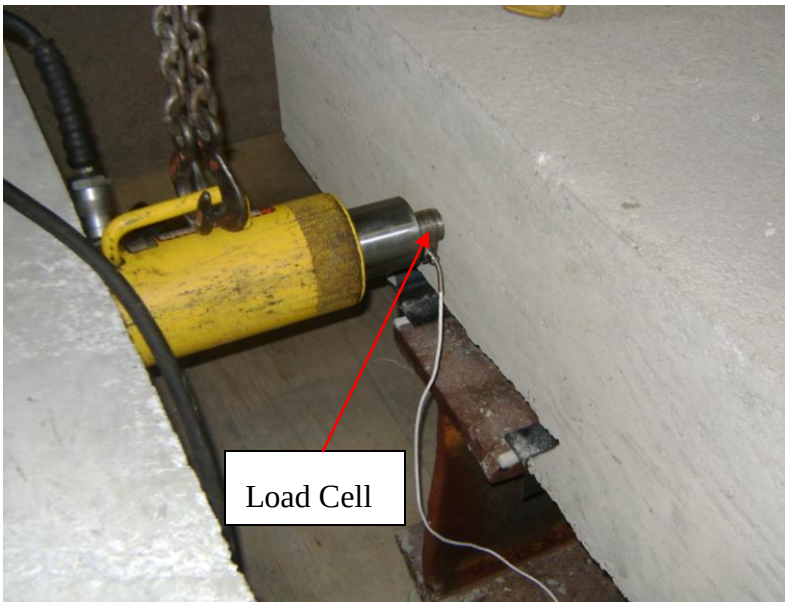

Figure 38: Load Cell for Horizontal Load

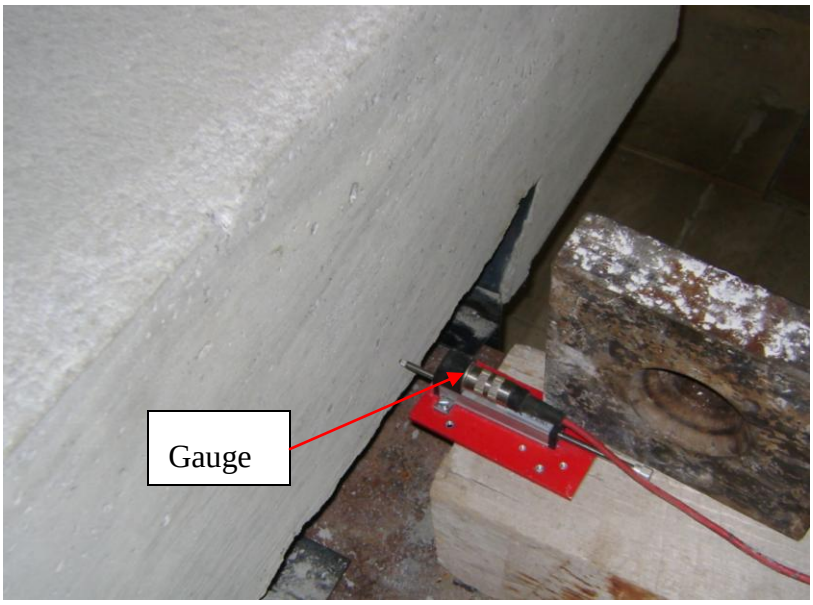

Figure 39: Gauge for Measuring Horizontal Movement

4.1.2. Summary of Test Results

Multiple test runs were conducted for each of the six different cases described earlier. The maximum friction coefficient values for each case were calculated. The results are shown in Table 2.

	Sample 1	Sample 2	Sample 3	AVG
Slick Strips (1 side)	0.569	0.482	0.450	0.501
Slick Strips (2 sides)	0.455	0.387	0.357	0.387
Teflon (2 in. X .5 in. @ 1ft)	0.233	0.233	0.255	0.240
Teflon (.25 in. full length)	0.246	0.203	--	0.225
HDPE	0.429	0.451	0.496	0.459
Metal on Metal	0.735	0.703	0.716	0.718

Table 2: Maximum Coefficients of Friction for Various Materials

Figure 40 illustrates the difference in the average friction coefficients for the various cases considered.

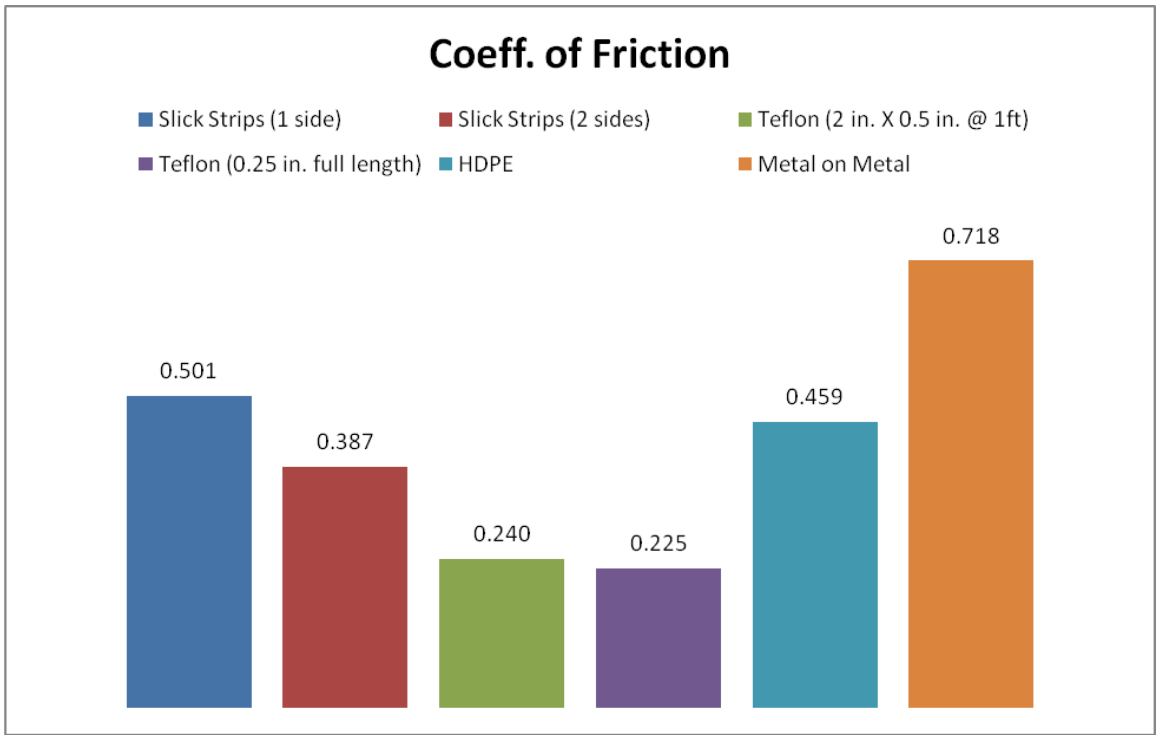

Figure 40: Bar Chart Comparison of Friction Coefficients

Slick Strips provide the easiest fabrication in the field. Using slick strips on both the girder and the channel provides a lower coefficient of friction. HDPE is comparable to Slick Strips but requires applying epoxy. Teflon is clearly the best option for a low friction bearing – roughly 1/3 the friction of metal on metal. However, it is the most expensive option and requires roughening of the plastic and application of a high strength epoxy.

4.2. Full Scale Production of the DCA System.

4.2.1. Introduction

The testing continued with the development of a full scale system. The full scale system is designed for a single span 50 ft steel bridge. Girder spacing was 8 ft with an 8 in. reinforced concrete deck. Standard AASHTO HL93 loading was used. The bridge has a width of 46 ft and consists of five girders. The bridge is shown in Figures 41 and 42.

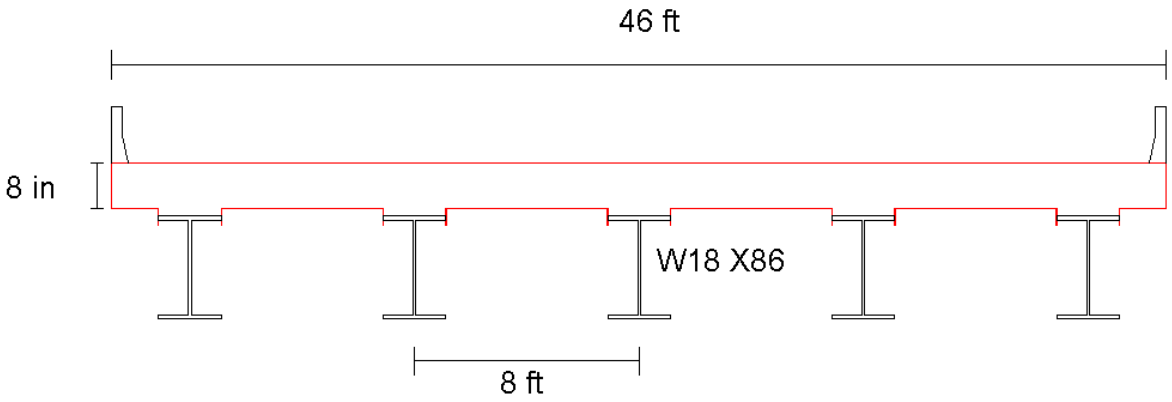

Figure 41: Bridge Cross Section

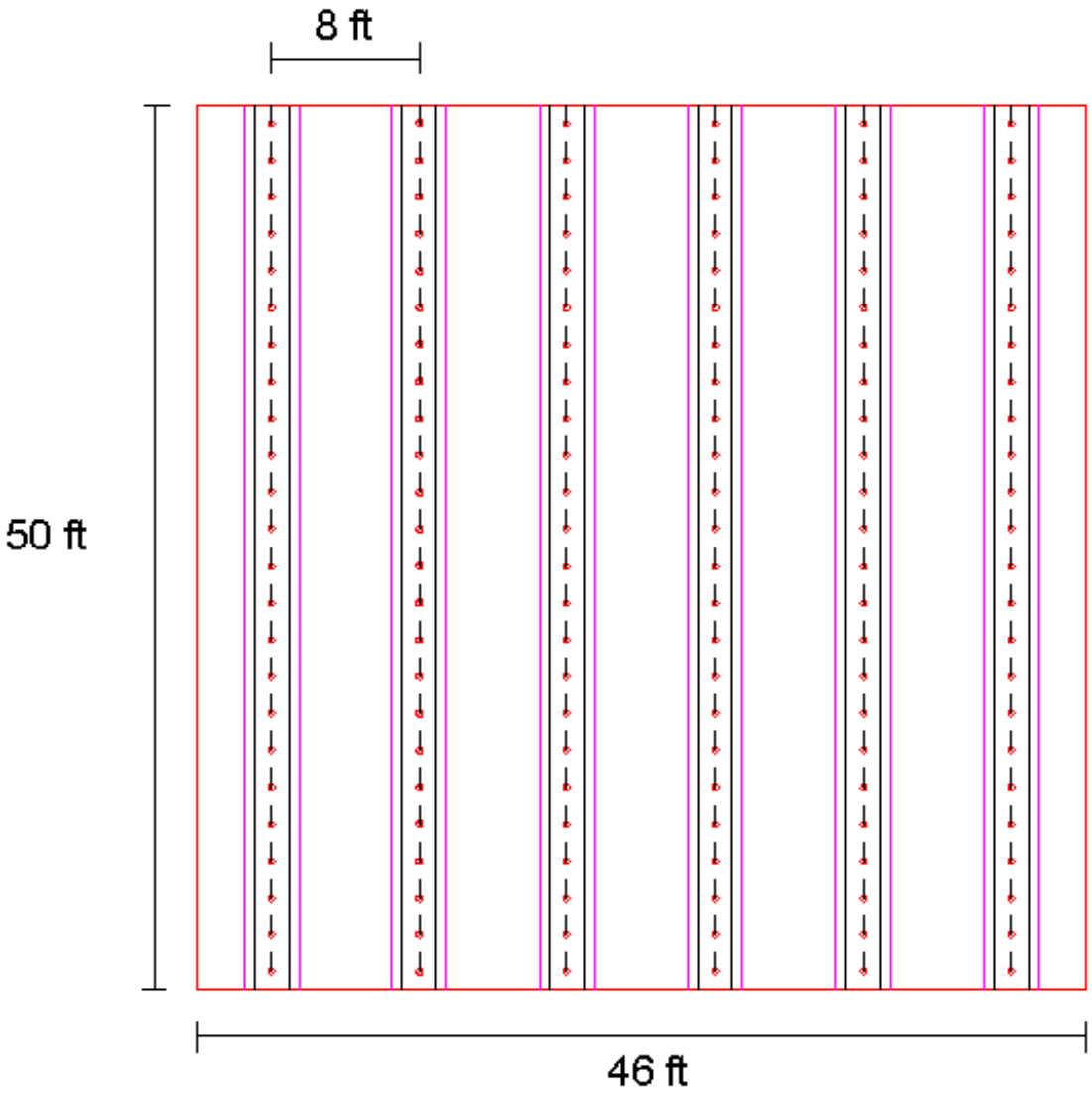

Figure 42: Bridge Plan View

The proposed specimens consist of two 50 ft long steel beams. The specimens will have a 4 ft wide by 8 in. thick reinforced concrete deck. One will utilize delayed composite action while the other will not have any sort of DCA. The DCA specimen will be post-tensioned using 0.6 in. strands. The cross sections for the beam specimens are shown in Figures 43-44.

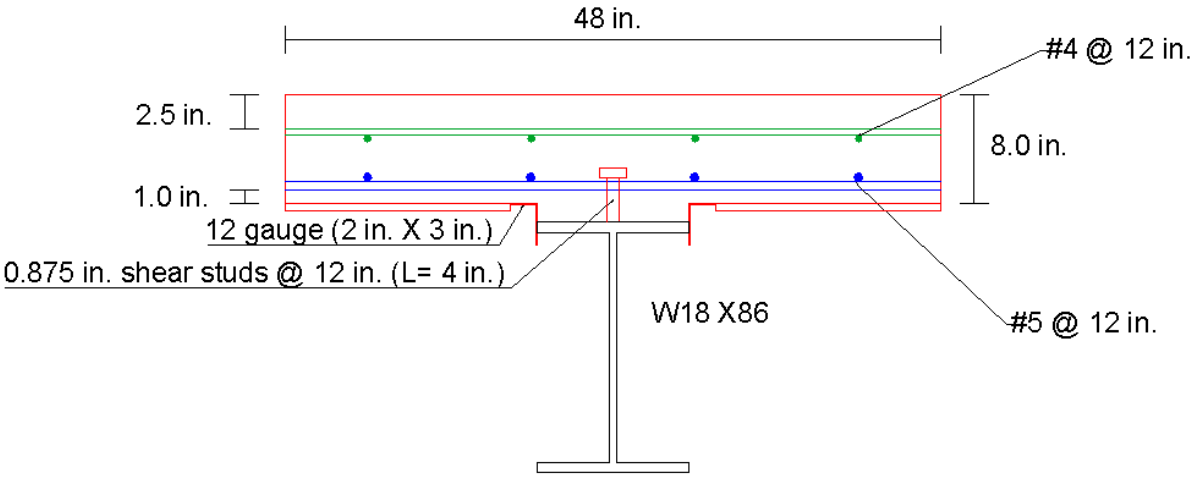

Figure 43: Specimen without DCA

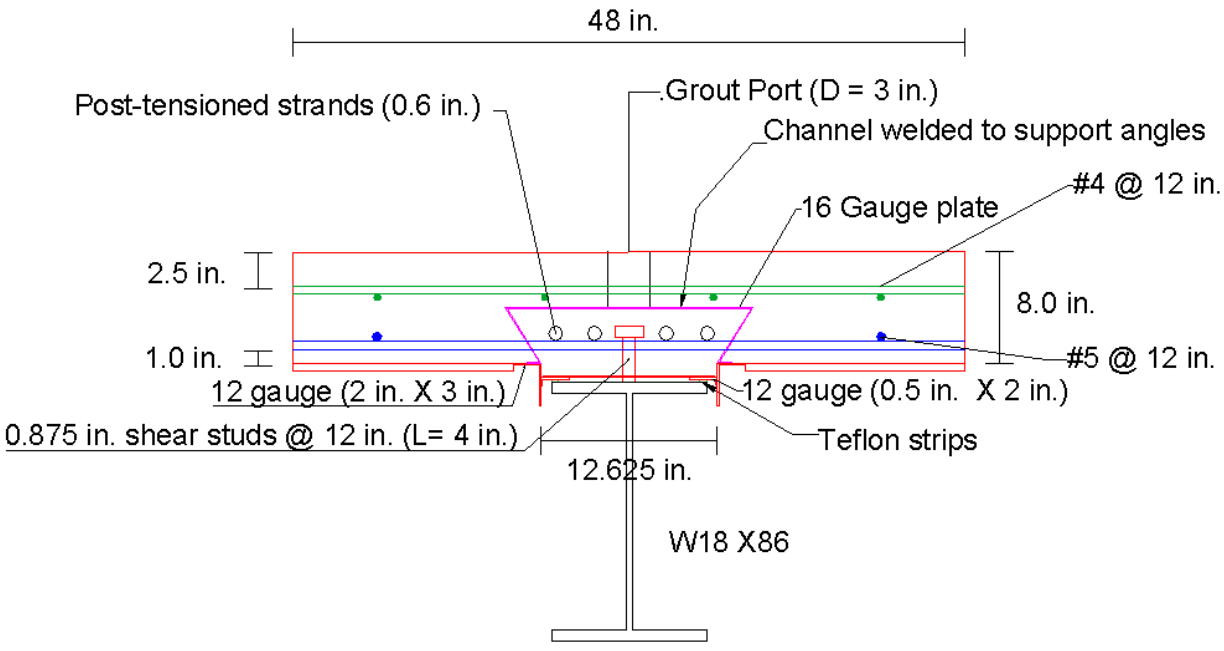

Figure 44: Specimen with DCA

Design calculations and cost comparisons were conducted to design the most efficient system possible. A W18X86 steel beam was calculated to be adequate to support dead load and AASHTO HL93 live load. The dead load, live load, and total factored moments of the interior bridge girder are shown in Table 3. See Appendix A for complete design calculations on the interior beam of the 50 ft single span bridge.

DL Moment	LL Moment	Total Factored Moment	Total Factored Shear
277 k-ft	605 k-ft	1406 k-ft	179 kips

Table 3: Summary of Moment and Shear Calculations

A W18X86 is used for both test specimens. The factored moment and shear capacities are shown in Table 4. Notice that the system with DCA and PT has a slightly lower moment capacity. This is due to the compression force from the post-tensioning. The shear capacity, which is the same for both specimens, is shown considering just the steel girder and is higher than the calculated shear on the beams.

Moment Capacity (No DCA)	Moment Capacity (DCA)	Shear Capacity
1577 k-ft	1530 k-ft	238 kips

Table 4: Shear and Moment Capacities

Shear studs (diameter = 7/8 in. and length = 4 in.) at 12 in. spacing were calculated to be adequate in horizontal shear. The required number of studs was 42, so 12 in. spacing was chosen giving a total of 50 shear studs per beam.

The following is a list of the expected significant steps in the fabrication and testing of the full scale system:

1) Weld the shear connectors and attach the low friction material to the steel beam.
2) Weld the prefabricated channel top plate, and support angles to form the DCA channel.
3) Construct the formwork and place the concrete.
4) Post-tension the DCA specimen using 0.6 in. strands.
5) Examine and compare both specimens for cracking.
6) Fill the channel with grout for the DCA specimen.
7) Test both specimens to ultimate failure in flexure.
8) Compare and summarize results.

4.2.2. Prefabricated Components

The fabrication of the channel for isolating the sheer studs and the support angles was done by Midwest Manufacturing in Omaha. The channel was fabricated in 10 ft pieces. The individual pieces are shown if Figures 45 - 46.

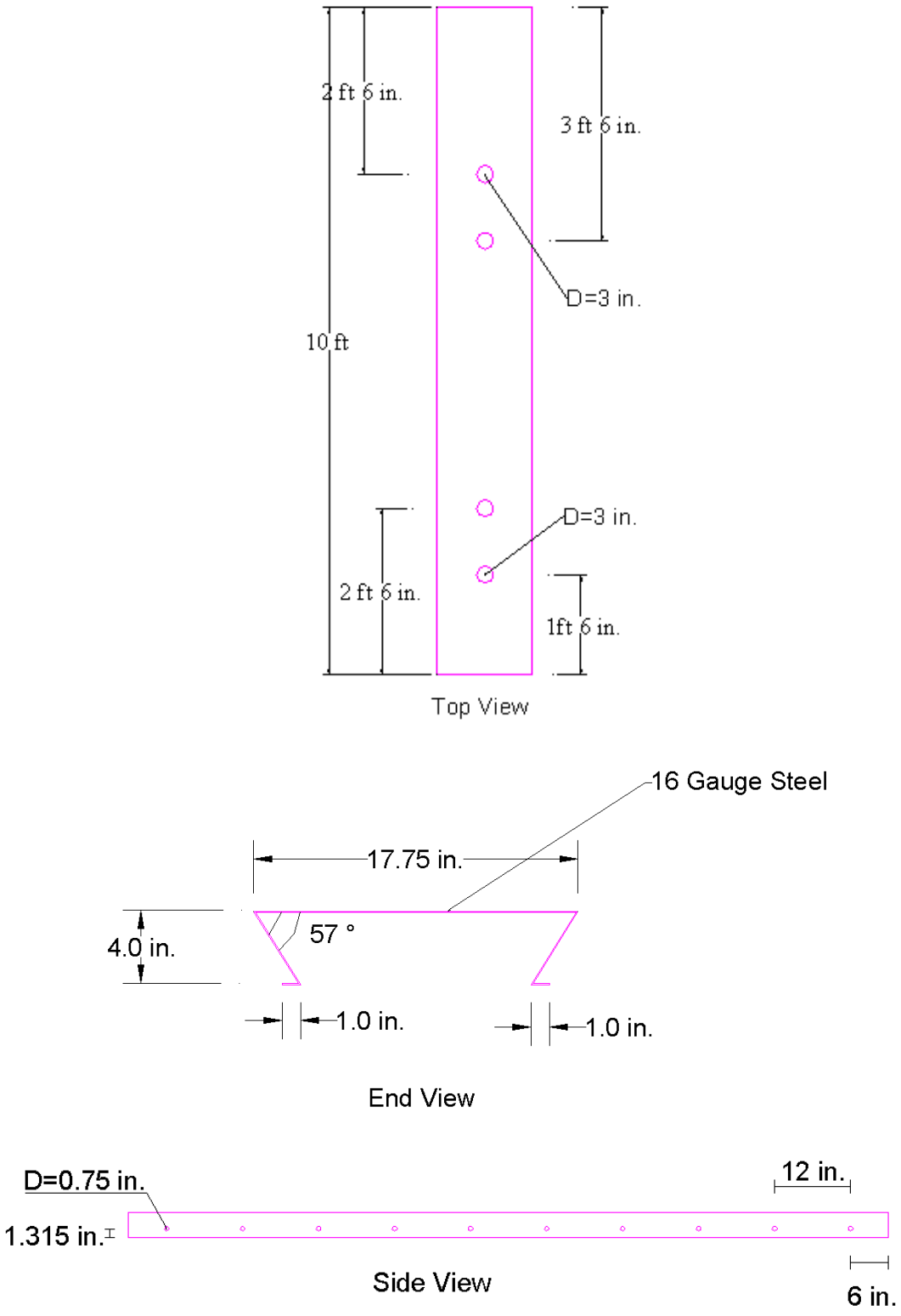

Figure 45: Channel for Isolating the Shear Studs

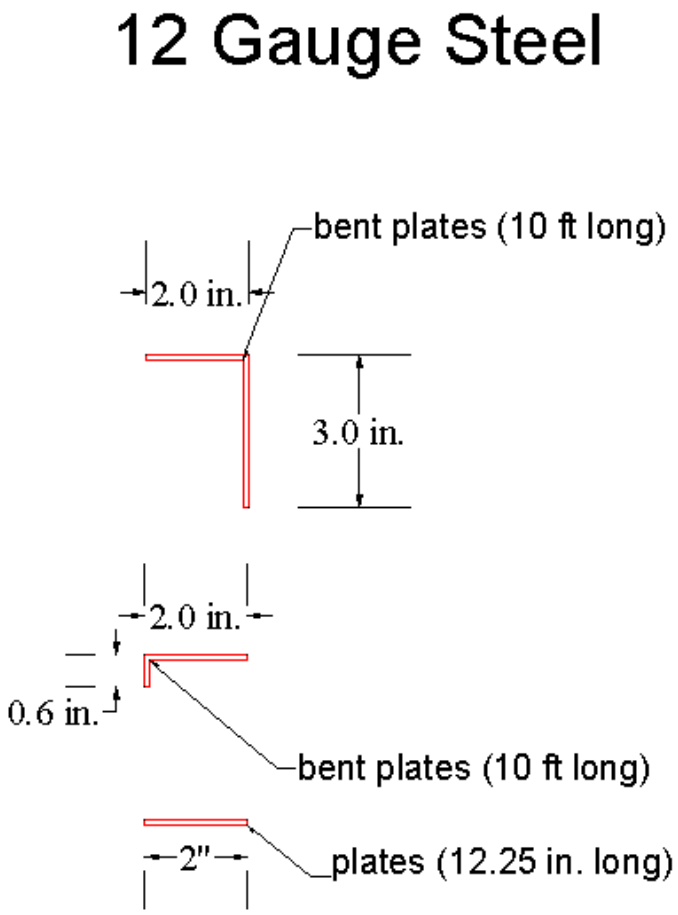

Figure 46: Support Angles

These pieces were used to construct the channel for the DCA system at the structures lab.

4.2.3. Lab Fabrication

The prefabricated steel plates and support angles were welded together to form one channel along the 50 ft steel beam for isolating the shear studs. The 2 in. by 3 in. bent plates were welded to the 2 in. by 0.6 in. steel plates to support the channel and the weight of the concrete from the initial placement of concrete.

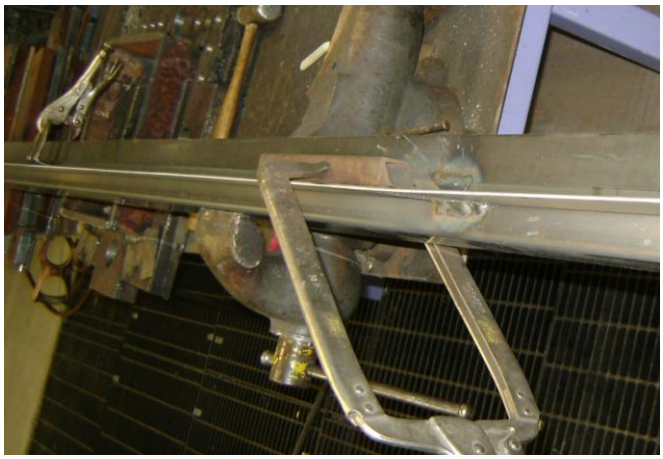

Figure 47: Support Angles

After the support angles were welded together, the low friction material was attached to the girder. UHMW plastic with adhesive (Slick Strips) was applied the full length of the girder to provide a low friction bearing. Strips were applied to both the girder and the underside of the support angle to maximize low friction behavior. UHMW strip was chosen due to its low friction characteristics and ease of application. Other options were discussed in Chapter 3, but UHMW tape (Slick Strips) provided the best option when considering cost, friction coefficient, and ease of application in the field.

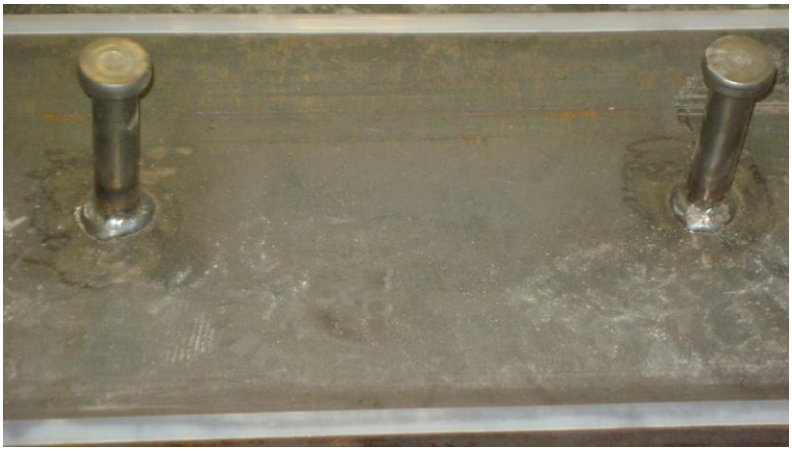

Figure 48: Low Friction Plastic Applied to Girder

The support angles, which also had UHMW plastic attached to the underside for further decreased friction, were set on the girder and welded together using small steel strips spaced at 12 in. to allow movement of the channel relative to the girder.

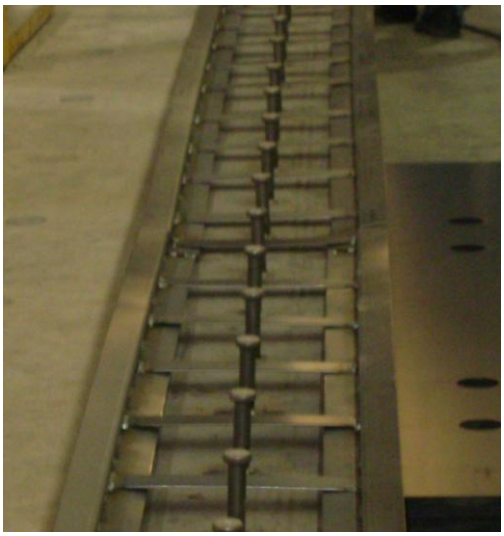

Figure 49: Welded Support Angles

The channel was welded to the top of the support angles for the full length of the beam.

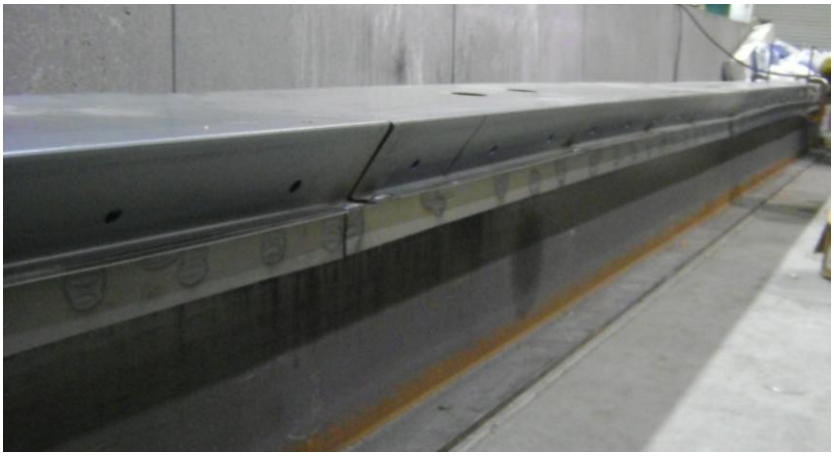

Figure 50: Channel Attached full Length of the Beam

The pieces of the steel channel were welded together as one continuous piece free to move along the length of the beam and lateral to the beam. The channel serves to isolate the shear studs, and holes in the top allow for grout to be poured later for composite behavior. Figure 51 shows a cross section of the completed steel channel.

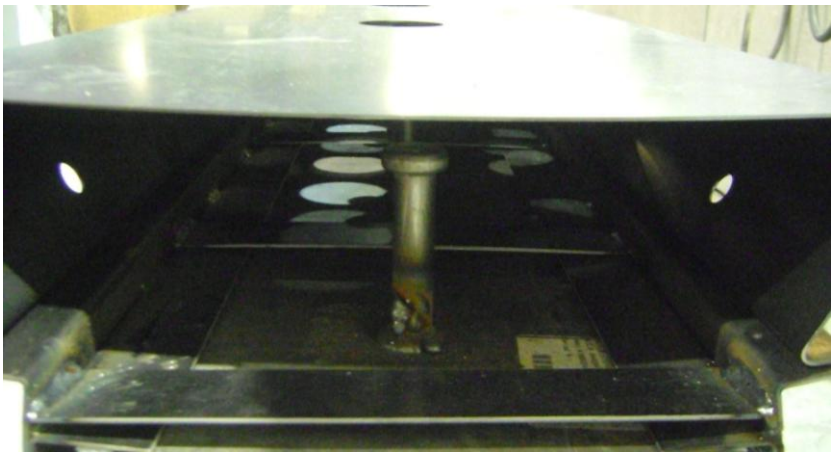

Figure 51: Cross Section of Channel for Isolating the Shear Studs

4.2.4. Formwork and Deck Reinforcement

Formwork was constructed (4 ft wide) for the full length of both beams. The sides of the formwork were 8 in. to provide an 8 in. reinforced concrete deck. PVC pipes were fastened to the holes on top of the channel to allow for concrete to be placed into the channel after the initial deck placement.

Figure 52: PVC Grout Holes

The deck reinforcement consisted of two layers. The top layer was designed as #4 bars at 12 in. spacing in both directions, with the bottom layer as #5 bars at 12 in. spacing in both directions. The reinforcement for the top layer ended up being #5 bars along the length of the beam with #4 bars in the lateral direction and all #5 bars in the bottom layer. 50 ft long #4 bars required a special order and cost more than #5 bars, so the larger rebar was used in the deck. The clear cover for the reinforcement was 1 in. for the bottom layer and 2.5 in. for the top. The specimens with completed formwork and deck reinforcement are shown in Figures 53-54.

Figure 53: Formwork and Deck Reinforcement for Specimen without DCA

Figure 54: Formwork and Deck Reinforcement for DCA Specimen

4.2.5. Placement of Concrete Deck

Concrete was placed using an NDOR standard bridge mix (3.5 ksi). The mix ingredients are shown in Table 5.

Material	Quantity
S47B	2105 lb
L47B	898 lb
CT1PF	562 lb
AAE90	41 oz
APZ80	168 oz
Water	287 lb
Water/cement	0.51

Table 5: Mix Design for Concrete Deck

Notice the mix had a water to cement ratio above 0.5. This was done as a means to develop more shrinkage with which to compare the two systems. The mix had a slump of 6.5 in. Both specimens were placed on the same day and from the same truck.

Figure 55: Pouring of DCA Specimen

Both specimens were covered with burlap and kept wet for five days.

Figure 56: Specimens Covered During Initial Curing

The strength of the concrete tested significantly higher than the specified 3.5 ksi compressive strength. The average one day compressive strength was 2678 psi. Figure 57 shows the compressive strength versus time relationship for the deck concrete. The average compressive strength was 6918 psi on the date of the test for ultimate flexural capacity.

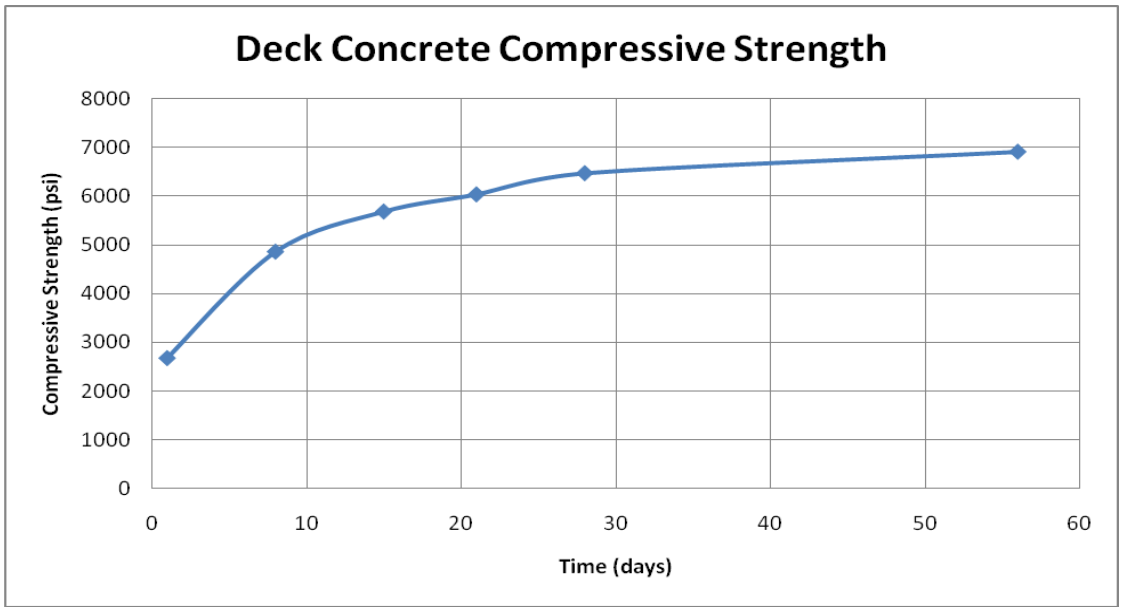

Figure 57: Deck Concrete Compressive Strength versus Time

4.2.6. Post-tensioning

The post-tensioning consisted of four 0.6 in. strands fed through the channel of the DCA system. The chucks were supported by HSS7X5X1 steel tubes on both ends of the specimen.

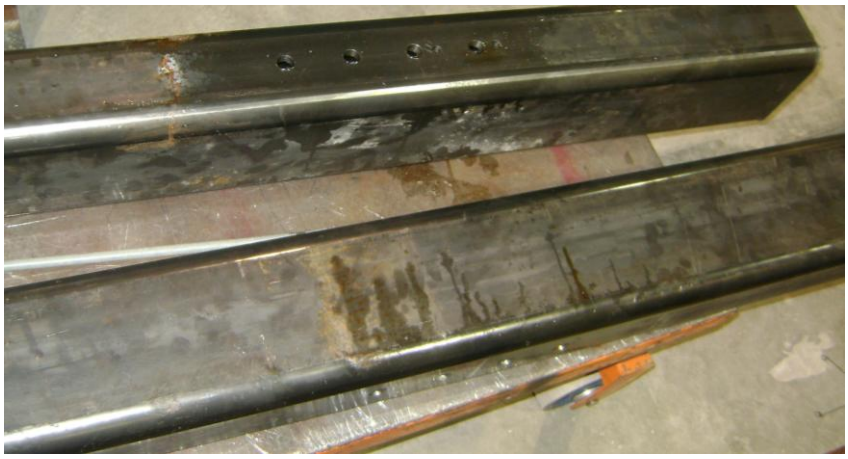

Figure 58: Steel Tube for Support of Post-tensioning

The strands were centered in the steel tube (2.5 in. from the bottom) at 3 in. spacing. The strands were tensioned to 202.5 ksi, which is 43.9 kips per strand. The stress on the concrete due to post-tensioning is calculated from the simple equation:

$$\sigma = \frac{P}{A}$$

Where σ is stress, P is prestressing force, and A is area. Assuming 20 percent prestress losses, the stress on the concrete was 366 psi. Three strands would have been adequate to have a stress greater than 250 psi. In a bridge with 8 ft spacing, 6 strands would be required to cause a compressive stress greater than 250 psi.

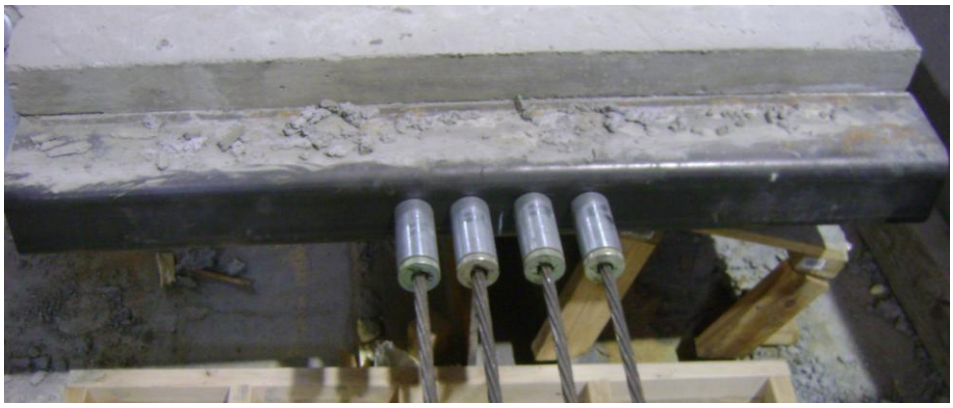

Figure 59: Post-tensioned Strand of DCA Specimen

The calculated elongation of each strand was 4.5 in. Actual elongation measured very near 4.5 in. This measurement was used to verify that the strands were actually tensioned to 202.5 ksi.

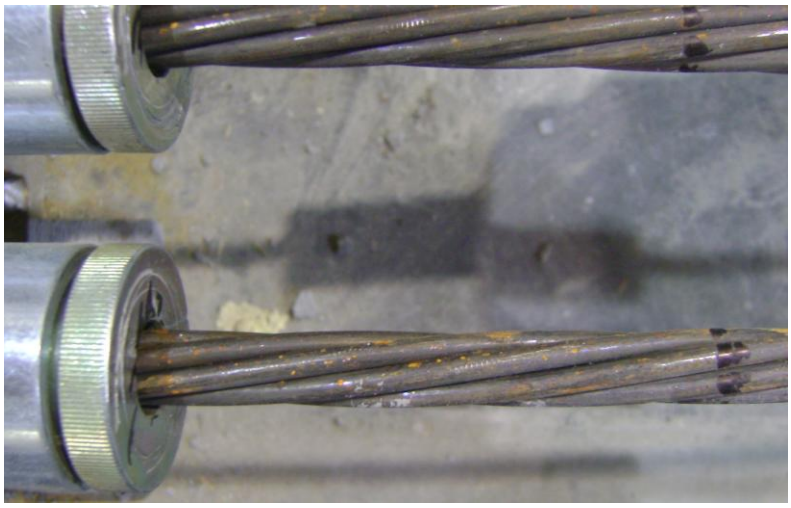

Figure 60: Elongation of Post-tensioned Strand

4.2.7. Placement of Channel Concrete

After the specimen with delayed composite action had been allowed to move relative to the sheer connecters without composite behavior for one month, the channel over the

sheer connecters was filled with grout. PVC pipe embedded through the deck and connected to holes in the top of the channel were filled with the concrete. Cones were used with concrete being dumped by hand from buckets. In a larger bridge application, it is recommended that a pump be used and connected to fittings that would be welded to the channel.

Figure 61: Pouring of Channel

The channel was placed moving from one end to the other. This was done to prevent air pockets in the channel. When one pipe was full the cone was moved to the next hole along the beam until the entire channel was filled to the top of the pipes as shown in Figure 62.

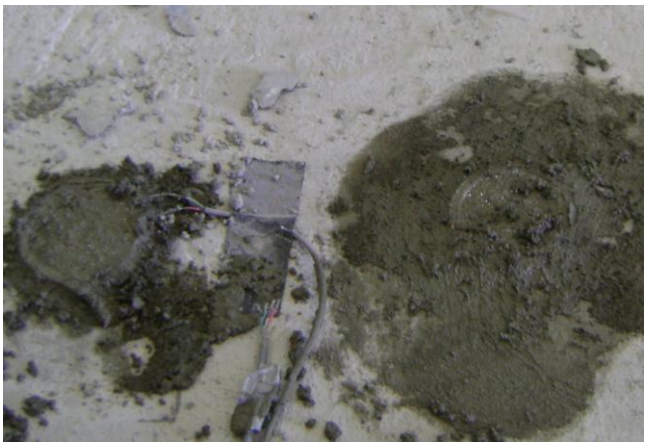

Figure 62: Channel Filled to Top

The mix used was an SCC (29 in. slump) sand gravel mix with a shrinkage reducing admixture (Tetraguard AS20). A sand gravel mix was used so that bigger aggregates would not create any air voids inside the channel. Table 6 shows the mix design for the channel concrete.

Material	Quantity
S47B	4300 lb
C1	965 lb
CFLYC	165 lb
AP900	159 oz
Water	426 lb
Tetraguard AS20	192 oz
Water/cement	0.444

Table 6: Mix Design for Channel Concrete

The mix was very easy to handle during the placement of the channel concrete. Because of the high flow ability of the concrete and the careful process of moving from one side of the channel to the other, the potential for air voids was reduced.

The designated compressive strength of the mix was 5,000 psi. The average compressive strength over time is shown in Figure 63. The 28 day compressive strength on the date of the test was 5897 psi.

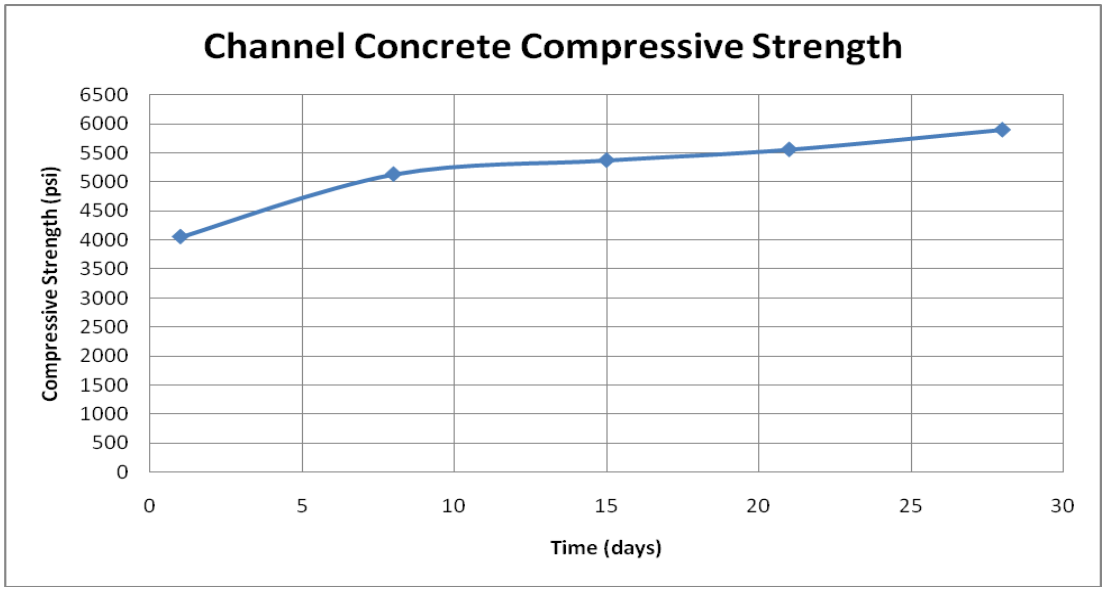

Figure 63: Channel Concrete Compressive Strength over Time

4.2.8. Crack and Strain Observation

4.2.8.1: Visual Inspection of Cracks

Both Specimens were observed for cracks after the deck pour and kept moist during the first week of curing. After this period, the visual crack observation took place. One specimen had immediate bond of the deck to the sheer connecters while the other specimen was free to move relative to the girder. Neither specimen showed cracks early on. It was expected that shrinkage cracks would be visible on the specimen without DCA, especially considering that a concrete mix with a high water-cement ratio was used.

This lack of cracking early on could be attributed to the relatively short span of 50 ft. A larger bridge application would have significantly longer spans which would make cracking due to shrinkage more likely. Another possible reason for the absence of cracks soon after pouring is the lack of exposure to the elements for the beam specimens. The beams received no sunlight or temperature variation typical of a normal bridge application.

Shrinkage cracks did appear on the specimen without DCA after a period of 7 weeks. Two cracks were located near mid-span, which is as expected. The cracks were located approximately five feet on either side of the girder mid-span, beginning on the side edge of the deck and extending approximately two thirds of the way across the top of the deck. Pictures of this crack can be viewed in Figures 64 - 65.

Figure 64: Shrinkage Crack Beginning on Edge Continuing on Top of Deck

Figure 65: Shrinkage Crack Extending Across Top of Deck

No shrinkage cracks were observed on the specimen with DCA and post-tensioning. The specimen without DCA did show some shrinkage cracks, though not as many as was anticipated. As mentioned earlier, this could be attributed to the conditions of the lab in comparison with outdoor elements and/or the shorter span of the specimens versus those found in typical bridge applications. The specimen with DCA and post-tensioning showed no signs of shrinkage cracks.

4.2.8.2: Detachable Mechanical Gauge Analysis of DCA Specimen

Detachable mechanical (Demec) Gauges were attached to both sides of the specimen that utilizes delayed composite action with post-tensioning. The gauges were attached 7 days after the concrete deck was cast. The first 7 days the specimen was covered with wet burlap. After the initial attachment of gauges, readings of the distance between the gauges were taken over time to record movement leading up to and after post-tensioning. Seventy-six gauges were attached 2 in. from the bottom along each side of the specimen. The spacing of the Demec gauges was 8 in.

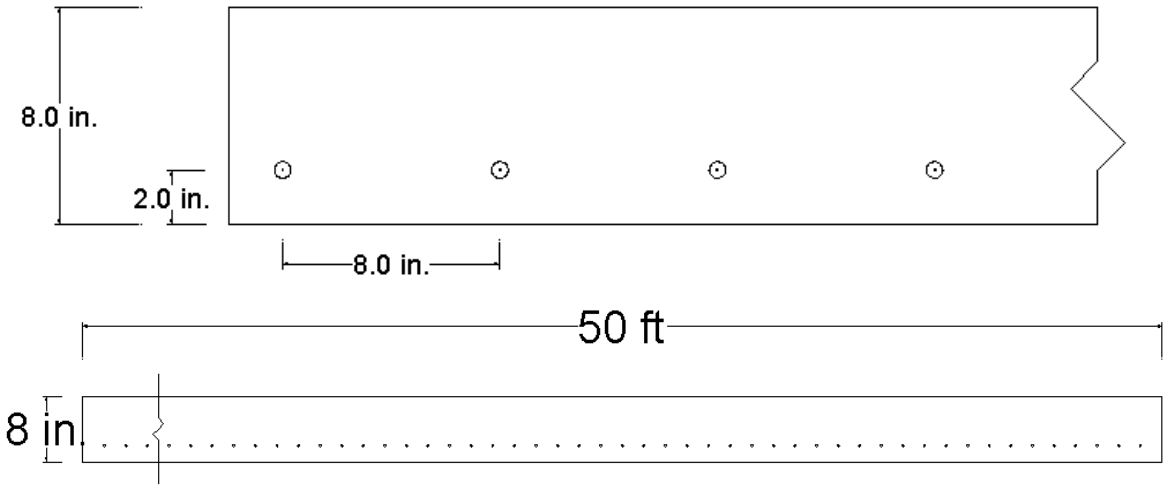

Figure 66: Demec Strain Gauges and Spacing Dimensions

Figure 67: Demec Strain Gauges

Figure 68: Instrument for Measuring Change in Strain of Demec Gauges

Initial and subsequent readings of the Demec gauges were taken at all points along the specimen. A change in length of 100 units is equal to a change in strain of 0.8 X 10^{-5}. This was used to calculate movement of the specimen due to strain. Strain is simply a calculation of change in length divided by the total length:

$$\varepsilon = \frac{\Delta L}{L}$$

The change in length at each Demec gauge along the specimen was calculated. Figure 64 shows the movement at each point along the length of the specimen at five different stages of time. As would be expected, the largest increase in movement due to strain occurred from the post-tensioning. A small increase in movement was measured after the much larger increase from post-tensioning.

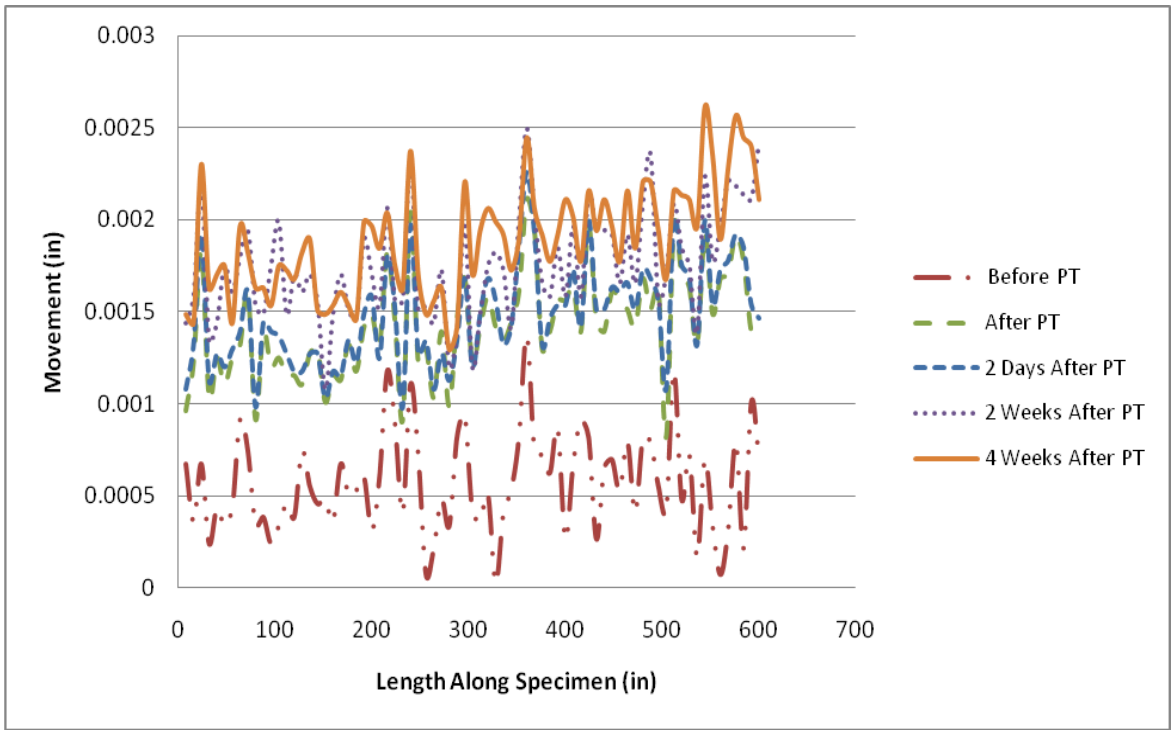

Figure 69: Change in Movement over Time

This same trend holds true when just the average movement for all points along the specimen are compared over time as shown in Figure 70. Notice movement occurs prior to post-tensioning. This can be attributed to the fact that the specimen was free to move due to delayed composite action. After post-tensioning, some movement still occurred over the length of the specimen.

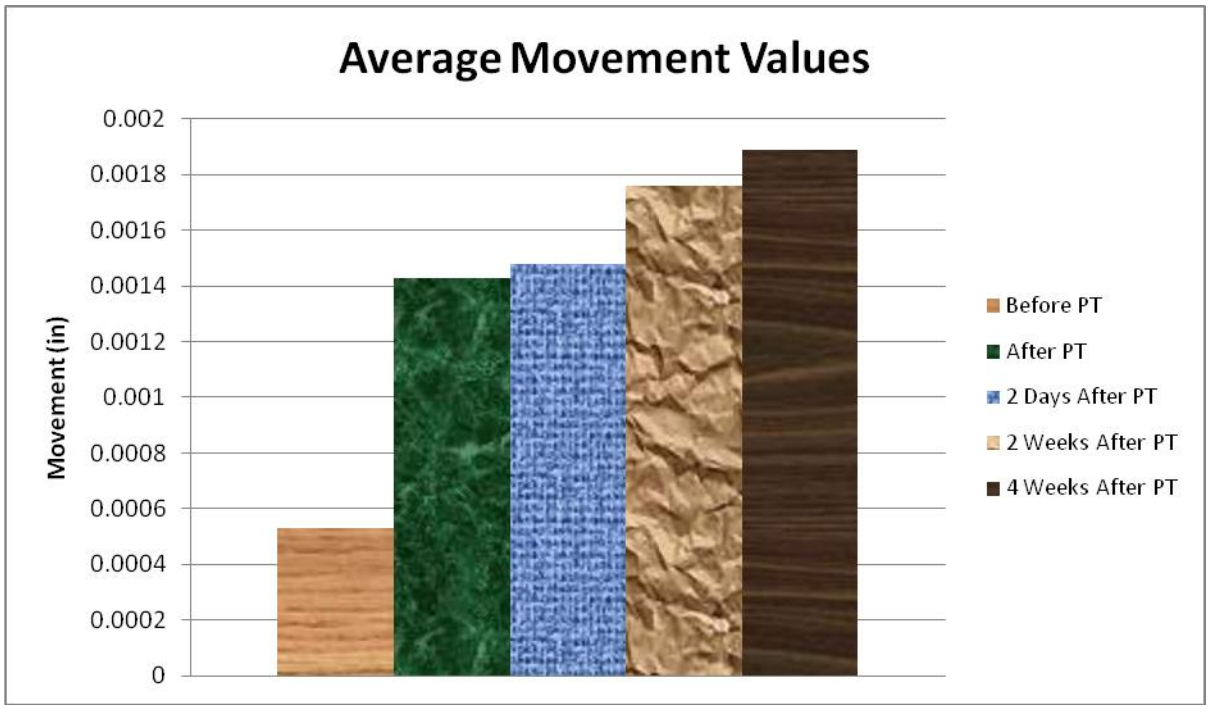

Figure 70: Change of Average Movement over Time

Using the strain, the total movement at mid-span was calculated. This was done for both sides on the north and south halves of the specimen. The average total movement at mid-span over time is shown in Figure 71.

Again notice that some movement was recorded before post-tensioning. This, as mentioned earlier, can be attributed to movement allowed by delayed composite action. The movement due to DCA is larger shortly after the concrete pour, and levels off before

post-tensioning takes place 18 days later. The largest jump was due to post-tensioning and can be seen in Figure 71. Again, movement occurs at a much slower rate after post-tensioning is applied.

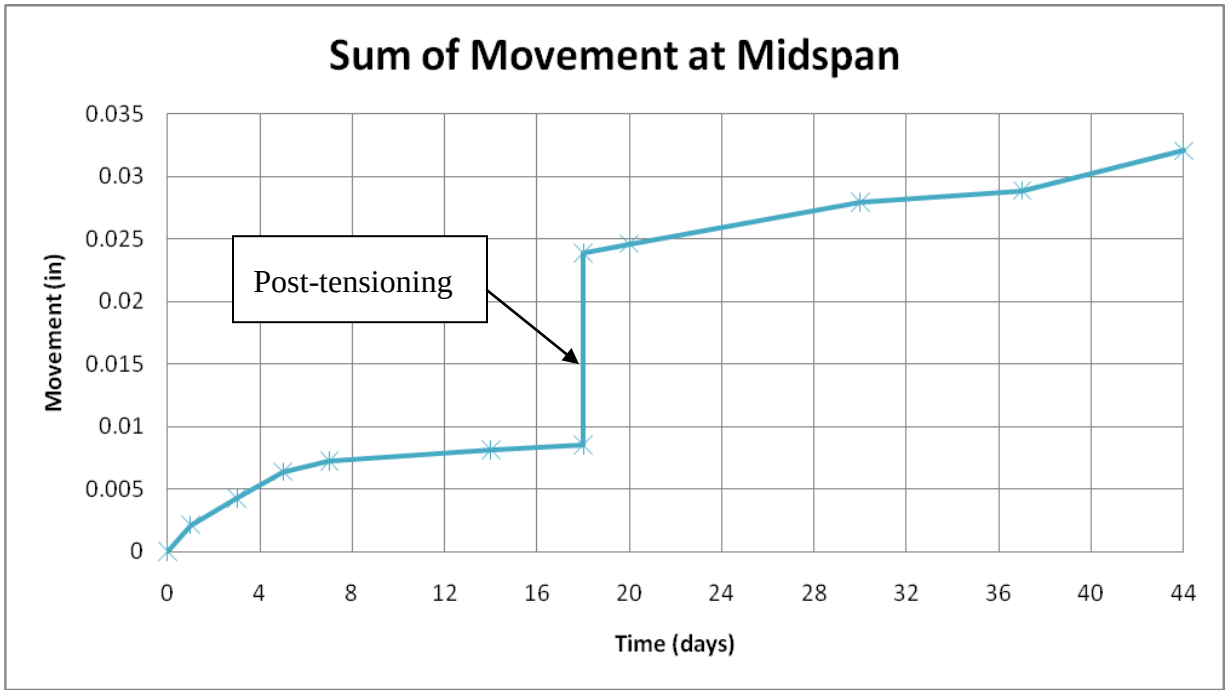

Figure 71: Sum of Total Movement at Mid-span over Time

The measured movement due to post-tensioning matches relatively closely with the theoretical value calculated using the stress strain relationship:

$$\frac{PL}{AE} = \Delta L$$

P is the load from post-tensioning. Four 0.6 in. strands were tensioned to 202.5 ksi for a total prestressing force of 176 kips. The length, L, considered was half the 50 ft span (300 in.) and the cross sectional area, A, equals 384 in^2 E, the concrete modulus of elasticity, was calculated based on the strength of the concrete at the time of post-

tensioning. Table 7 shows a comparison of the measured and theoretical values of the movement due to post-tensioning.

	ε (microstrain)	Deflection (in)
Measured	46.91	0.0141
Theoretical	51.02	0.0153

Table 7: Measured and Theoretical Movement Due to Post-tensioning

The cumulative sum of movement moving from one edge of the specimen to mid-span is shown in Figure 72. As would be expected, the points increase in a very similar pattern to the results mentioned previously. Some deflection occurs before and after post-tensioning, but the largest increase is due to post-tensioning.

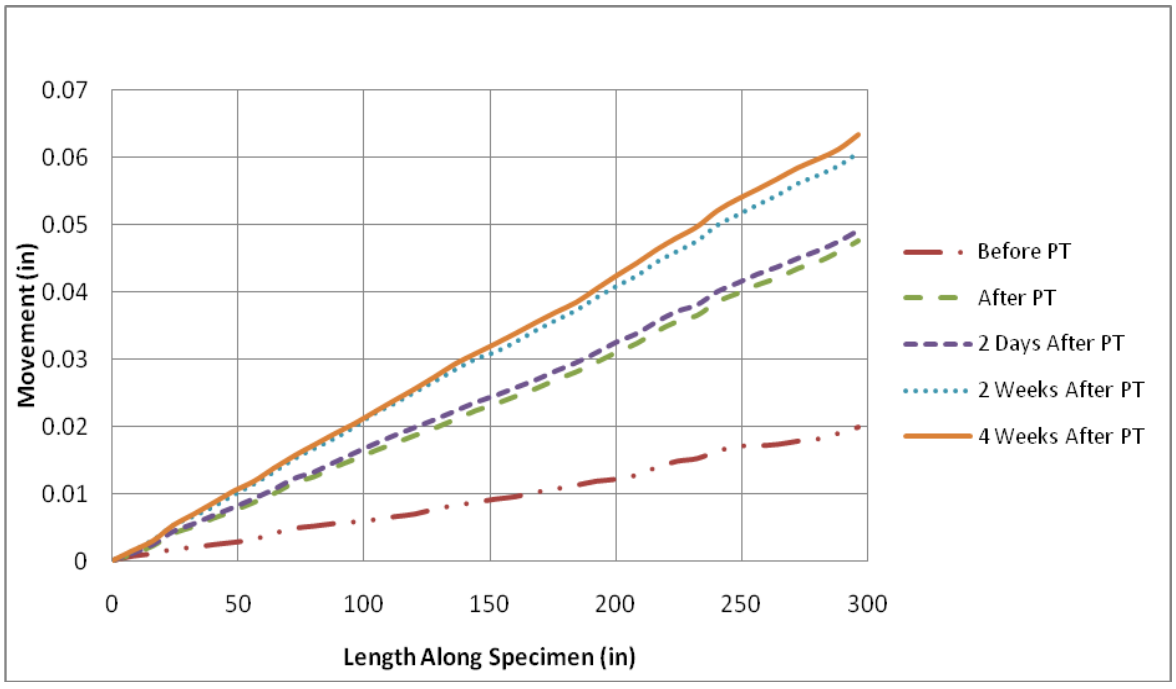

Figure 72: Change in Movement along the Length of the Specimen

The specimen behaved as would be expected considering both the effects of delayed composite action and post-tensioning. Some movement occurred due to the freedom of the deck to move relative to the girder as a result of the DCA. This is the desired effect of DCA and is illustrated very clearly in the test results. A larger portion of the movement occurred due to post-tensioning. The theoretical and measured deflections due to post-tensioning are a close match. In summary, this analysis shows that delayed composite action is effective at allowing movement of the deck relative to the girder.

4.2.8.3: Concrete Strain Gauges

Strain Gauges were attached to record changes in strain over time for both specimens. Twelve strain gauges were placed on each beam. The location and numbering of the gauges was identical for both specimens and is shown in Figure 73. Gauges 1-3 are located on the side of the specimen a distance of 4 in. from the top of the 8 in. deck. Gauges 4-7 are located on top of the deck and centered 2 ft from the edge. Gauges 8-12 are also located on the edge. At mid-span, three gauges were placed at 2 in. increments down the side of the deck. Gauges 8 and 12 are located 4 in. from the top of the 8 in. deck.

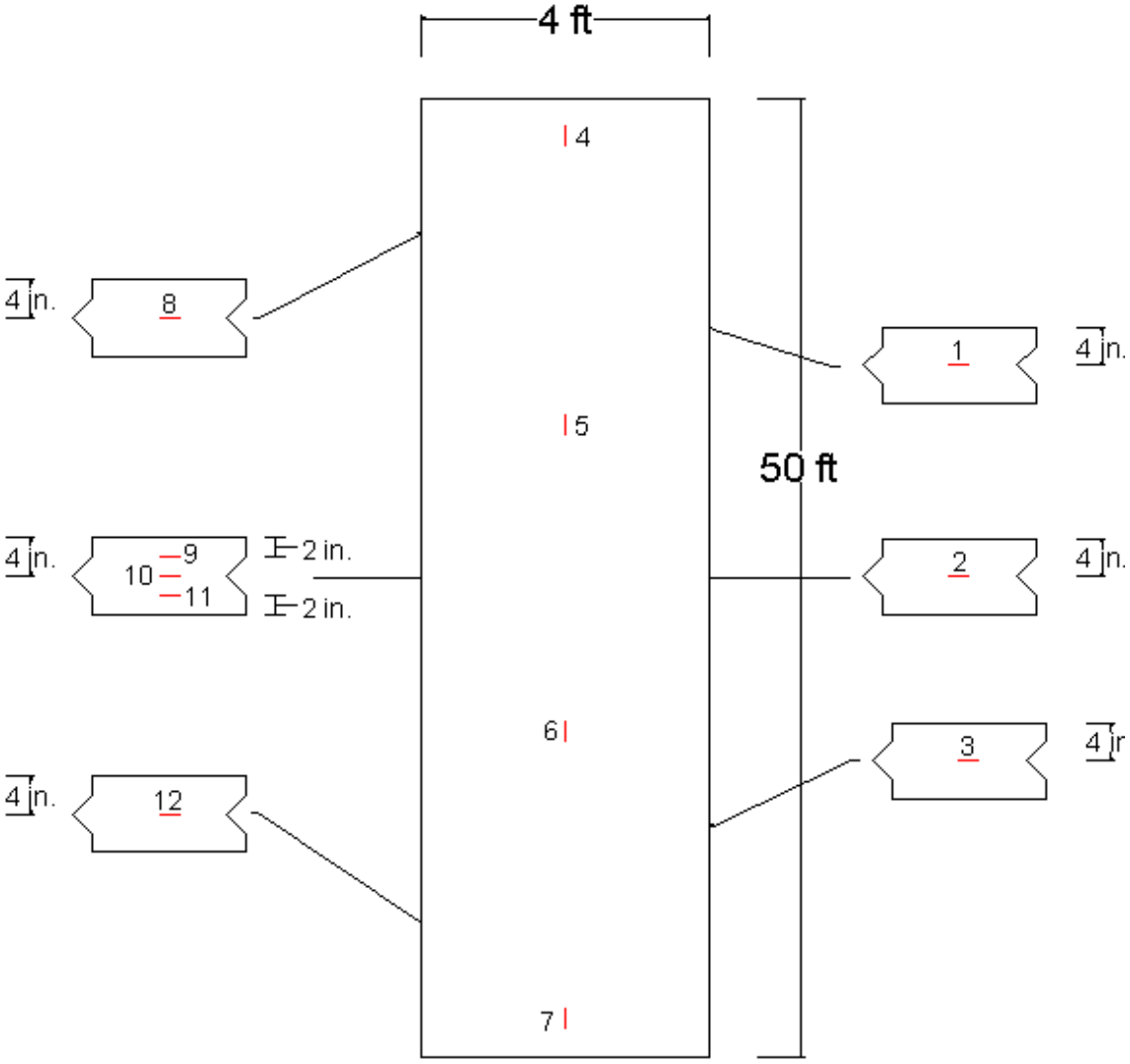

Figure 73: Location of Strain Gauges

Several of the strain gauges did not provide data over the full time period leading up to testing. However, comparison of Gauges 3 and 7 over the time period leading up to post-tensioning provide useful information.

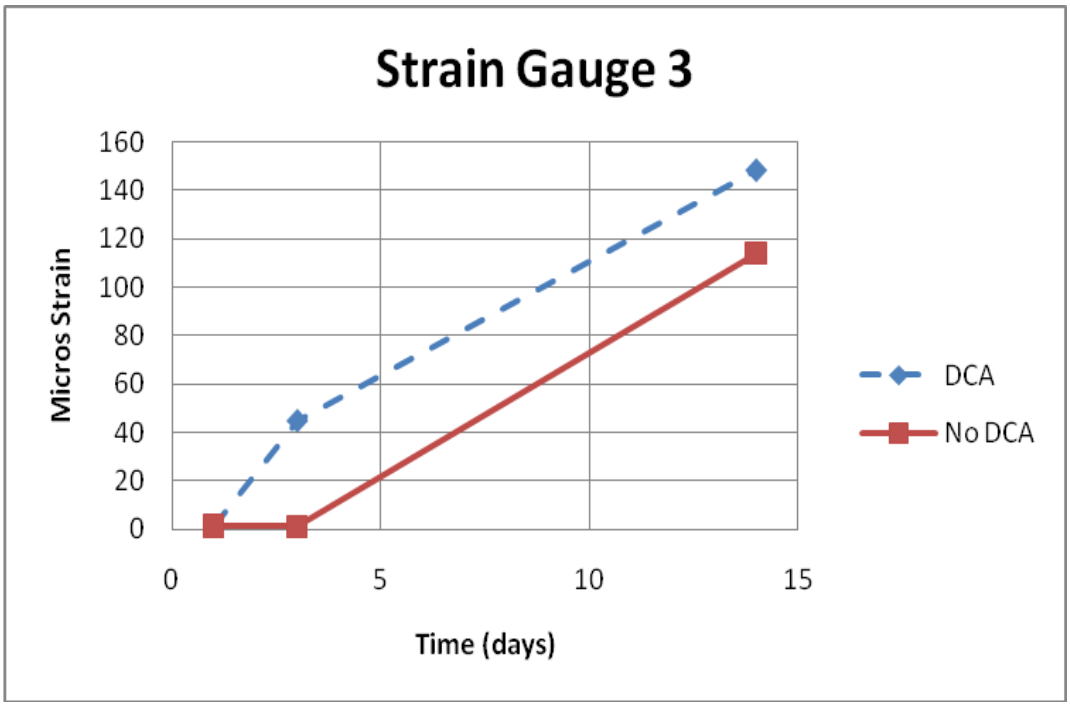

Figure 74: Comparison of Strain Gauge 3

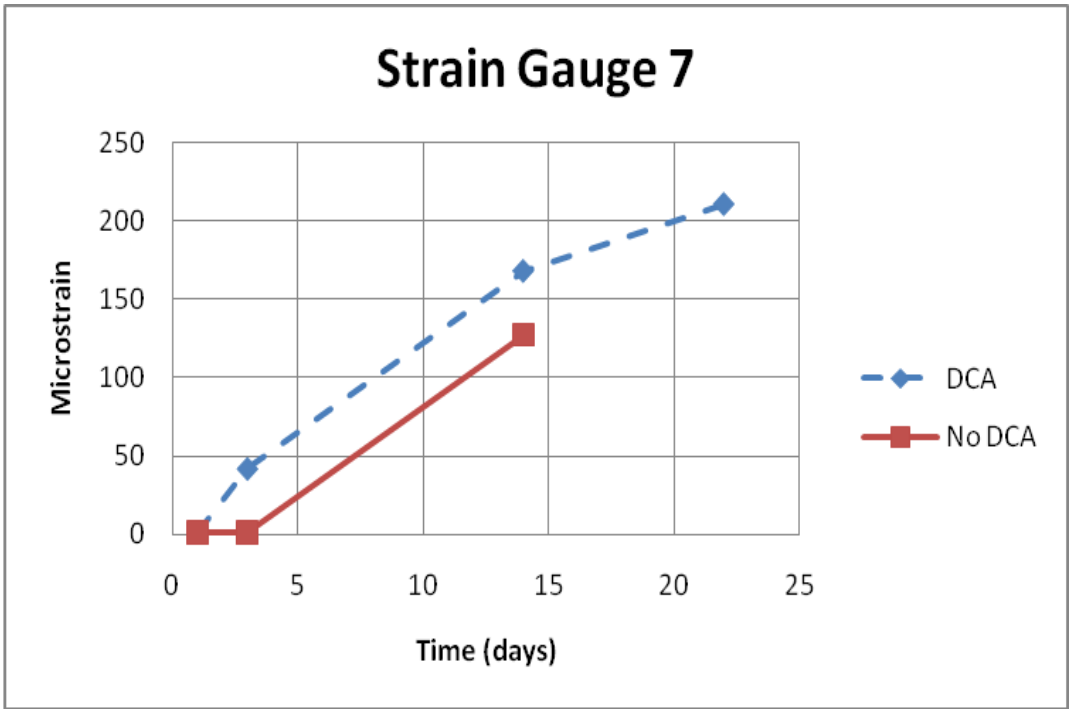

Figure 75: Comparison of Strain Gauge 7

Both strain gauges show similar trends. The deck with DCA moved more than the deck without DCA. This is expected since the beam with DCA is free to move relative to the sheer connectors.

An average change in strain for all correctly read gauges provides the information shown in Figure 76.

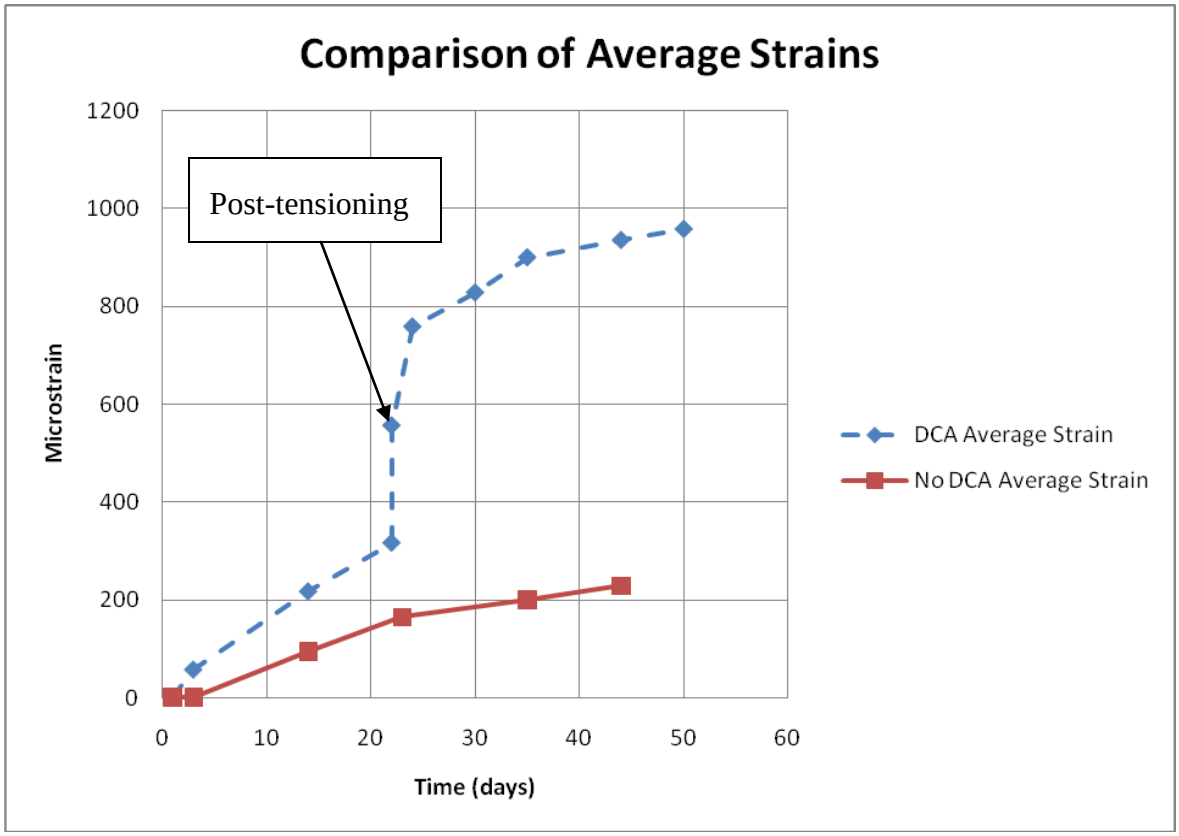

Figure 76: Change in Average Strain for Both Systems

Notice that both specimens recorded strain over time, but the DCA specimen had more movement than the specimen without DCA in the time leading up to post-tensioning (as observed in comparison of gauges 3 and 7). This is expected since the beam with DCA was free to move while the deck without DCA was bonded to the sheer

connectors. Additionally, the specimen with post-tensioning showed considerable response to the post-tensioning, as seen above. The strain gauge results also show that the system with DCA behaved as desired for both movement before and during post-tensioning as compared to the system without DCA or post-tensioning.

4.2.8.4: Pulse/Echo Testing

Pulse echo readings were taken on both specimens over time. The pulse echo testing apparatus sends a pulse through the concrete and a frequency measurement is read across two points. The purpose of the pulse echo testing was to detect cracking beneath the surface by measuring an increase in the pulse echo reading. Readings were taken at five foot increments along the length of the beam. Each Location had three different spacings at which the readings were taken: 4 in., 10 in., and 18 in. Figure 77 shows the different reading locations for the pulse echo testing.

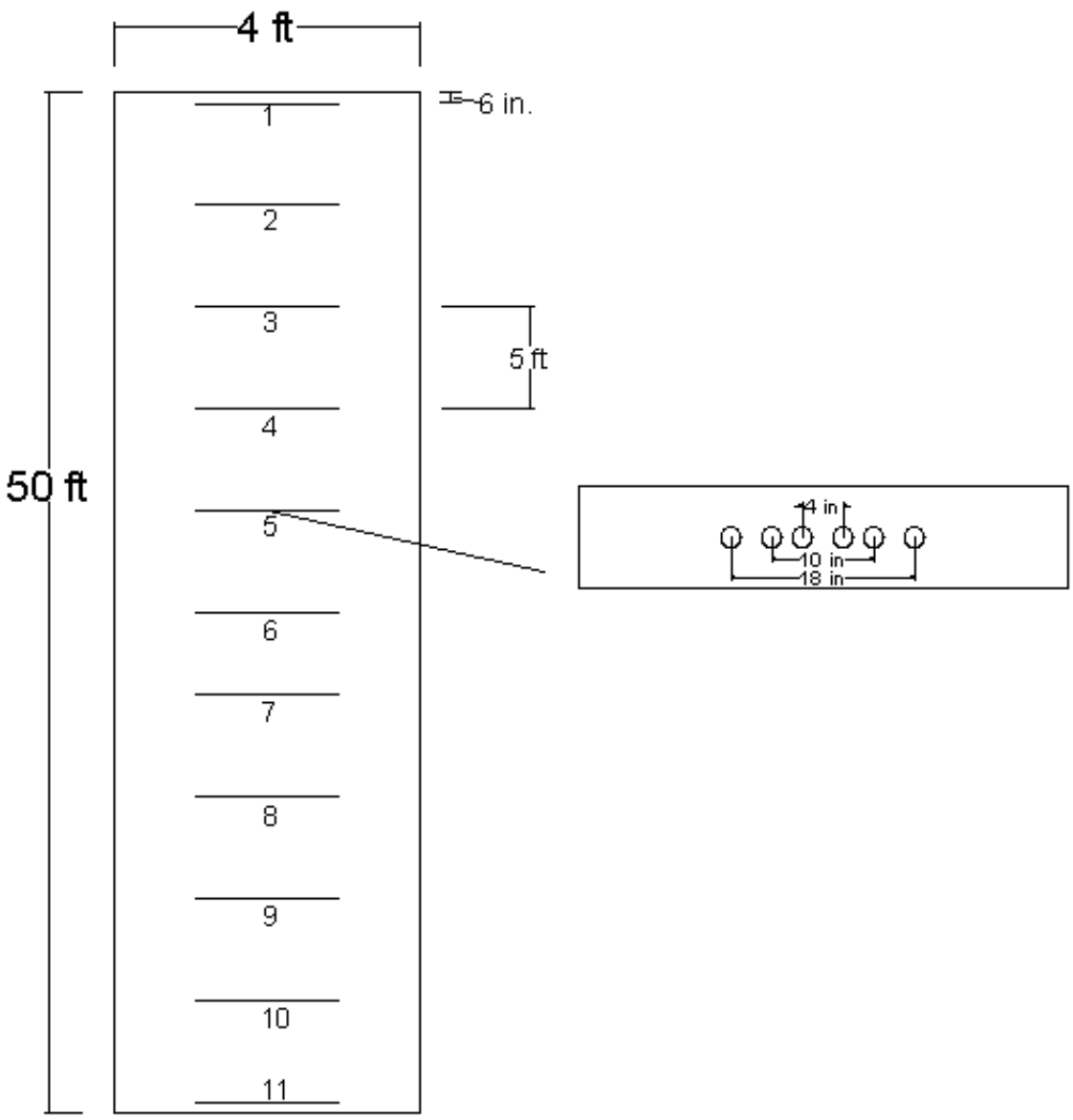

Figure 77: Pulse Echo Test Locations for both Specimens

Figure 78 shows the pulse echo testing apparatus. It consists of two censors that measure a frequency between each other.

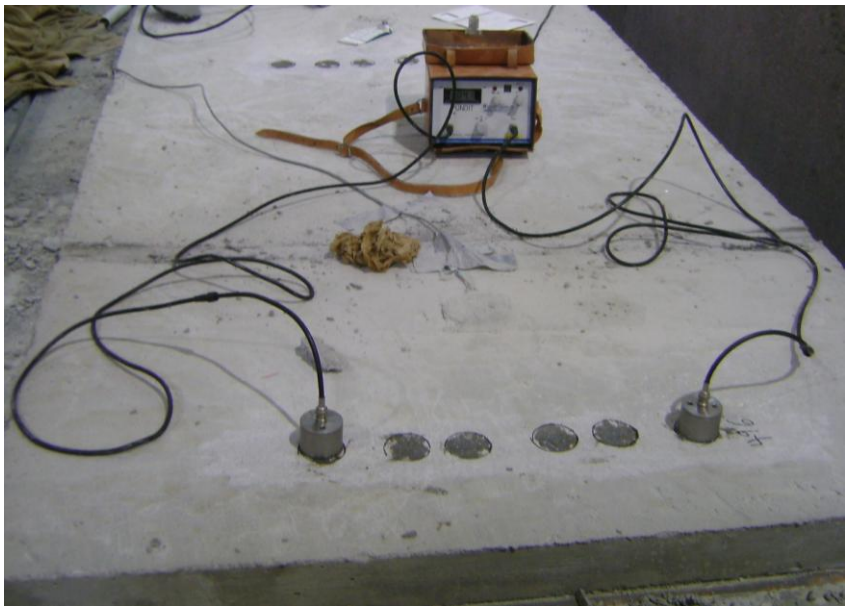

Figure 78: Testing Apparatus

The results of this testing were the least conclusive of the analysis methods for checking strain and cracks; however, the results are still summarized in the following paragraphs.

Data was collected at all eleven points along the beams for each of the three test locations. (Each location is a different spacing.)

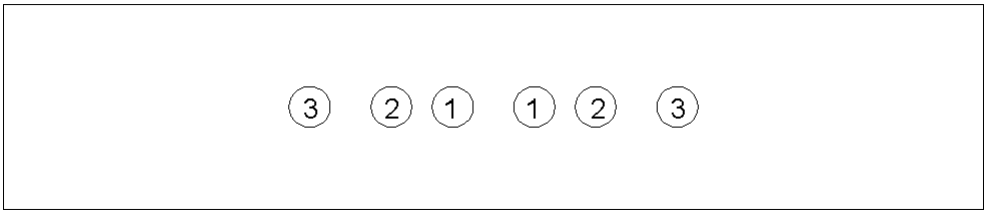

Figure 79: Three Test Locations

Location 1 did not provide any noticeable trends. Locations 2 and 3 did show slight increases in readings over time for the specimen without DCA compared to the specimen with DCA.

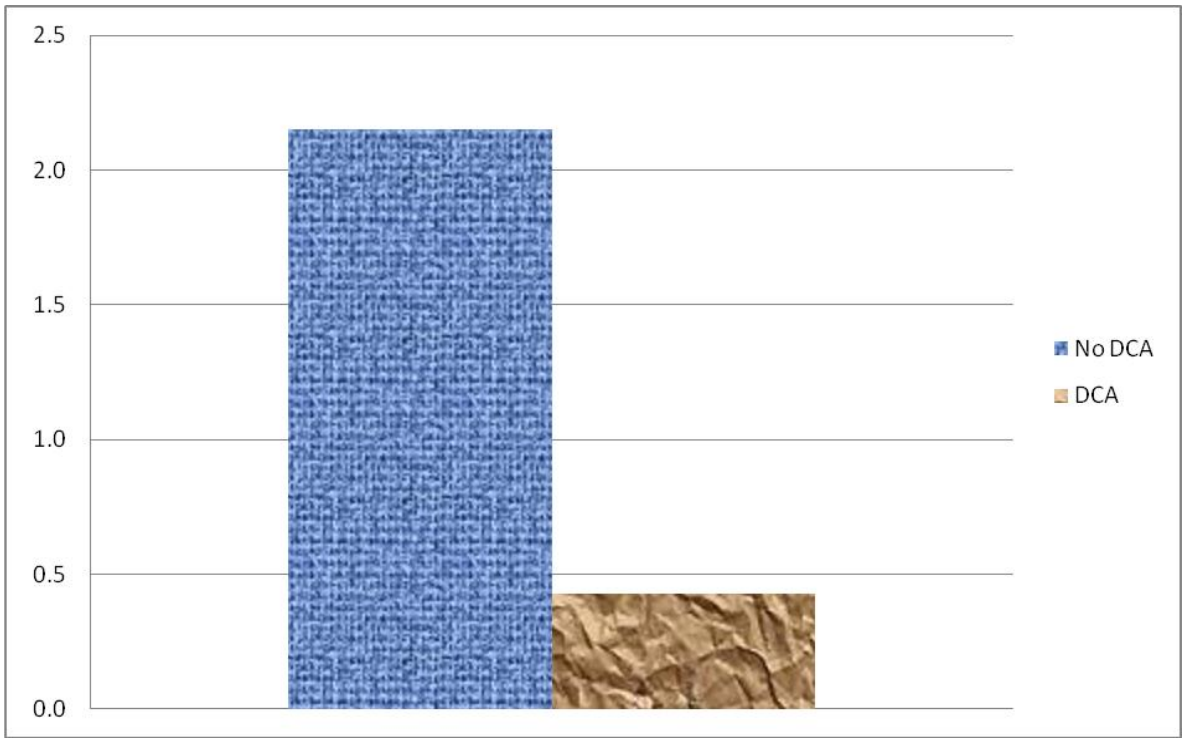

Figure 80: Average Change in Reading over Time (Location 2)

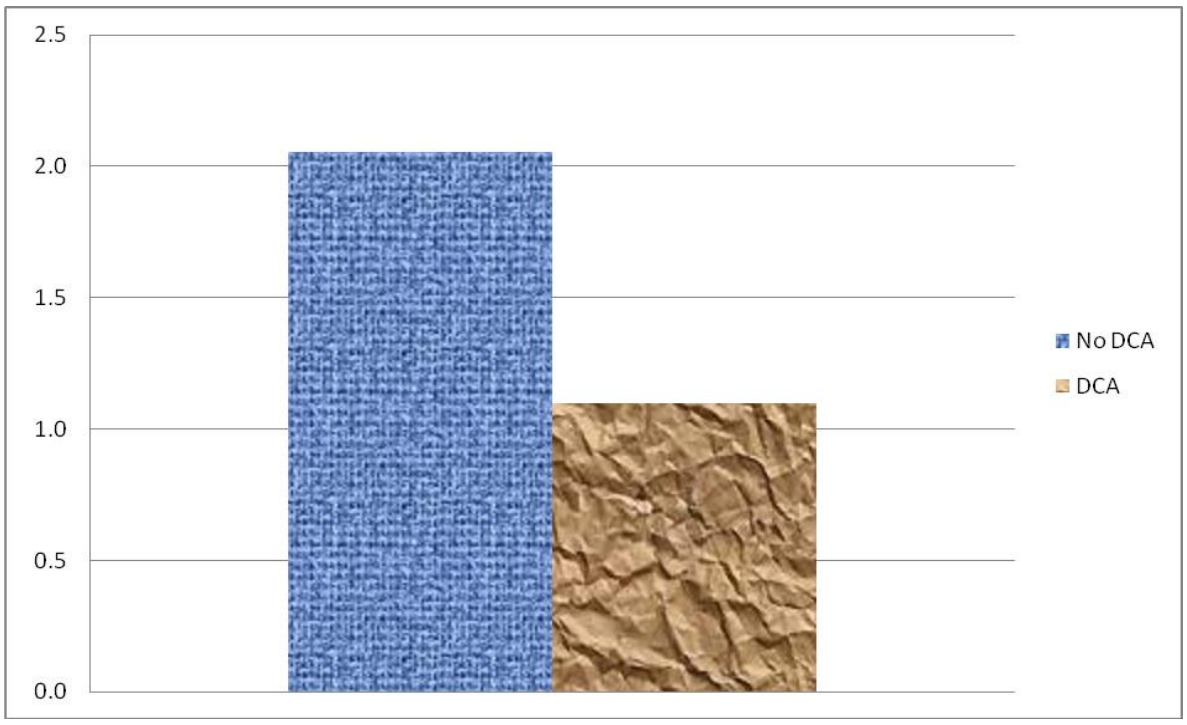

Figure 81: Average Change in Reading over Time (Location 3)

Though the change is slight, the pulse echo testing indicates that the beam without DCA had a slightly higher rate of increase in the readings than the specimen with DCA. This is what would be expected if cracks were forming beneath the surface. The pulse echo testing compares the change in reading over a 37 day period of time. These findings match the findings in the visual inspection for cracks. The specimen without DCA did experience shrinkage cracks after a longer period of time.

4.2.9. Ultimate Flexural Strength Test

After the specimens were observed and tested for cracks and strain, both were then tested for ultimate flexural capacity. If the specimens reach their calculated capacities, then composite behavior has been achieved. Ideally, the DCA specimen should achieve the same fully composite behavior as the specimen without a channel isolating it from its sheer connectors. Both specimens were tested two months after the deck pour (one month after the channel pour for the DCA specimen with post-tensioning).

The specimens were tested with a load at mid-span of the 50 ft length between simple supports. The test setup consisted of a load cell and deflection gauge at mid-span. Also, several strain gauges were attached throughout the beam.

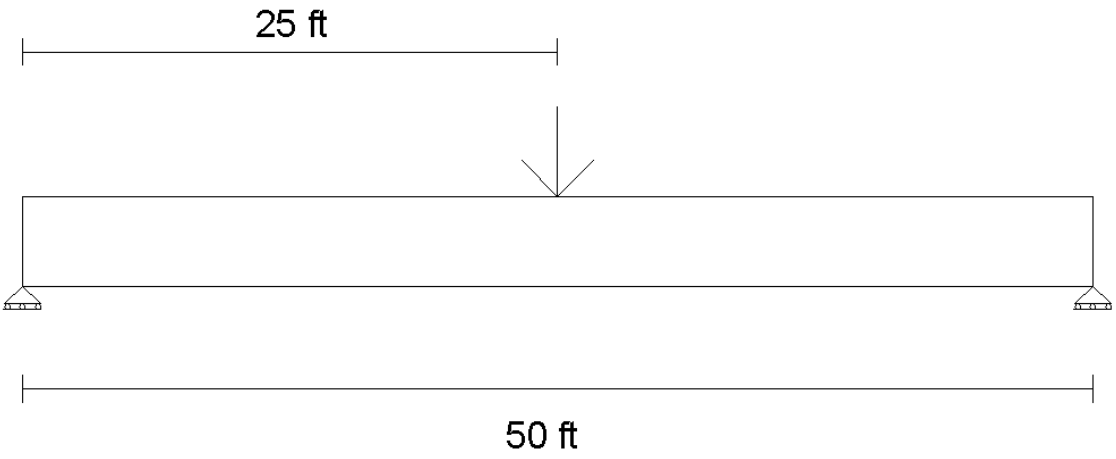

Figure 82: 50 ft Simple Span

Figure 83: Flexure Test Setup

Twelve strain gauges were attached to each specimen, placed as described earlier in the strain gauge analysis leading up to the flexural test. Several of the gauges were damaged or quit working and had to be replaced. The location of the strain gauges is shown in Figure 84.

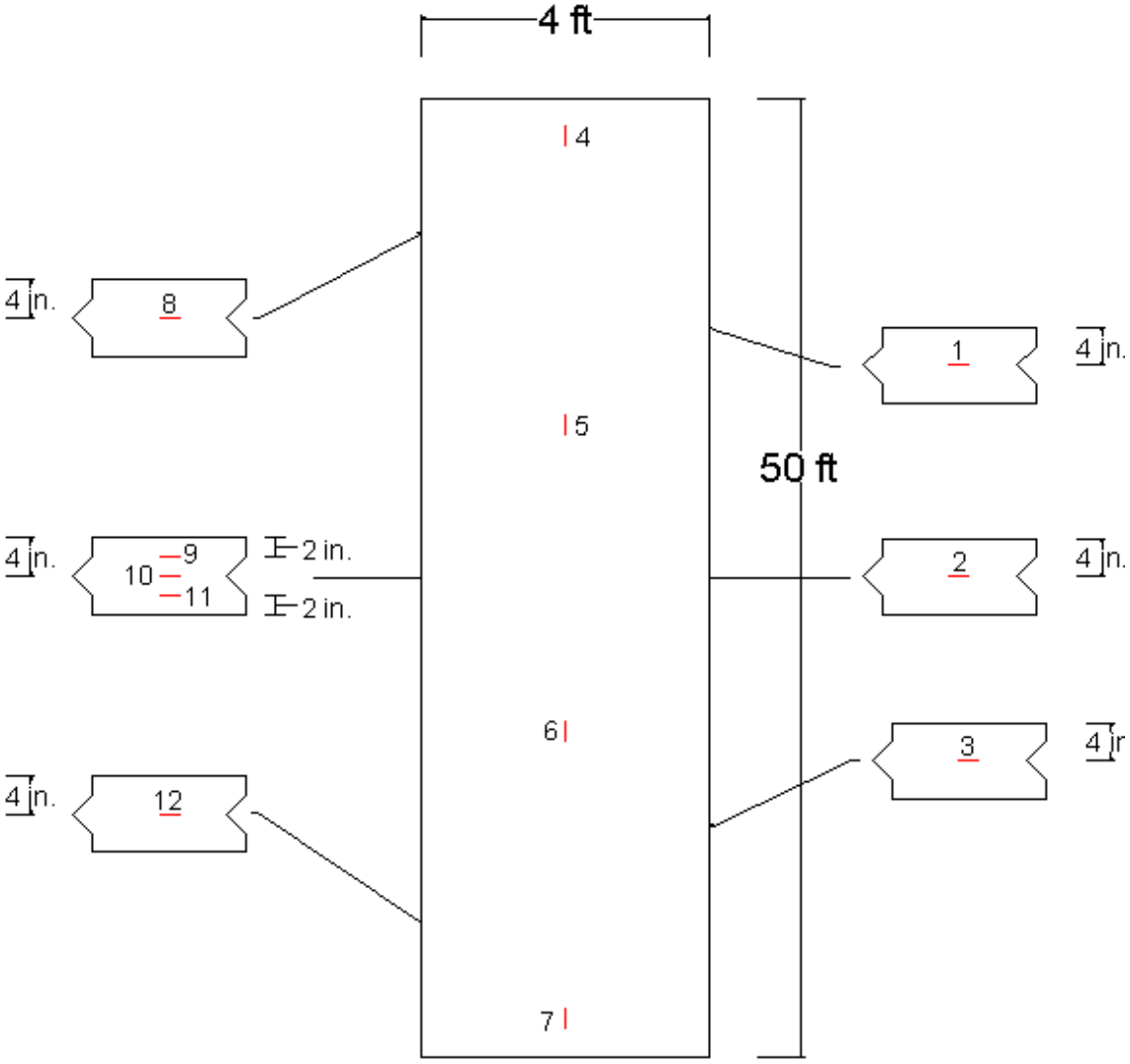

Figure 84: Location of Strain Gauges

Just as before, gauges 1-3 are located on the side of the specimen at a distance of 4 in. from the top of the 8 in. deck. Gauges 4-7 are located on top of the deck centered 2 ft from the edge. Gauges 8-12 are also located on the edge. At mid-span, three gauges were placed at 2 in. increments down the side of the deck. Gauges 8 and 12 are located 4 in. from the top of the 8 in. deck.

The beams were loaded till failure, which occurred due to compression of the deck at mid-span for both beams (See Figure 85).

Figure 85: Compression Failure at Mid-span

The beam with DCA was cut in order to examine if any separation existed between the channel and concrete deck on either side. Separation could affect composite behavior. No separation was observed and can be seen in Figure 86.

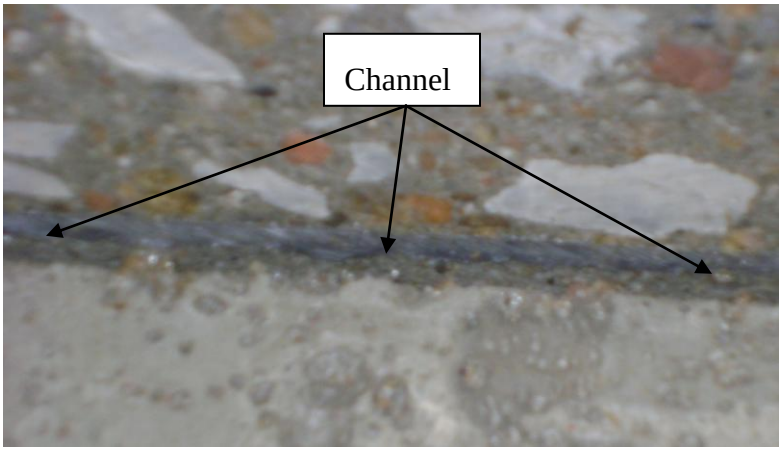

Figure 86: Channel Embedded within Concrete

No web or flange buckling was observed for either test, which is as expected. Both beams failed near their predicted failure loads. The results of the test are summarized in the next section.

4.2.10. Analysis of Test Results

Figure 87 shows the load deflection curves (at mid-span) for both the beam utilizing DCA with post-tensioning and the beam without.

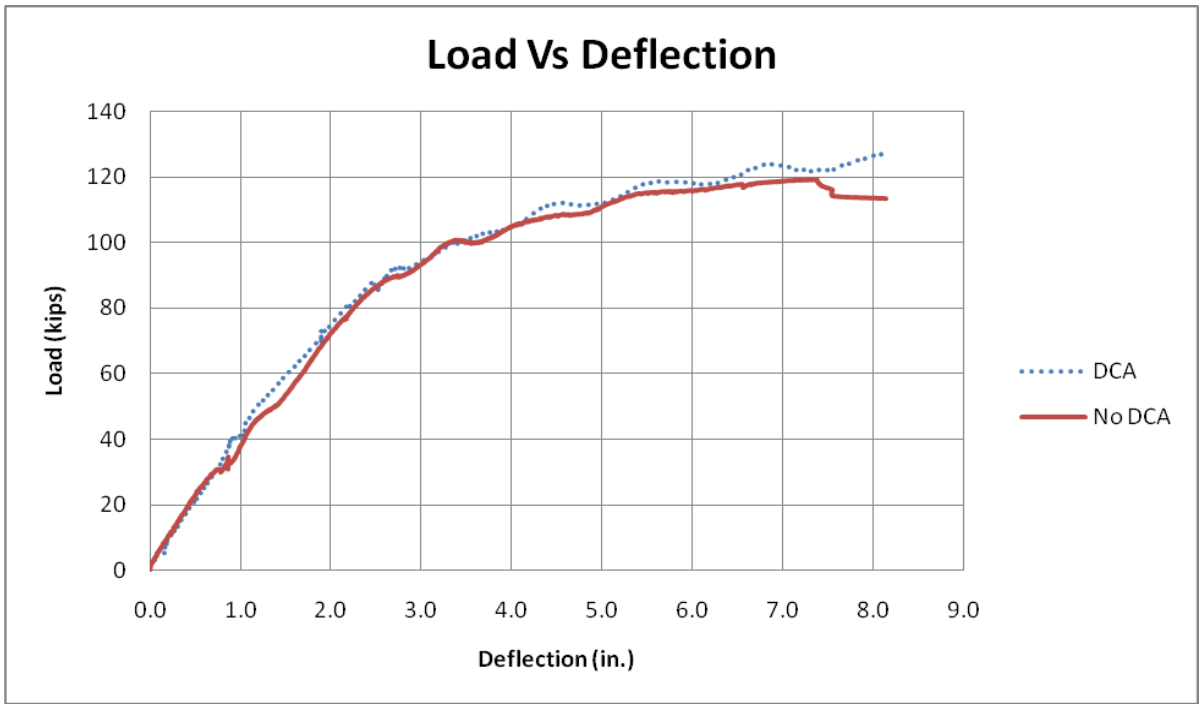

Figure 87: Load Deflection Curves

Notice that the curves are very similar, including the ultimate deflection of about 8 in. at mid-span. The load versus deflection charts for both specimens follow very similar paths, which is as expected if both beams have the same composite behavior. Table 8

shows the calculated theoretical failure loads and the tested failure loads for both specimens.

	Calculated Failure (kips)	Actual Failure (kips)
DCA Beam with PT	122	127
Beam without DCA or PT	125	120

Table 8: Theoretical and Tested Failure Loads

Both Specimens failed near their calculated capacities. Notice that the beam with DCA and post-tensioning had a slightly lower calculated failure. This is due to the effects of post-tensioning, which causes a compression force above the neutral axis and decreases its capacity.

The results of the strain gauges seem to indicate that the specimen utilizing DCA achieved composite behavior. Three strain gauges were placed on the side of the 8 in. deck at mid-span. The strains of each point along the deck are shown in Figure 88.

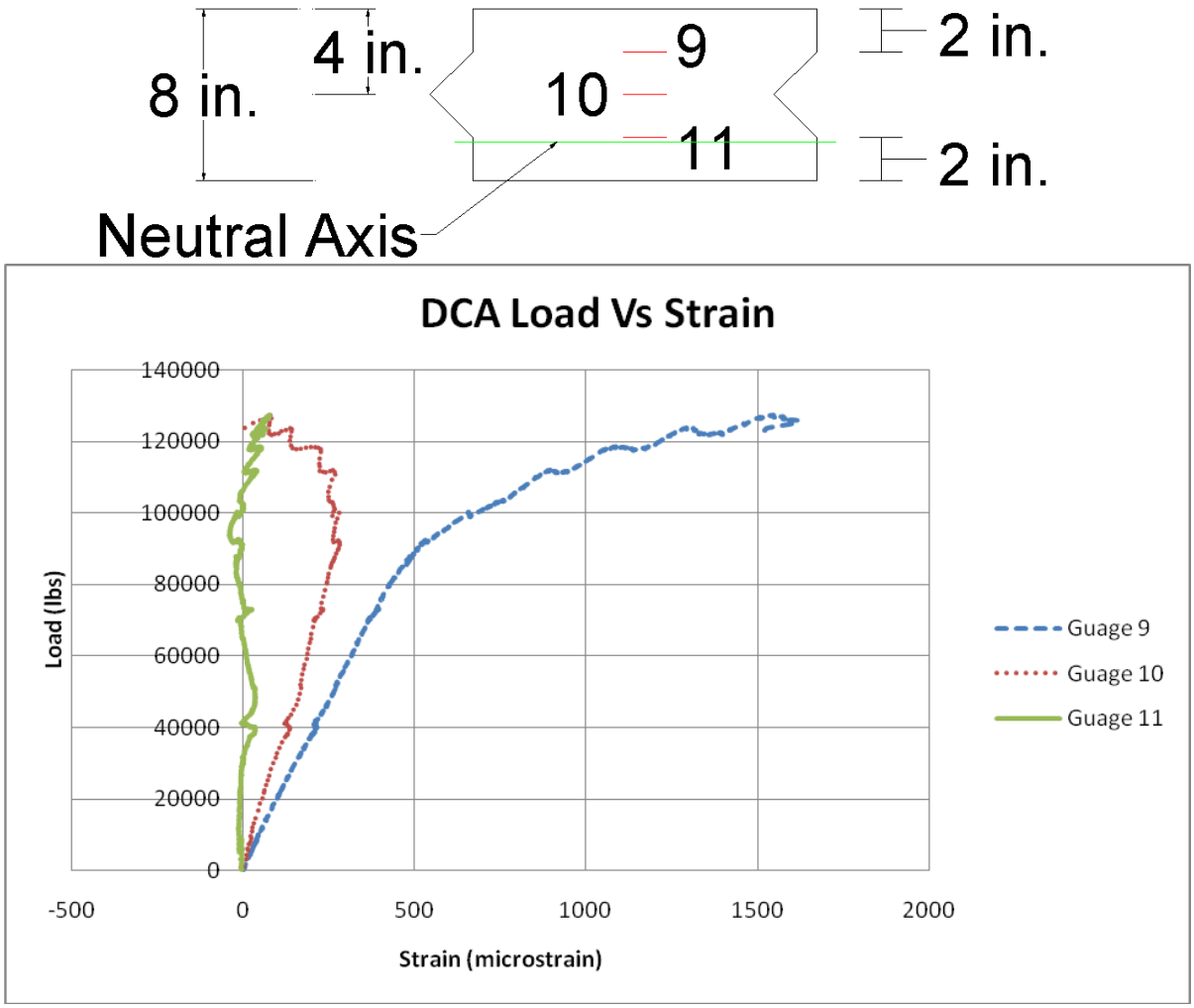

Figure 88: DCA Strain Readings at Mid-span

Gauge 9 theoretically should have the highest compressive strain as it is closest to the compression face. Gauge 10 should show compression, but less than gauge 9 as it is further from the compression face. Gauge 11, which is near the neutral axis should show little strain. This is exactly what is observed when looking at the specimen with DCA.

The results indicate that both specimens achieved fully composite behavior. The steel channel seems to have no impact on the composite action, ultimate strength, or deflection of the beams.

Chapter 5.

Analysis and Design of Complete Bridge

5.1. Overview of Design

5.1.1. Introduction

A 240 ft long two span bridge was designed using the DCA coupled with PT bridge system. The purpose of the design is to demonstrate the viability of the DCA with PT system for a larger bridge application. A cost comparison is given as well as strain and total movement of the deck due to creep, shrinkage, and temperature effects.

The bridge designed is the same section designed by the Federal Highway Administration (FHWA) in their LRFD Design Example for Steel Girder Superstructure Bridge. This section was chose to save time and effort. The main focus of the design example is the addition of the DCA with PT system and cost and strain calculations. The bridge consists of two 120 ft spans with five girders at a spacing of 9 ft 9 in., as shown in Figures 89 and 90.

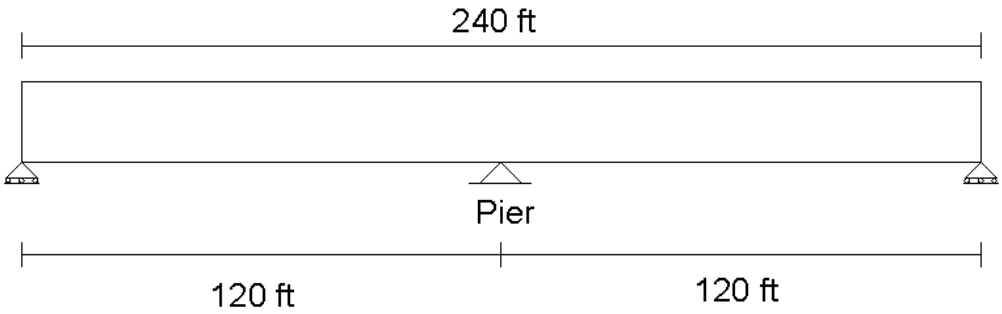

Figure 89: Two Span Bridge with Dimensions

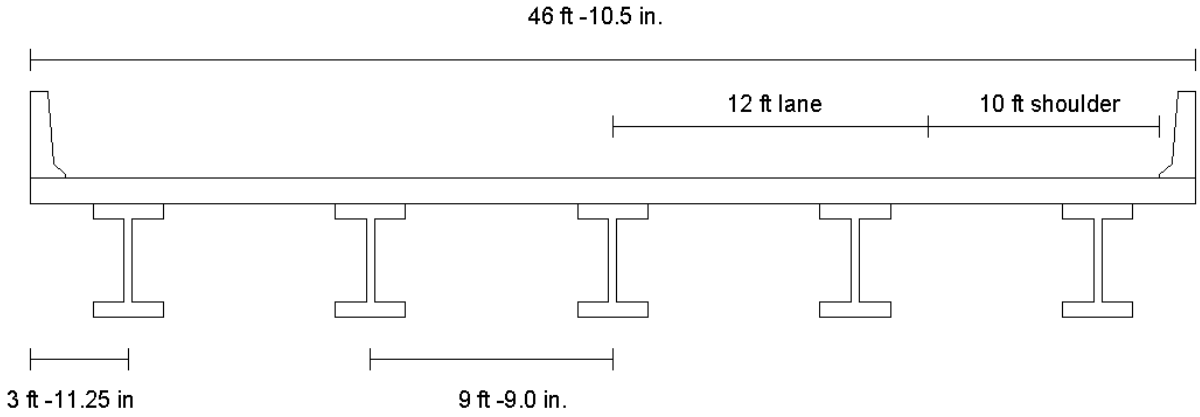

Figure 90: Bridge Width and Girder Spacings

The bridge has an 8.5 in. reinforced concrete deck. In addition to parapets and a 2 in. wearing surface, standard HL 93 live loading was used in the calculations. A girder cross section is shown in Figure 91. More detailed drawings of the cross section with dimensions are presented later.

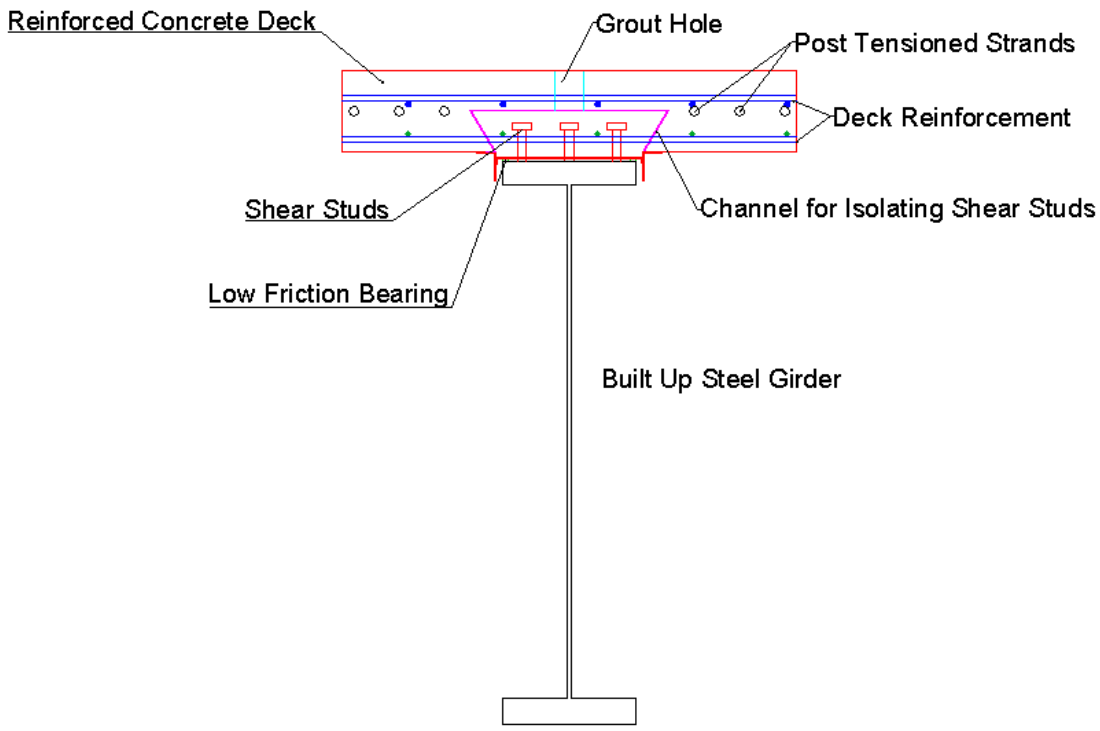

Figure 91: Bridge Cross Section

The system used is the same as that described in the full scale testing in Chapter 4. The channel allows isolating of the shear studs and movement of the deck relative to the girder through use of a low friction bearing (UHMW adhesive).

5.1.2. Deck Design

The reinforced concrete deck is 8.5 in. thick over the interior supports and 9 in. thick for the overhang. The primary reinforcement for the top and bottom layers was calculated to be # 5 at 6 in. spacing and # 5 at 8 in. spacing, respectively. At the overhang, reinforcement was identical with the exception of 2 #5 bars bundled at 6 in. rather than just one # 5 at 6 in. This is needed for the extra negative moment in the overhang.

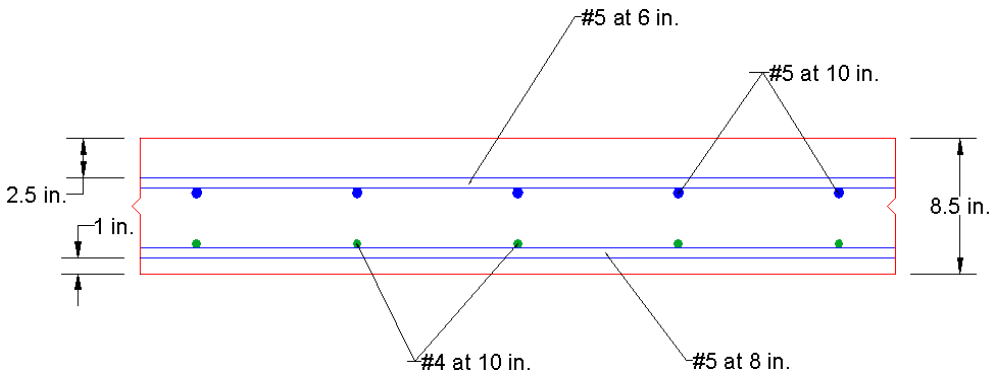

Figure 92: Deck Cross Section over Interior Span

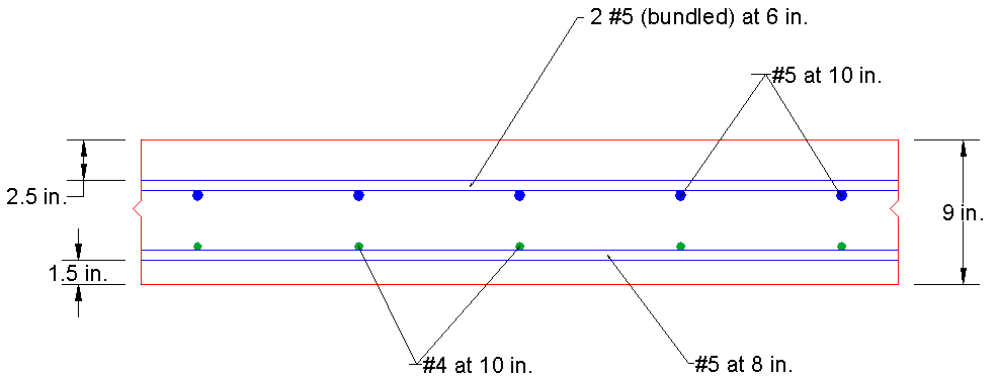

Figure 93: Deck Cross Section at Overhang

The deck cross sections do not include the post-tensioning, which will be discussed later in this chapter. Appendix B has the complete deck design calculations.

5.1.3. Girder Design

The girders were designed as built up steel sections. The complete girder design calculations can be seen in Appendix B. The girder consists of 3 plates welded to form an I girder. The web plate is 0.5 in. thick by 54 in. tall. The top and bottom flange plates are both 14 in. wide and have variable thickness over the length of the beam, as shown in Figure 94.

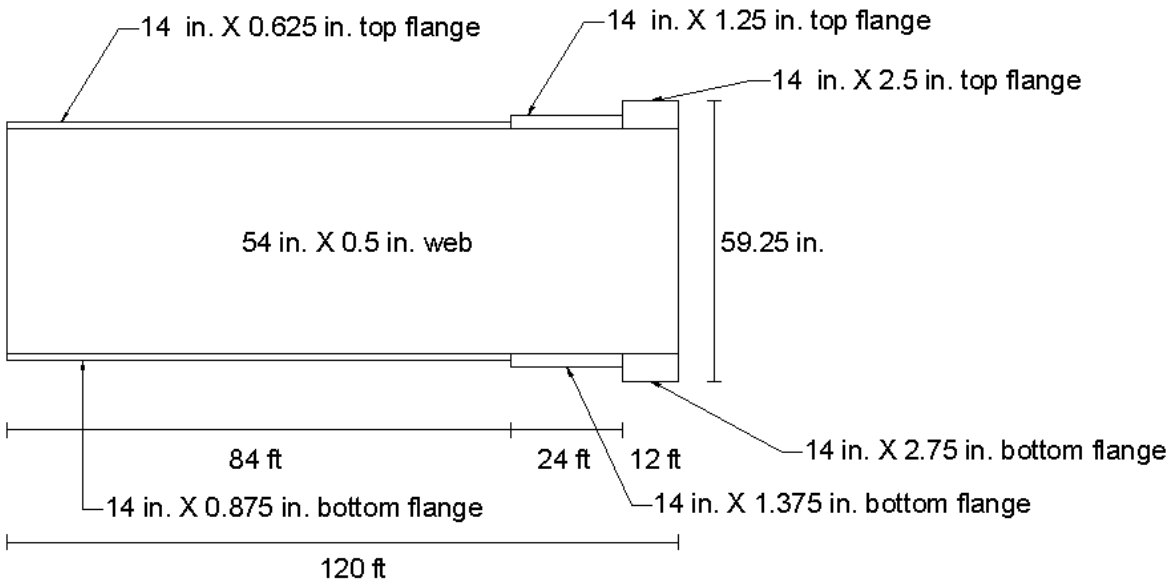

Figure 94: I Girder over the Length of the Span

The steel girder was checked for flexure, shear, and service limit at the positive and negative moment sections. These detailed calculations are shown in Appendix B. Table 9 shows the moment calculations for locations of maximum positive and negative

moment. Maximum positive moment occurs at 0.4L from the exterior support, and the location of maximum negative moment occurs over the pier.

	Dead Load	Live Load	Total Factored Moment
Maximum Moment (+)	1632.7 k-ft	1908 k-ft	5439 k-ft
Maximum Moment (-)	4161 k-ft	2450 k-ft	9621 k-ft

Table 9: Maximum Positive and Negative Moment Calculations

The maximum shear occurs at the pier and is shown in Table 10.

	Dead Load	Live Load	Total Factored Shear
Maximum Shear	150.9 k	131.4 k	423.5 k

Table 10: Maximum Shear

The stresses for Service II limits are summarized in Table 11.

	f_{botgdr}	f_{topgdr}	f_{deck}
Maximum Moment (+)	44 ksi	-23.06 ksi	-0.99 ksi
Maximum Moment (-)	-35.01 ksi	24.12 ksi	0.94 ksi

Table 11: Service II Stresses

The girder section was designed and checked to meet all the requirements listed in Tables 9-11. Table 12 shows the nominal flexural resistance compared to the required moment strength and shows the stress limit of $0.95F_{yf}$ compared to the stresses at the top and bottom of the girder at maximum positive moment (0.4L). Maximum shear occurs at the location of the pier.

ϕMn	Mu	$.95F_{yf}$	f_{botgdr}	f_{topgdr}
5970 k-ft	5439 k-ft	47.5 ksi	44 ksi	-23.1 ksi

Table 12: Moment and service Limit Calculations at Maximum Positive Moment

The calculations at maximum negative moment are summarized in Table 13.

ϕFn	F_{max}	F_{yw}	f_{cw}	ϕVn	Vu
50 ksi	48.84 ksi	50 ksi	-32.3 ksi	430.7 k	423 k

Table 13: Flexure, Service Limit, and Shear Calculations

Notice that the ultimate moment capacity was not used to check the girder in flexure. Because the section was not compact and the neutral axis was in the web, the flexural resistance of the girder at maximum negative moment was calculated considering lateral torsional buckling. The service limit for this case is $f_{cw} \leq F_{yw}$. Shear was not adequate without stiffeners. The shear capacity in Table 13 includes transverse intermediate stiffeners spaced at 80 in. See Appendix B for the shear capacity with stiffeners calculations.

Figure 95 shows the complete cross section at mid-span for the bridge complete with reinforcement details and dimensions.

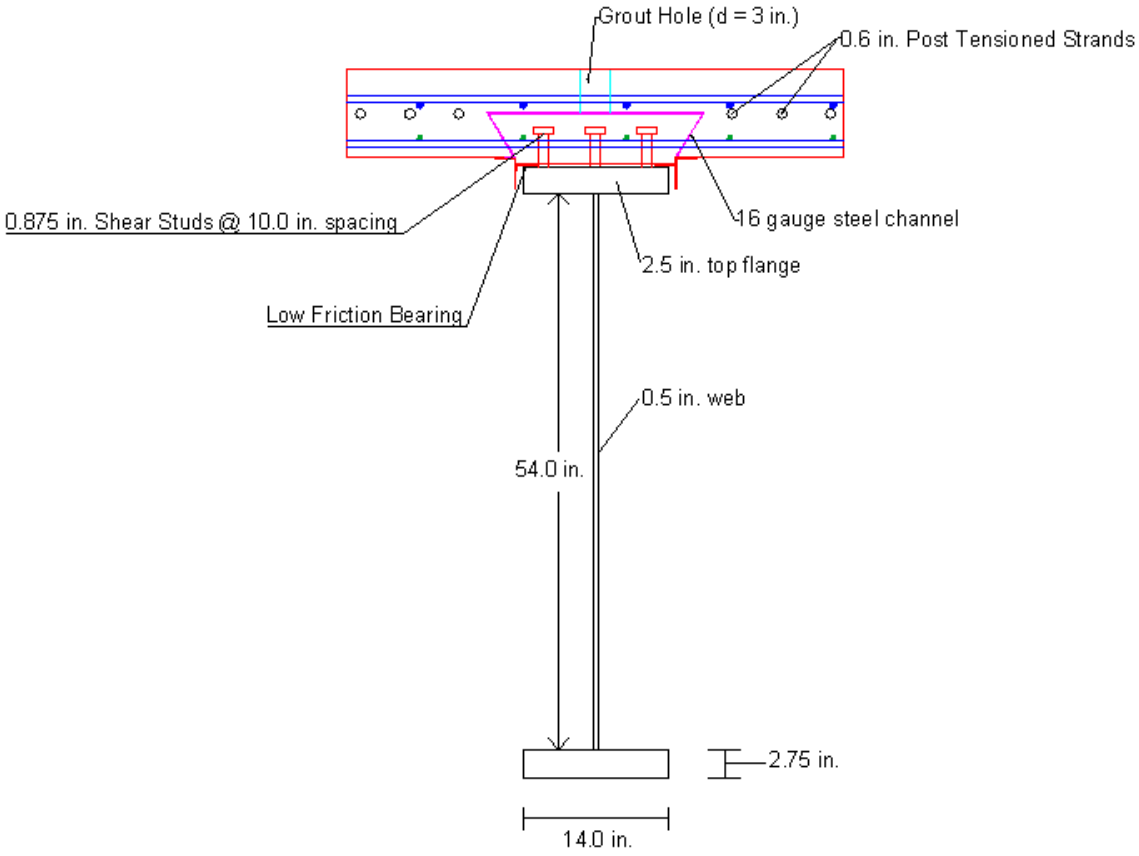

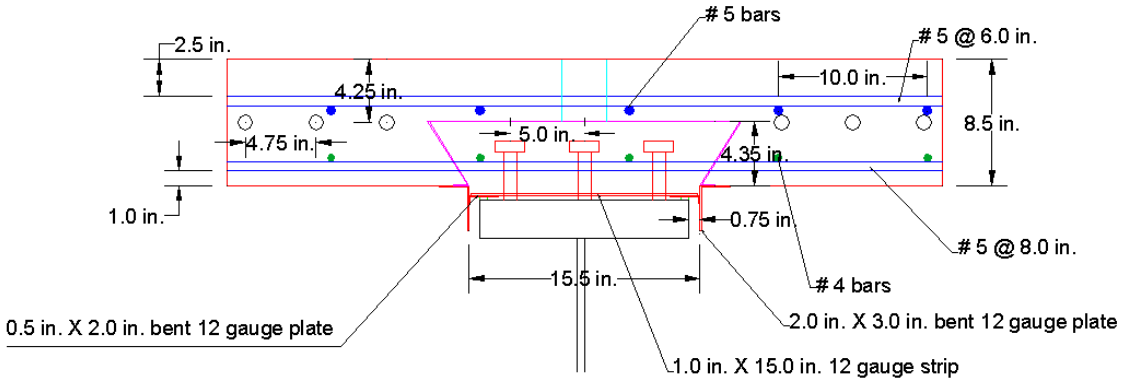

Figure 95: Complete Cross Section at Mid-span

5.2. Post-tensioning Calculations

The bridge utilizes post-tensioning in the deck. The number of 0.6 in. strands required was calculated based on making the stress at the top of the deck after live load equal to zero or in compression. Twelve strands were required by this calculation. The goal of the post-tensioning is to have permanent compression in the deck to prevent cracking even after the initial creep and shrinkage strain have occurred without composite action to the girder. Appendix B has the post-tensioning calculations. Figure 96 shows two girders with the 12 post-tensioned strands spaced between the girders in the deck.

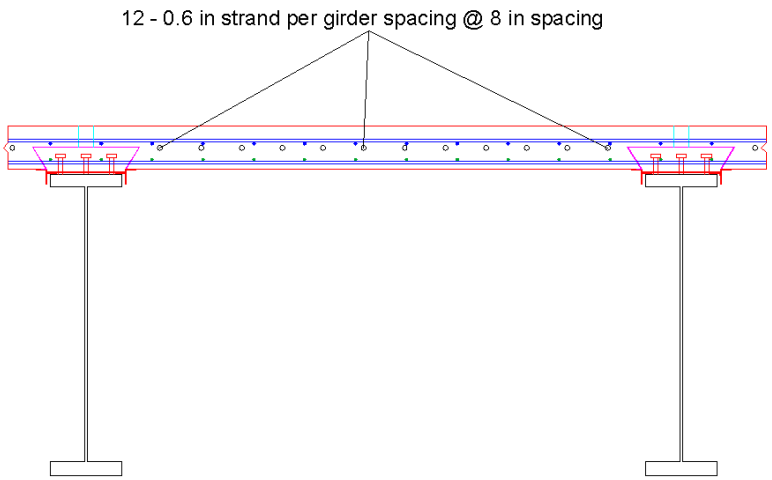

Figure 96: Post-tensioned Strands Spaced Between Girders

5.3. Cost Comparison

Use of the delayed composite action coupled with post-tensioning bridge deck system introduces new expenses into the cost of a bridge. These expenses are due to the following:

- Low friction bearing material
- Steel Channel for isolating the shear studs
- Post-tensioning
- Increased labor

Based on the cost of the materials for testing done at University of Nebraska on a 50 ft girder, cost analysis was done for the 240 ft two span bridge described in this chapter. Labor was not included in the analysis as it is very hard to estimate for a new construction process. The increase in cost of materials per square ft of bridge is shown in Table 14.

Material	Cost per ft^2
Low Friction Bearing	0.15
Steel Channel	0.52
Post-tensioning (12 strands per girder)	0.54
Total	$1.20

Table 14: Increase in Cost of Materials

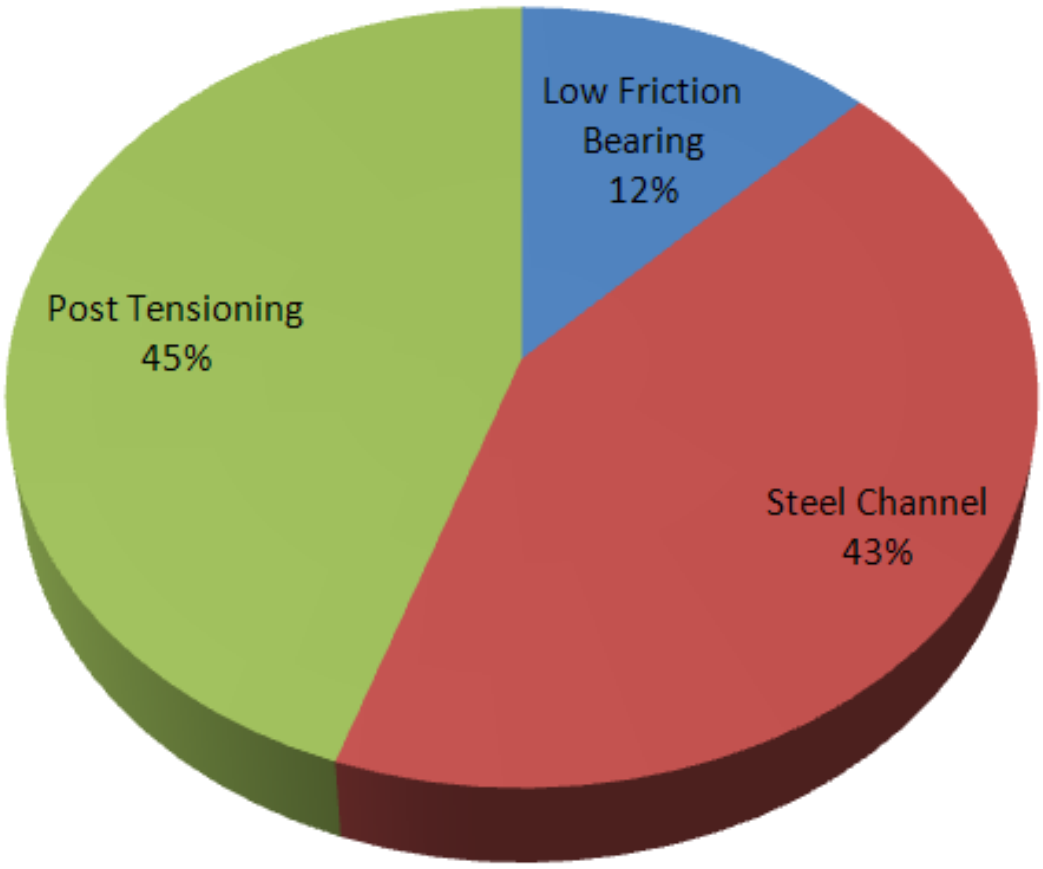

Figure 97: Cost of Additional Materials

As can be seen in Figure 97, the primary contributors to the increase in cost of the DCA system are the steel channel for isolating the shear studs and the post tensioning. The low friction bearing material was the least expensive of the additional materials for the DCA with PT bridge deck system.

Chapter 6.
Conclusions

The delayed composite action with post-tensioning bridge deck system performed as expected. The system was effective in allowing movement of deck relative to the girder and reducing creep and shrinkage cracks. This was demonstrated through several methods of analysis. The system responded as expected to the post-tensioning. The permanent compression force on the deck should eliminate cracking due to tensile stresses from early creep, shrinkage, and temperature effects, as well as later during the life of the bridge.

The steel channel did not prevent full composite behavior of the deck with the girder. The specimen with DCA and PT exceeded the expected capacity assuming full composite behavior. In addition to effectively delaying composite behavior and allowing movement of the deck relative to the girder to avoid tensile stress from creep, shrinkage, and temperature effects the specimen suffered no loss in capacity. The test specimen with DCA and PT demonstrated nearly identical load deflection behavior compared to the specimen of identical parameters without DCA and PT.

Use of the system for a larger full scale bridge is also feasible. The amount of strain and movement that is allowed in the deck prior to bonding to the girder is considerable. This should reduce cracking due to creep, shrinkage, and temperature effects which is in fact the desired effect of the system.

Use of the DCA with PT bridge system does increase the overall cost of the bridge. The cost analysis shows an increase of $1.20 per square ft of bridge. Most of this cost comes from the steel channel and post tensioning. This does not include any increase in labor for a new construction method of a cast-in-place bridge deck.

The system is effective at eliminating cracks from creep, shrinkage, and temperature effect early in the life of the concrete deck, while the strength of the concrete is still low. Once the channel is grouted, the system (as demonstrated by test results) behaves exactly as a bridge system without DCA and PT. Research of this bridge system shows promise at being a viable option for in-field bridge applications.

References

AASHTO. "AASHTO LRFD Bridge Design Specifications." 3rd Edition, Washington D.C., 2010.

ACI Committee 318. “Building Code Requirements for Structural (ACI 318-08).” American Concrete Institute, 2008.

American Institute of Steel Construction. “Steel Construction Manual (13th Edition).” 2008.

Azizinamini, Atorod, Aaron Yakel. “Steel Bridge System with Delayed Composite Action” National Bridge Research Organization, (2003).

Federal Highway Administration, “LRFD Design Example for Steel Girder Superstructure Bridge” FHWA 2003

Kitagawa, Hiragi, Watanabe, Tachibana, and Ushijima: Push-over shear test on Post Rigid (PR) Studs, The 55th Annual Conference of Japan Society of Civil Engineers (I), September 2000 (in Japanese).

Medberry, S.B., and Shahrooz, B.M. (2002), "Perfobond Shear Connector for Composite Construction," Engineering Journal, AISC, Vol. 39, No. 1, pp. 2-12.

Nawy, Edward. *Prestressed Concrete: A Fundamental Approach (5th Edition)* Prentice Hall, 2009.

Oguejiofor, E.C. and Hosain, M.U. (1992), "Perfobond Rib Connectors for Composite Beams", Composite Construction in Steel and Concrete II, Proceedings, pp. 883-898.

Precast/Prestressed Concrete Institute. “PCI Design Handbook (7th Edition).” 2010.

Price, K.D., Cassity, P.A., and Azizinamini, A. (2000), "The Nebraska High Performance Steel Two-Box Girder System," Proceedings - Steel Bridge Design and Construction for the New Millennium with emphasis on High Performance Steel, Baltimore, Maryland, November, pp. 120-137, 2000.

Slutter, R.G., and Driscoll, G.C. (1965), "Flexural Strength of Steel-Concrete Composite Beams," Journal of the Structural Division, ASCE, 91, ST2 (April), 1965.

Sudo, Hiragi, Kurita, Watanabe, Tachibana, and Kitagawa: Physical property tests on Time-setting resin mortar used for composite systems, The 55th Annual Conference of Japan Society of Civil Engineers (I), September 2000 (in Japanese).

Sun, Tadros, Lafferty, and Fallaha, “High Performance Precast Concrete Bridge Deck System for the Skyline Bridge,” CBC (2004).

Tachibana, Hiragi, Watanabe, and Kitagawa: Outline of Shiratori-bridge, a Post Rigid System (PR System) bridge, The 55th Annual Conference of Japan Society of Civil Engineers (I), September 2000 (in Japanese).

Tadros, Maher and Baishya, Mantu, “Rapid Replacement of Bridge Decks,” NCHRP Report 407, (1998).

Appendix A: Single Span 50 ft Bridge Calculations

Given:

- 50 ft single span steel girder bridge
- Grade 50 ksi steel beam
- Deck concrete f'c = 4 ksi (tested as 6 ksi)
- 8 inch deck
- Full composite behavior
- AASHTO HL 93 standard truck and lane loads
- Interior Girder

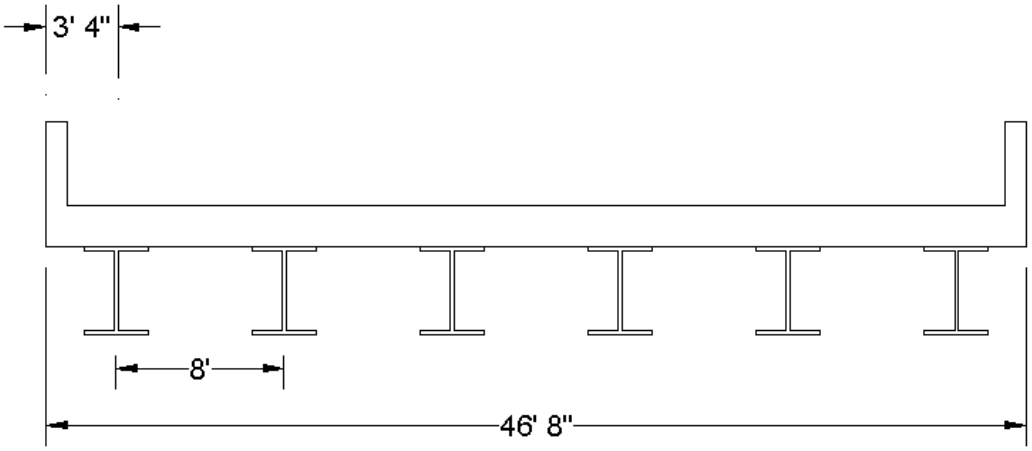

Check the shear and moment capacity of a <u>W18X86</u> against the required shear and moment capacities.

<u>Dead Load</u>

Girder weight: $w = .086\ k/ft$ $\quad M(girder) = \frac{.086\,(50)^2}{8} = 26.9\ k-ft$

$$V(girder) = \frac{.086(50)}{2} = 2.2k$$

Deck weight: $w = 8\left(\frac{8}{12}\right)(.150) = 0.8\ k/ft$ $\quad M(deck) = \frac{.8(50)^2}{8} = 250\ k-ft$

$$V(girder) = \frac{.8(50)}{2} = 20k$$

Live Load

Lane Load: 0.64k/ft

Maximum moment is at midspan, Maximum shear at supports

$$M(Lane\ Load) = \frac{.64(50)^2}{8} = 200\ k - ft$$

$$V(Lane\ Load) = \frac{.64(50)}{2} = 16k$$

Truck Load

Maximum moment occurs when loaded as shown.

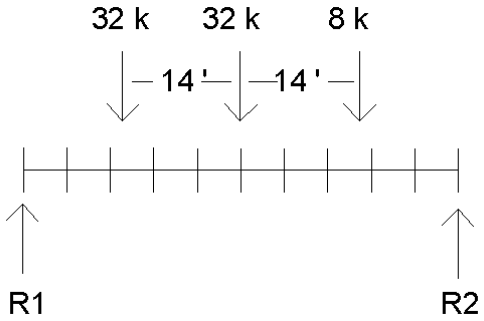

Calculate Reactions R1 and R2.

$$R1(50) = 8(11) + 32(25) + 32(39) \qquad R1 = 42.72\ k \qquad R2 = 29.28\ k$$

$$M(truck\ load) = 42.72(25) - 32(14) = 620\ k - ft$$

Maximum shear occurs when loaded as shown.

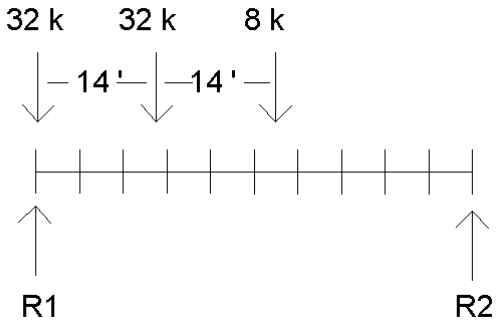

Calculate Reactions R1 and R2.

$R1(50) = 32(50) + 32(36) + 8(22)$ $R1 = 58.56\ k$ $R2 = 13.44\ k$

$V(truck\ load) = 58.56\ k$

These values were verified with a stuctural analyses software program.

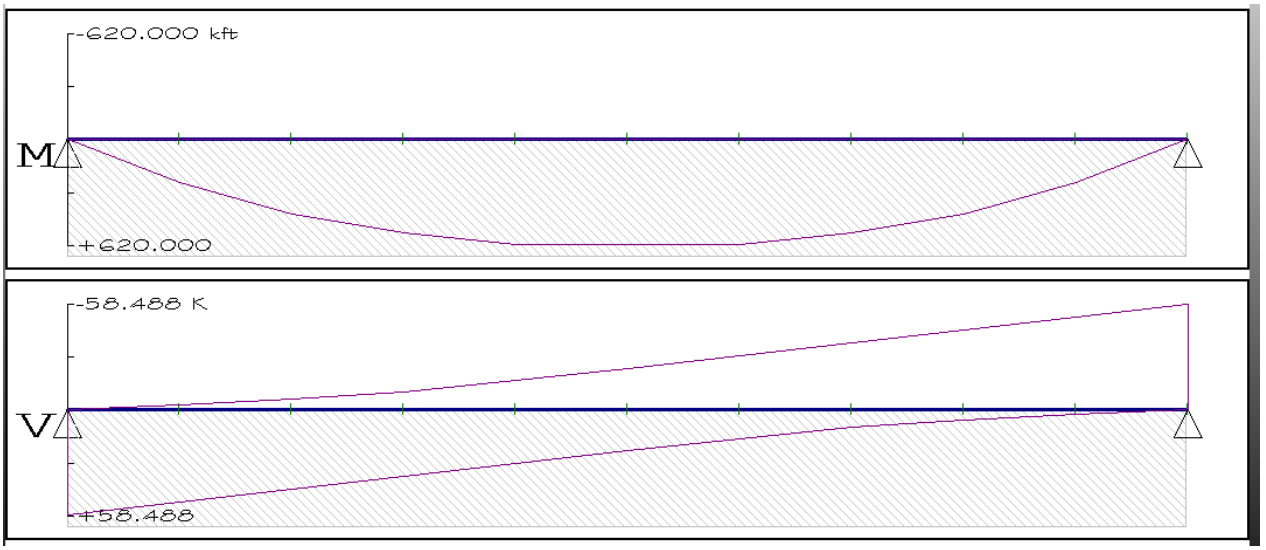

Total Moment and Shear Values

Moment

Total undistributed Live Load:

Impact Factor: 1.33

$$M(Live\ Load) = 200 + 1.33(620) = 1025k - ft$$

Moment Distribution Factors

1 Lane Loaded: $DF_1 = .06 + \left(\frac{S}{14}\right)^{0.4}\left(\frac{S}{L}\right)^{0.3}\left(\frac{k_g}{12Lt_s^3}\right)^{0.1}$

S = 8 ft (girder spacing)

L = 50 ft (span)

t_s= 8 in (depth of deck)

$k_g = n(I + Ae_g^2)$ $\quad n = \frac{E_{steel}}{E_{deck}} = \frac{29000}{3834} = 7.56$ $\quad I = 1530in^4$ $\quad A = 25.3in^2$

$$e_g = \frac{18.4}{2} + 4 = 13.2\ in$$

$$k_g = n\left(I + Ae_g^2\right) = 7.56[1530 + 25.3(13.2)^2] = 44914$$

$$DF_1 = .06 + \left(\frac{8}{14}\right)^{0.4}\left(\frac{8}{50}\right)^{0.3}\left(\frac{44914}{12(50)(8)^3}\right)^{0.1} = .441$$

2 Lanes Loaded: $DF_2 = .075 + \left(\frac{S}{9.5}\right)^{0.6}\left(\frac{S}{L}\right)^{0.2}\left(\frac{k_g}{12Lt_s^3}\right)^{0.1}$

$$DF_2 = .075 + \left(\frac{8}{9.5}\right)^{0.6}\left(\frac{8}{50}\right)^{0.2}\left(\frac{44914}{12(50)(8)^3}\right)^{0.1} = .591$$ **Controls**

Distributed Live Load: $M(LL) = 0.591(1025) = 605\ k - ft$

Total Moment: $1.25(DL) + 1.75(LL) = 1.25(277) + 1.75(605) = 1406k - ft$

Shear

Total undistributed Live Load:

$$V(Live\ Load) = 16 + 1.33(58.6) = 94\ k$$

Shear Distribution Factors

$$DF_1 = .36 + \frac{S}{25} = .36 + \frac{8}{25} = .68$$

$$DF_2 = .2 + \frac{S}{12} + \left(\frac{S}{35}\right)^2 = .2 + \frac{8}{12} + \left(\frac{8}{35}\right)^2 = .919$$

DF2 controls

Distributed Live Load

$$V(LL) = 0.919(94) = 86.4\ k$$

Total shear: $1.25(22.2) + 1.75(86.4) = 179$ k

Calculate Moment Capacity of section

Sum Moments about top: Check if entire steel girder is in tension

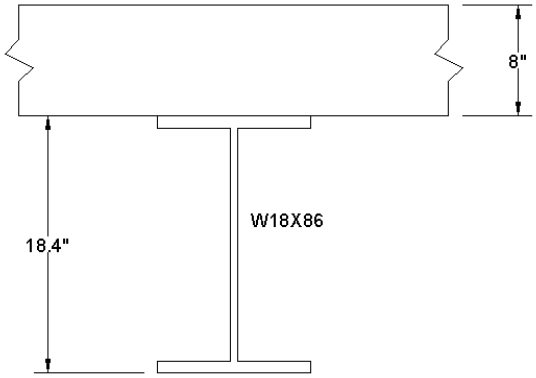

Specimen with no DCA:

Calculate a:

$$T = C \qquad 50(25.3) = .85(6.9)(48)(a) \quad a = 4.49\ in \qquad \Phi = 1$$

$$\Phi M_n = -.85(6.9)(4.49)(48)\left(\frac{4.49}{2}\right) + 25.3(50)(9.2 + 8) = 18920.3k - in = 1577k - ft$$

1577 k-ft > 1406 k-ft OK

Failure Load: P=2(1577k-ft /25.125 ft) = 125.5 k

DCA Specimen Including Effects of Post-tensioning:

Calculate a:

$$T = C \qquad 50(25.3) = .85(6.9)(48)(a) \quad a = 4.49\ in \qquad \Phi = 1$$

$$\Phi M_n = -.85(6.9)(4.49)(48)\left(\frac{4.49}{2}\right) + 25.3(50)(9.2+8) - 4(0.8)(202.5)(.217)(4) = 18357.8\ k-in = 1530\ k-ft$$

1530k-ft > 1406 k-ft OK

Failure Load: P=2(1530k-ft /25.125 ft) = 121.8 k

Shear Capacity: From AISC Table 3-6, Vn for a W18X86 is 265 k.

ΦVn =0.9(265) = 238 k > 179 k OK

Calculation of Shear Studs (AASHTO)

Factored resistance of shear connectors: $Q_r = \Phi_{sc} Q_n \qquad \Phi_{sc} = .85$

$$Q_n = 0.5 A_{sc} \sqrt{(f'c E_c)} \leq A_{sc} F_u$$

Use 7/8“ diameter shear connectors.

$$A_{sc} = \frac{\pi\left(\frac{7}{8}\right)^2}{4} = .601\ in^2$$

f’c = 4 ksi (tested as 6 ksi)

E_c = 4696 ksi

F_u =60 ksi

$Q_n = 0.5(.601)\sqrt{[(6)(4696)]} = 50.44\ \text{k} > .601(60) = 36.08$ Use Q_n = 36.08 k

$Q_r = .85(36.08) = 30.67\ k$

Calculate # of shear connectors: $n = \frac{V_h}{Q_r}$

V_h is the lesser of the following: $V_h = .85f'c(b)t_s$ or

$V_h = F_{yw}Dt_w + F_{yt}b_t t_t + F_{yc}b_f t_f = F_y A$

b= min of the following:

1) Span/4: $\frac{50}{4} = 12.25\ ft = 150\ in$
2) 12 times the average slab thickness plus the greater of the web thickness or one half the width of the top flange of the girder: $12(8) + \frac{11.1}{2} = 101.55\ in$
3) Average girder spacing: **8 ft= 96 in. Controls**

t_s =8 in

F_y = 50 ksi

A=25.3 in^2

$V_h = .85(6)(96)(8) = 3916\ k$ or $V_h = 50(25.3) = 1265\ k$ **Use 1265 k**

$$n = \frac{1265}{30.67} = \mathbf{42}$$

Use 1 stud @ 1 ft spacing. **50 studs**

Minimum length: $4\left(\frac{7}{8}\right) = 3.5\ in$ **Use 4 in. length**

Appendix B: Two Span 240 ft Bridge Calculations

Deck Calculations

Deck Design

Load Assumptions

$K := 1000lb$

$kcf := \frac{K}{ft^3}$

Deck Width:	$w_{deck} := 46.875ft$
Roadway Width:	$w_{raodway} := 44ft$
Bridge Length:	$L_{total} := 240ft$
Steel Yield Strength:	$F_y := 50ksi$
Steel Tensile Strength:	$F_u := 60ksi$
Concrete Strength (28 days):	$f_c := 4ksi$
Rebar Strength:	$f_y := 60ksi$
Steel Density:	$W_s := .490kcf$
Concrete Density:	$W_c := .150kcf$
Parapet Weight (one)	$W_{par} := .530\frac{K}{ft}$
Future Wearing Surface Weight	$W_{fws} := .140kcf$
FWS thickness	$t_{fws} := 2.5in$
Deck Thickness:	$t_s := 8in$
Girder Spacing:	$S := 9.75ft$
Number of Girders:	$N := 5$
Deck top Cover:	$Cover_t := 2.5in$
Deck Bottom Cover:	$Cover_b := 1in$

Use of structural analysis program give unfactored dead load moment shown below

The maximum positive dead load moment occurs at 0.4S. The unfactored values are shown in the table below.

	Unfactored (+) Moment (k-ft)
Slab	0.38
Parapet	0.19
FWS	0.09

The maximum negative dead load moment occurs over the girder. The unfactored values are shown in the table below.

	Unfactored (-) Moment (k-ft)
Slab	-0.74
Parapet	-1.66
FWS	-0.06

Use of Table S A4.1-1 give unfactored live load moment shown below

	Max Moment (k-ft)
Positive LL	6.74
Negative LL	-6.65

Factored Positive Moment Using Table S A4.1-1

Dynamic Load Allowance: $IM := 0.33$

LL factor: $\gamma_{LL} := 1.75$

$Mu_{posLL} := \gamma_{LL} \cdot 6.74 \frac{K \cdot ft}{ft}$ $\quad Mu_{posLL} = 11.795 K \cdot \frac{ft}{ft}$

$Mu_{posDL} := 1.25\left(.38 \frac{K \cdot ft}{ft}\right) + 1.25\left(.19 \cdot \frac{K \cdot ft}{ft}\right) + 1.5\left(.09 \cdot \frac{K \cdot ft}{ft}\right) = 0.847 K \cdot \frac{ft}{ft}$

$Mu_{posTotal} := Mu_{posLL} + Mu_{posDL} = 12.642 K \cdot \frac{ft}{ft}$

Factored Negative Moment Using Table S A4.1-1

$Mu_{negLL} := \gamma_{LL} \cdot -6.65 K \cdot \frac{ft}{ft} = -11.638 K \cdot \frac{ft}{ft}$

$Mu_{negDL} := 1.25\left(-.74 \frac{K \cdot ft}{ft}\right) + 1.25\left(-1.66 \frac{K \cdot ft}{ft}\right) + 1.5\left(-.06 \cdot \frac{K \cdot ft}{ft}\right) = -3.09 K \cdot \frac{ft}{ft}$

$Mu_{negTotal} := Mu_{negLL} + Mu_{negDL} = -14.728 K \cdot \frac{ft}{ft}$

Deck Reinforcement for Positive Flexure

Assume #5 bars

$d_e := t_s - Cover_b - \frac{.625 in}{2} = 6.687 in$

$\phi_f := 0.9$

$b := 12 in$

$R_n := \frac{Mu_{posTotal} \cdot 12 in}{\phi_f \cdot b \cdot d_e^{\,2}} = 0.314 \frac{K}{in^2}$

$\rho := .85 \cdot \left(\frac{f_c}{f_y}\right) \cdot \left[1 - \sqrt{1 - \frac{2 \cdot (.314)}{.85 \times 4}}\right] = 5.5 \times 10^{-3}$

$$A_s := \rho \cdot \frac{b}{ft} \cdot d_e = 0.441 \cdot \frac{in^2}{ft}$$

$$bar_{srequired} := \frac{.31in^2}{A_s} = 8.428\,in$$

Use 8 inch spacing: $bar_{spacing} := 8in$

Check max reinforcement limit

$$a := \frac{.31in^2 \cdot f_y}{.85 \cdot f_c \cdot bar_{spacing}} = 0.684\,in \qquad c := \frac{a}{.85} = 0.804\,in$$

$\frac{c}{d_e} = 0.12$ which is less than .42. Design is OK

Deck Reinforcement for Negative Flexure

$$d_{eneg} := t_s - Cover_t - \frac{.625in}{2} = 5.188\,in \qquad t_s := 8.5in$$

$$R_{nneg} := \frac{-Mu_{negTotal} \cdot 12in}{\phi_f \cdot b \cdot d_{eneg}^2} = 0.608 \frac{K}{in^2}$$

$$\rho := .85 \cdot \left(\frac{f_c}{f_y}\right) \cdot \left[1 - \sqrt{1 - \frac{2 \cdot (.505)}{.85 \cdot 4}}\right] = 9.156 \times 10^{-3}$$

$$A_s := \rho \cdot \frac{b}{ft} \cdot d_{eneg} = 0.57 \cdot \frac{in^2}{ft}$$

$$bar_{srequired} := \frac{.31in^2}{A_s} = 6.526\,in$$

Use 6 inch spacing: $bar_{spacing} := 6in$

Check max reinforcement limit

$$a := \frac{.31in^2 \cdot f_y}{.85 \cdot f_c \cdot bar_{spacing}} = 0.912\,in \qquad c := \frac{a}{.85} = 1.073\,in$$

$\frac{c}{d_{eneg}} = 0.207$ which is less than .42. Design is OK

Overhang Negative moment Reinforcement

$R_n := .76\frac{K}{in^2}$ $d_e := 6.19in$

$\rho := .85\cdot\left(\frac{f_c}{f_y}\right)\cdot\left[1-\sqrt{1-\frac{2\cdot(.76)}{.85\times 4}}\right] = 0.015$

$A_s := \rho\cdot\frac{b}{ft}\cdot d_e = 1.079\frac{in^2}{ft}$

Use 2 #5 bars bundled at 6 inch spacing.

$A_s := 2\cdot.31in^2\cdot\frac{12in}{6in} = 1.24in^2$

Longitudinal Reinforcement

Bottom Reinforcement

$S_e := 9.25\ ft$

$A_{sbot\%} := \frac{220}{\sqrt{S_e}}$ $A_{sbot\%} = 72.336$ must be < 67%

Use: $A_{sbot} := .67$

$As_{ft} := .31in^2\cdot\frac{12in}{8in} = 0.465in^2$

$As_{bot} := As_{ft}\cdot.67 = 0.312in^2$

$As_{botspacing} := \frac{.31in^2}{\frac{As_{bot}}{ft}} = 11.94in$

Use: #5 bars at 10 inch spacing for bottom longitudinal reinforcement.

Top Reinforcement

$$A_s \geq .11 \frac{A_g}{f_y}$$

$$A_g := 8.5in \cdot \left(12 \frac{in}{ft} \right) = 102 \cdot \frac{in^2}{ft}$$

$$0.11 \cdot \frac{A_g}{60} = 0.187 \cdot \frac{in^2}{ft}$$

$$A_{sreq} := \frac{.187 \frac{in^2}{ft}}{2} = 0.094 \frac{in^2}{ft}$$

Use #4 bars at 10 in spacing

$$As_{top} := .2in^2 \cdot \frac{12in}{10in} = 0.24 in^2$$

Deck Reinforcement Summary

Top

Primary: #5 bars at 6 in spacing

Longitudinal: #5 bars at 10 in spacing

Overhang: 2 #5 bars bundled at 6 in spacing

Bottom

Primary: #5 bars at 8 in spacing

Longitudinal: #4 bars at 10 in spacing

Girder Calculations

Girder Design (Interior Beam)

$K := 1000lb$

$kcf := \frac{K}{ft^3}$

$ksf := \frac{K}{ft^2}$

$ksi := 1\frac{K}{in^2}$

Load Assumptions

Number of Spans:	$N_{spans} := 2$
Span Length:	$L_{span} := 120ft$
Number of Girders:	$N_{girders} := 5$
Girder Spacing:	$S := 9.75ft$
Deck Overhang:	$S_{overhang} := 3.9675ft$
Cross Frame Spacing	$L_b := 20ft$
Web Yield Strength:	$F_{yw} := 50ksi$
Flange Yield Strength:	$F_{wf} := 50ksi$
Concrete Strength (28 days):	$f_c := 4ksi$
Rebar Strength:	$f_y := 60ksi$
Total Deck Thickness	$t_{deck} := 8.5in$
Effective Deck Thickness	$t_{effdeck} := 8.0in$
Total Overhang Thickness	$t_{overhang} := 9.0in$
Effective Overhang Thickness	$t_{effoverhang} := 8.5in$
Steel Density	$W_s := .490kcf$
Concrete Density	$W_c := .150kcf$
Additional DL per Girder	$W_{misc} := .015\frac{K}{ft}$
Stay-in-Place deck form weight	$W_{deckforms} := .015ksf$
Parapet Weight (each)	$W_{par} := 0.53\frac{K}{ft}$
Future Wearing Surface Weight	$W_{fws} := 0.14kcf$
Future Wearing Surface Thickness	$t_{fws} := 2.5in$
Deck Width	$w_{deck} := 46.875ft$

Roadway Width $w_{roadway} := 44.0ft$

Haunch Depth (from top of web) $dhuanch := 3.5in$

Average Daily Truck Traffic (Single Lane) $ADTT_{SL} := 300$

Section Properties

Interior Beam

Effective flange width is smallest of these three: $Span_{eff} := 60ft$

1) $W_{eff1} := \frac{Span_{eff}}{4} = 15 \cdot ft$

2) $W_{eff2} := 12 t_{effdeck} + \frac{14in}{2} = 8.583 ft$ Controls

3) $W_{eff3} := S = 9.75 ft$

Area of longitudinal deck reinforcement in negative moment region

$$A_{deckreinf} := 2 \cdot .31 in^2 \cdot \frac{W_{eff2}}{5in} = 12.772 in^2$$

Positive Moment Section Properties in Table Below

Section	Area (in^2)	Centroid (in)	Io (in^4)	Itotal (in^4)
Girder	48	25.85	6562	22115
Composite Girder	48	25.85	22115	51907.2
Total Composite Section	151	50.8	22664	66340
	Sbotgdr (in)	**Stopgdr (in)**		
Girder	855.5	745.9		
Total Composite Section	1306.8	14010.3		

Negative Moment Section Properties in Table Below

Section	Area (in^2)	Centroid (in)	Io (in^4)	Itotal (in^4)
Girder	100.5	28.72	6604	65426.6
Composite Girder	100.5	28.72	65427	97931.2
Total Composite Section	203.5	46.7	65976	130196
	Sbotgdr (in)	**Stopgdr (in)**		
Girder	2278.2	2142.9		
Total Composite Section	2787.8	10376.2		

Dead Load Effects

$$DL_{deck} := W_c \cdot S \cdot \frac{t_{deck}}{12\frac{in}{ft}} = 1.036\frac{K}{ft}$$

$$W_{top\,flange} := 14in$$

$$DL_{deckforms} := W_{deckforms} \cdot \left| S - W_{top\,flange} \right| = 0.129\frac{K}{ft}$$

$$DL_{misc} := W_{misc} = 0.015\frac{K}{ft}$$

$$DL_{par} := W_{par} \cdot \frac{2}{N_{girders}} = 0.212\frac{K}{ft}$$

$$DL_{fws} := \frac{W_{fws} \cdot t_{fws} \cdot 44ft}{N_{girders}} = 0.257\frac{K}{ft}$$

Use of Structural analysis program to calculate unfactored DL moments and shears

Span 1 is Symmetrical to Span 2

Dead Load Contribution	Max Positive Moment (k-ft)	Max Negative Moment (k-ft)
Steel Girder	150.3	-421.5
Deck and Haunch	928.6	-2418.3
Other DL on Girder	136.7	-357.1
Parapets	192.2	-436.1
Future Wearing Surface	232.7	-528.2

Dead Load Contribution	**Max Shear at Pier (kips)**
Steel Girder	-16.84
Deck and Haunch	-85.18
Other DL on Girder	-12.65
Parapets	-16.36
Future Wearing Surface	-19.82

Live Load Effects

Calculate longitudinal stiffness parameter at 3 locations

$$K_g = n\left(I + A \cdot e_g^{\,2}\right)$$

	1 (max positive M)	**2 (Intermediate)**	**3 (Pier)**	**Average**
Length (ft)	84	24	12	
n	8	8	8	
I (in^4)	22115	34640	65427	
A (in^2)	48	63.75	100.5	
eg (in)	36.52	35.28	35.53	
Kg (in^4)	689147	911796	1538481	818611

Calculate distribution factors for 1 and 2 lane loadings

$K_g := 81861$

$t_s := t_{deck}$

$$g_{int\_moment\_1} = .06 + \left(\frac{S}{14}\right)^{.4}\left(\frac{S}{L}\right)^{0.3}\left(\frac{K_g}{12L \cdot t_s^{\,3}}\right)^{.1}$$

$$g_{int\_moment\_1} := .06 + \left(\frac{9.75}{14}\right)^{.4}\left(\frac{9.75}{120}\right)^{0.3}\left[\frac{818611}{12 \cdot 120 \cdot (8)^3}\right]^{.1} = 0.472$$

$$g_{int\_moment\_2} = .075 + \left(\frac{S}{9.5}\right)^{.6}\left(\frac{S}{L}\right)^{0.2}\left(\frac{K_g}{12L \cdot t_s^{\,3}}\right)^{.1}$$

$$g_{int\_moment\_2} := .075 + \left(\frac{9.75}{9.5}\right)^{.6}\left(\frac{9.75}{120}\right)^{0.2}\left[\frac{818611}{12 \cdot 120 \cdot (8)^3}\right]^{.1} = 0.696$$

$$g_{int\_shear\_1} = .36 + \frac{S}{25}$$

$$g_{int\_shear\_1} := .36 + \frac{9.75}{25} = 0.75$$

$$g_{int\_shear\_2} = .2 + \frac{S}{12} - \left(\frac{S}{35}\right)^2$$

$$g_{int\_shear\_2} := .2 + \frac{9.75}{12} - \left(\frac{9.75}{35}\right)^2 = 0.935$$

Use of Structural analysis program to calculate unfactored LL moments and shears

Span 1 is Symmetrical to Span 2

Live Load	
Max Positive Moment	1908 k-ft
Max Negative Moment	-2450 k-ft
Max Positive Shear	110.5 kips
Max Negative Shear	-131.4 kips

Total Factored Moment

Maximum Positive Moment at 0.4L

$M_{DC} := 150K\cdot ft + 922.4K\cdot ft + 135.8K\cdot ft + 192.2K\cdot ft = 1.4\times 10^{3}\cdot K\cdot ft$

$M_{DW} := 232.7K\cdot ft$

$M_{LL} := 1908K\cdot ft$

$M_{Total} := 1.25\cdot M_{DC} + 1.5\cdot M_{DW} + 1.75\cdot M_{LL} = 5.439\times 10^{3}\cdot K\cdot ft$

Stress Due to Positive Moment at 0.4L

Noncomposite Dead Load

$M_{noncompDL} := 150K\cdot ft + 922.4K\cdot ft + 135.8K\cdot ft = 1.208\times 10^{3}\cdot K\cdot ft$

$S_{top} := 745.9in^{3}$

$f_{noncomDL} := \frac{-M_{noncompDL}}{S_{top}} = -19.437ksi$

Parapet Dead Load (Composite)

$M_{parapet} := 192.2K\cdot ft$

$S_{top} := 3398.4in^{3}$

$f_{parapet} := \frac{-M_{parapet}}{S_{top}} = -0.679ksi$

Future Wearing Surface Dead Load (Composite)

$M_{fws} := 232.7K\cdot ft$

$S_{top} := 3398.4in^{3}$

$f_{fws} := \frac{-M_{fws}}{S_{top}} = -0.822ksi$

Live Load and Dynamic Load Allowance

$M_{LL} := 1908\,K\cdot ft$

$S_{top} := 14010.3\,in^3$

$f_{LL} := \frac{-M_{LL}}{S_{top}} = -1.634\,ksi$

Total

$f_{Str} := 1.25 f_{noncomDL} + 1.25 f_{parapet} + 1.5 f_{fws} + 1.75 f_{LL} = -29.238\,ksi$

Shear, moment, and stress calculations are summarized below at maximum positive moment, maximum negative moment, and maximum shear

Maximum Positive Moment

Factored Limit State	Moment (k-ft)	fbotgdr (ksi)	f topgdr (ksi)
Strength I	5439	57.77	-29.24
Service II	4114	44	-23.06

Maximum Negative Moment

Factored Limit State	Moment (k-ft)	fbotgdr (ksi)	f topgdr (ksi)
Strength I	-9621	-48.84	44.99
Service II	-7346	-35.01	24.12

Maximum Shear

Factored Limit State	Shear (kips)
Strength I	423.5
Service II	321.7

Check Section Proportion limits, Plastic Moment Capacity, Nominal Flexural Resistance Flexure Service Limit, and Shear

Positive Moment Region

Proportion Limits

1) $0.1 \le \frac{I_{yc}}{I_y} \le 0.9$ $\quad I_{yc} := \frac{0.625in \cdot (14in)^3}{12} = 142.917in^4$

$$I_y := \frac{0.625in \cdot (14in)^3}{12} + \frac{54in \cdot \left(\frac{1}{2}in\right)^3}{12} + \frac{.875in \cdot (14in)^3}{12} = 343.562in^4$$

$\frac{I_{yc}}{I_y} = 0.416$ $\quad$ OK

2) Web Slenderness

$$\frac{2D_c}{t_w} \le 6.77\sqrt{\frac{E}{f_c}} \le 200$$

From Previous Calculations:

$f_{botgdr} := 57.77ksi$ $\quad f_{topgdr} := -29.24ksi$

$t_{topfl} := .625in$ $\quad D_{web} := 54in$ $\quad t_{botfl} := .875in$

$Depth_{gdr} := t_{topfl} + D_{web} + t_{botfl} = 55.5in$

$$Depth_{comp} := \frac{-f_{topgdr}}{f_{botgdr} - f_{topgdr}} Depth_{gdr} = 18.651in$$

$D_c := Depth_{comp} - t_{topfl} = 18.026in$

$t_w := \frac{1}{2}in$ $\quad E := 29000ksi$

$f_{comp} := -f_{topgdr} = 29.24ksi$

$\frac{2 \cdot D_c}{t_w} = 72.104$ $\quad 6.77\sqrt{\frac{E}{f_{comp}}} = 213.206$ $\quad$ OK

3) Flange Proportions

$b_f \geq 0.3 D_c$

$b_f := 14\,in$

$0.3 D_c = 5.408\,in$ OK

Plastic Moment Capacity

Bottom Flange (Tension Flange)

$F_{yt} := 50\,ksi$ $b_t := 14\,in$ $t_t := .875\,in$

$P_t := F_{yt} \cdot b_t \cdot t_t = 612.5\,K$

Web

$F_{yw} = 50\,ksi$ $D_w := 54\,in$ $t_w = 0.5\,in$

$P_w := F_{yw} \cdot D_w \cdot t_w = 1.35 \times 10^3 \cdot K$

Top Flange (Compression Flange)

$F_{yc} := 50\,ksi$ $b_c := 14\,in$ $t_c := .625\,in$

$P_c := F_{yc} \cdot b_c \cdot t_c = 437.5\,K$

Slab

$f_c = 4\,ksi$ $b_s := 103\,in$ $t_s := 8\,in$

$P_s := .85 \cdot f_c \cdot b_s \cdot t_s = 2.802 \times 10^3 \cdot K$

Calculate location of Neutral Axis

$$Y := t_s \cdot \frac{\left| P_c + P_w + P_t \right|}{P_s} = 6.853\,in$$

$$d_c := \frac{-t_c}{2} + 3.5\,in + t_s - Y = 4.334\,in$$

$$d_w := \frac{D_w}{2} + 3.5\,in + t_s - Y = 31.647\,in$$

$$d_t := \frac{t_t}{2} + D_w + 3.5\,in + t_s - Y = 59.084\,in$$

$$M_p := \frac{Y^2 \cdot P_s}{2 t_s} + \left| P_c \cdot d_c + P_w \cdot d_w + P_t \cdot d_t \right| = 7.419 \times 10^3 \cdot K \cdot ft$$

Nominal Flexural Resistance

$M_n = 1.3 R_h \cdot M_y$

$R_h := 1$ The same steel is used for the web, top, and bottom flanges

$$F_y = \frac{M_{D1}}{S_{NC}} + \frac{M_{D2}}{S_{LT}} + \frac{M_{AD}}{S_{ST}}$$

$M_y = M_{d1} + M_{D2} + M_{AD}$ $F_y := 50\,ksi$

$M_{D1} := 1.25 \cdot 1208\,K \cdot ft = 1.51 \times 10^3 \cdot K \cdot ft$

$M_{D2} := 1.25 \cdot 192\,K \cdot ft + 1.5 \cdot 233\,K \cdot ft = 589.5\,K \cdot ft$

Bottom Flange:

$S_{NC} := 855.5\,in^3$ $S_{LT} := 1192.7\,in^3$ $S_{ST} := 1306.8\,in^3$

$$M_{AD} := S_{ST} \cdot \left(F_y - \frac{M_{D1}}{S_{NC}} - \frac{M_{D2}}{S_{LT}} \right) = 2.493 \times 10^3 \cdot K \cdot ft$$

$M_{ybot} := M_{D1} + M_{D2} + M_{AD} = 4.592 \times 10^3 \cdot K \cdot ft$

Top Flange:

$S_{NC} := 745.9\,in^3$ $S_{LT} := 3398.4\,in^3$ $S_{ST} := 14010.3\,in^3$

$$M_{AD} := S_{ST} \cdot \left(F_y - \frac{M_{D1}}{S_{NC}} - \frac{M_{D2}}{S_{LT}} \right) = 2.758 \times 10^4 \cdot K \cdot ft$$

$M_{ybot} := M_{D1} + M_{D2} + M_{AD} = 2.968 \times 10^4 \cdot K \cdot ft$

My is the minimum of the Mybot values

$M_y := 4592\,K \cdot ft$

$M_n := 1.3 \cdot R_h \cdot M_y = 5.97 \times 10^3 \cdot K \cdot ft$

Flexure Service Limit

$f_f \le 0.95 F_{yf}$

$f_{botgdr} := 44ksi$ $f_{topgdr} := -23.06ksi$ $F_{yf} := 50ksi$

$.95 F_{yf} = 47.5ksi$ which is greater than both stress values at top and bottom

Shear

Shear is maximum at the location of the pier, and will be checked in the negative moment region calculations.

Negative Moment Region

Proportion Limits

1)

$0.1 \le \frac{I_{yc}}{I_y} \le 0.9$

$\frac{2.75in \cdot (14in)^3}{12} = 628.833in^4$

$I_y := \frac{2.75in \cdot (14in)^3}{12} + \frac{54in \cdot \left(\frac{1}{2}in\right)^3}{12} + \frac{2.5in \cdot (14in)^3}{12} = 1.201 \times 10^3 in^4$

$\frac{I_{yc}}{I_y} = 0.119$ OK

2) Web Slenderness

$$\frac{2D_c}{t_w} \le 6.77\sqrt{\frac{E}{f_c}} \le 200$$

From Previous Calculations:

$D_c := 32.668in - 2.75in = 29.918in$

$t_w := \frac{1}{2}in$ $E := 29000ksi$

$f_{comp} := 48.84ksi$

$\frac{2 \cdot D_c}{t_w} = 119.672$ $6.77 \cdot \sqrt{\frac{E}{f_{comp}}} = 164.968$ OK

3) Flange Proportions

$b_f \ge 0.3D_c$ $b_f := 14in$

$0.3D_c = 8.975in$ OK

$\frac{b_t}{2t_t} \le 12$ $t_t := 2.5in$

$\frac{b_t}{2t_t} = 2.8$ OK

Plastic Moment Capacity

Check if Section is Compact

$$\frac{2D_{cp}}{t_w} \le 3.76\sqrt{\frac{E}{F_{yc}}}$$

$D_{cp} := 38.83in$

$2\frac{D_{cp}}{t_w} = 155.32$ $3.76\sqrt{\frac{E}{F_{yc}}} = 90.553$

Section is not compact; therefore the plastic moment capacity is not used to compute the moment capacity.

Nominal Flexural Resistance

The nominal flexural resistance is calculated based on lateral torsional buckling

$F_n = R_b \cdot R_h \cdot F_{cr}$

$R_h = 1$ From previous Calculation

$\lambda_b := 4.64$ for sections where $D_c > \frac{D}{2}$

$D_c = 29.918\,in$ $f_c := 48.84\,ksi$

$D := 54.0\,in$ $\frac{D}{2} = 27\,in$

$t_w = 0.5\,in$ $\frac{2D_c}{t_w} = 119.672$

$\lambda_b \cdot \sqrt{\frac{E}{f_c}} = 113.065$

$\frac{2D_c}{t_w} \geq \lambda_b \cdot \sqrt{\frac{E}{f_c}}$ Therefore $R_b := 1$

$F_{cr} = \frac{1.904E}{\left(\frac{b_f}{2t_f}\right)^2 \cdot \sqrt{\frac{2D_c}{t_w}}} \leq F_{yc}$ $t_f := 2.75\,in$

$\frac{1.904E}{\left(\frac{b_f}{2t_f}\right)^2 \cdot \sqrt{\frac{2D_c}{t_w}}} = 779.001\,ksi$

Therefore $F_{cr} := F_{yc} = 50\,ksi$

$F_n := R_b \cdot R_h \cdot F_{cr} = 50\,ksi$ $\phi_f := 1$

$F_r := \phi_f \cdot F_n = 50\,ksi$

$50\,ksi > 48.84\,ksi$ OK

The Section is adequate for flexure in the negative moment region.

Flexure Service Limit

$$f_{cw} \le \frac{0.9E\cdot\alpha\cdot k}{\left(\frac{D}{t_w}\right)^2} \le F_{yw}$$

$\alpha := 1.25$ for webs without longitudinal stiffeners

$D := 54in$

From previous calculation:

$f_{botgdr} := -35.01ksi$ $f_{topgdr} := 24.12ksi$ $t_{botfl} := 2.75in$

$Depth_{gdr} := 59.25in$

$$Depth_{comp} := \frac{-f_{botgdr}}{f_{topgdr} - f_{botgdr}} \left| Depth_{gdr} \right| = 35.081in$$

$D_c := Depth_{comp} - t_{botfl} = 32.331in$ $t_f := 2.75in$

$$k := 9\cdot\left(\frac{D}{D_c}\right)^2 = 25.107$$ Which is greater than 7.2

$$\frac{0.9E\cdot\alpha\cdot k}{\left(\frac{D}{t_w}\right)^2} = 70.225ksi$$ Which is greater than 50 ksi. Use 50 ksi

$$f_{cw} := f_{botgdr}\cdot\left(\frac{D_c}{D_c + t_f}\right) = -32.266ksi$$ OK

Shear

$V_n = C\cdot V_p$

$k := 5$

$$\frac{D}{t_w} = 108$$

$$1.10\sqrt{\frac{E\cdot k}{F_{yw}}} = 59.237 \qquad 1.38\sqrt{\frac{E\cdot k}{F_{yw}}} = 74.315 \qquad \frac{D}{t_w} \ge 1.38\sqrt{\frac{E\cdot k}{F_{yw}}}$$

$$C := \frac{1.52}{\left(\frac{D}{t_w}\right)^2}\left(\frac{E \cdot k}{F_{yw}}\right) = 0.378$$

$V_p := .58 \cdot F_{yw} \cdot D \cdot t_w = 783 \text{ K}$

$V_n := V_p \cdot C = 295.907 \text{ K}$ $\phi_v := 1.0$

$V_r := \phi_v \cdot V_n = 295.907 \text{ K}$

$295.9 \text{K} < 423.5 \text{K}$ Therefore web stiffeners must be used

Shear Stiffener Design

$\frac{D}{t_w} \geq 150$ $\frac{D}{t_w} = 108$ Use Stiffeners

Spacing: Assume 80 in.

$$d_o \leq D \cdot \left[\frac{260}{\left(\frac{D}{t_w}\right)}\right]^2 \qquad D \cdot \left[\frac{260}{\left(\frac{D}{t_w}\right)}\right]^2 = 312.963 \text{in}$$

Use $d_o := 80 \text{in}$ $\phi_f := 1$ $F_y := 50 \text{ksi}$

$f_u \leq .75 \phi_f \cdot F_y$ $f_u := 48.84 \text{ksi}$

$.75 \phi_f \cdot F_y = 37.5 \text{ksi}$

$$V_n = R \cdot V_p \cdot \left[C + \frac{.87(1 - C)}{\sqrt{1 + \left(\frac{d_o}{D}\right)^2}}\right] \geq C \cdot V_p$$

$$k := 5 + \frac{5}{\left(\frac{d_o}{D}\right)^2} = 7.278$$

$$\frac{D}{t_w} = 108.0 \geq 1.38\sqrt{E \cdot \frac{k}{F_{yw}}} = 89.7$$

$$C := \frac{1.52}{\left(\frac{D}{t_w}\right)^2} \cdot \left(\frac{E \cdot k}{F_{yw}}\right) = 0.55$$ $F_r := 50 \text{ksi}$

$$R := \left[0.6 + 0.4\left(\frac{F_r - f_u}{F_r - .75\phi_f \cdot F_y}\right)\right] = 0.637$$

$$V_p := .58F_{yw} \cdot D \cdot t_w = 783 \cdot K$$

$$R \cdot V_p \cdot \left[C + \frac{.87(1 - C)}{\sqrt{1 + \left(\frac{d_o}{D}\right)^2}}\right] = 383.67 \cdot K$$

$$C \cdot V_p = 430.73 \cdot K$$

Use max of two values

$V_n := 430.73K$

$V_r := \phi_v \cdot V_n = 430.73K$ which is greater than 423.5K OK

Shear Stud Calculations

$K := 1000lb$

$\frac{Height_{stud}}{Diamter_{stud}} = \frac{6}{0.875} = 6.86 \geq 4$ OK $ksi := \frac{1000lb}{in^2}$

Pitch of 10 in. $p := 10in$

$Q_r = \phi_{sc} \cdot Q_n$ $\phi_{sc} := 0.8$

$Q_n = 0.5 A_{sc} \cdot \sqrt{f_c \cdot E_c} \leq A_{sc} \cdot F_u$

Assume 7/8 in. studs. $d := .875in$

$A_{sc} := \pi \cdot \frac{d^2}{4} = 0.601 \cdot in^2$

$f_c := 4ksi$ $E_c := 3834ksi$ $F_u := 60ksi$

$Q_n := 0.5 A_{sc} \cdot \sqrt{f_c \cdot E_c} = 37.233K$

$A_{sc} \cdot F_u = 36.079K$ Use: $Q_n := A_{sc} \cdot F_u = 36.079K$

$Q_r := \phi_{sc} \cdot Q_n = 30.667K$

Number of Shear Connectors: $n = \frac{V_h}{Q_r}$

Total horizontal shear force equals lesser of the following:

$V_h = .85 f_c \cdot b \cdot t_s$ or $V_h = F_{yw} \cdot D \cdot t_w + F_{yt} \cdot b_t \cdot t_t + F_{yc} \cdot b_f \cdot t_f$

$b := 103in$ $t_s := 8in$ $F_{yw} := 50ksi$ $D := 54in$

$t_w := 0.5in$ $F_{yt} := 50ksi$ $b_t := 14in$ $t_t := .875in$

$F_{yc} := 50ksi$ $b_f := 14in$ $t_f := .625in$

$.85 f_c \cdot b \cdot t_s = 2.802 \times 10^3 \cdot K$

$F_{yw} \cdot D \cdot t_w + F_{yt} \cdot b_t \cdot t_t + F_{yc} \cdot b_f \cdot t_f = 2.4 \times 10^3 \cdot K$

$V_h := F_{yw} \cdot D \cdot t_w + F_{yt} \cdot b_t \cdot t_t + F_{yc} \cdot b_f \cdot t_f = 2.4 \times 10^3 \cdot K$

$n := \frac{V_h}{Q_r} = 78.259$

$L := 35.6ft$

$n := \frac{3 \cdot L}{p} = 128.16$

$A_r := 12.772in^2$ $F_{yr} := 60ksi$

$V_h := A_r \cdot F_{yr} = 766.32K$

$n := \frac{V_h}{Q_r} = 24.988$

$L := 36.4ft$

$n := \frac{3 \cdot L}{p} = 131.04$

Use 3 studs per row with rows spaced at 10 in over the length of the beam.

Post-tensioning Calculations

Stress at Pier

Stress at top of deck after live load

After Post Tensioning

$$f_t = \frac{P}{A_{deck}} - \frac{P \cdot e}{S_{tdeck}}$$

$K := 1000lb$

$ksi := 1\frac{K}{in^2}$

Assume 20 % prestress losses.

$P := 12 \cdot (0.8)(202.5ksi)\,.217in^2 = 421.848K$

$A_{deck} := 103in \cdot 8in = 824in^2$

$I := \frac{103in \cdot (8in)^3}{12} = 4.395 \times 10^3 \cdot in^4$

Post tensioning applied in center of deck

$e := 0in$ $\quad y_t := 4.25in$

$S_{tdeck} := \frac{I}{y_t} = 1.034 \times 10^3 \cdot in^3$

$M_{DL} := 0$

$$f_{t\_noncomp} := \frac{P}{A_{deck}} - \frac{P \cdot e}{S_{tdeck}} + \frac{M_{DL}}{S_{tdeck}} = 0.512ksi$$

$\frac{P}{A_{deck}} = 0.512ksi$

$\frac{P \cdot e}{S_{tdeck}} = 0 \cdot ksi$

$\frac{M_{DL}}{S_{tdeck}} = 0 \cdot ksi$

After Parapet, Wearing Surface, and Live Load (Unfactored Loads)

$$f_t = \frac{-M_{LL}}{S_{tcomp}}$$

$M_{LL} := 3414K \cdot ft$ Including parapet and wearing surface

$S_{tcomp} := 10376.2in^3$ Previous calculation for equivalent steel section
Multiply by n = 8 to convert to concrete

$$f_{t\_comp} := \frac{-M_{LL}}{8 \cdot S_{tcomp}} = -0.494\,ksi$$

Total Stress at Final

$$f_{t\_total} := f_{t\_noncomp} + f_{t\_comp} = 0.018\,ksi$$

Stress at 0.4 L (Maximum positive Moment)

Stress at top of deck after live load

After Post Tensioning

$$f_t = \frac{P}{A_{deck}} - \frac{P \cdot e}{S_{tdeck}} + \frac{M_{DL}}{S_{tdeck}}$$

$K := 1000\,lb$

$ksi := 1\,\frac{K}{in^2}$

$P = 421.848\,K$

$A_{deck} = 824\,in^2$

$I := \frac{103\,in \cdot (8\,in)^3}{12} = 4.395 \times 10^3 \cdot in^4$

Post tensioning applied in center of deck

$S_{tdeck} := \frac{I}{y_t} = 1.034 \times 10^3 \cdot in^3$

$f_{t\_noncomp} := \frac{P}{A_{deck}} - \frac{P \cdot e}{S_{tdeck}} = 0.512\,ksi$

$\frac{P}{A_{deck}} = 0.512\,ksi$

$\frac{P \cdot e}{S_{tdeck}} = 0 \cdot ksi$

After Parapet, Wearing Surface, and Live Load (Unfactored Loads)

$$f_t = \frac{M_{LL}}{S_{tcomp}}$$

$M_{LL} := 2896\,K\cdot ft$ Including parapet and wearing surface

$S_{tcomp} := 6042.14\,in^3$ Previous calculation for equivalent steel section
Multiply by n = 8 to convert to concrete

$$f_{t\_comp} := \frac{M_{LL}}{8\cdot S_{tcomp}} = 0.719\,ksi$$

Total Stress at Final

$f_{t\_total} := f_{t\_noncomp} + f_{t\_comp} = 1.231\,ksi$

Strain and Movement Calculations

Movement due to creep and shrinkage

Shrinkage

$\varepsilon_{bid} = k_s \cdot k_{hs} \cdot k_f \cdot k_{td} \cdot .48 \cdot 10^{-3}$

$K := 1000 lb$

$ksi := \frac{1K}{in^2}$

$k_s = 1.45 - 0.13 \cdot \frac{V}{SA}$

$\frac{V}{SA} = \frac{Area}{Length_{perimeter}}$

$A := 117in \cdot 8in = 936 \cdot in^2$

$L_p := (117 + 117 + 8 + 8)in$

$\frac{A}{L_p} = 3.744 in$

$1.45 - 0.13 \cdot \frac{A}{L_p \cdot in} = 0.963$

Use $k_s := 1$

$k_{hs} = 2 - .014 H$

Assume $H := 70$

$k_{hs} := 2 - .014 H = 1.02$

$k_f = \frac{5}{1 + f_{ci}}$

Assume $f_{ci} := 3 \ ksi$

$k_f := \frac{5}{1 + f_{ci}} = 1.25$

$k_{td} = \frac{t}{61 - 4 \cdot f_{ci} + t}$

$t := 89$ days

$k_{td} := \frac{t}{61 - 4 f_{ci} + t} = 0.645$

$\varepsilon_{bid} := k_s \cdot k_{hs} \cdot k_f \cdot k_{td} \cdot .48 \cdot 10^{-3} = 3.947 \times 10^{-4}$

Creep

$\psi_b = 1.9 k_s \cdot k_{hc} \cdot k_f \cdot k_{td} \cdot t_i^{-.118}$

$t_f := 90$ days $t_i := 1$ day

$k_{hc} := 1.56 - .008H = 1$

$k_{td} := \frac{t_f - t_i}{61 - 4f_{ci} + (t_f - t_i)} = 0.645$

$\psi_b := 1.9 k_s \cdot k_{hc} \cdot k_f \cdot k_{td} \cdot t_i^{-.118} = 1.532$ $f_c := 4$ ksi

$\Delta f_{pCR} = \frac{E_p}{E_{ci}} f_{cgp} \cdot \psi_b \cdot K_{id}$

$K_{id} = 1 + \frac{E_p}{E_{ci}} \cdot \frac{A_{ps}}{A_g} \left(1 + \frac{A_g \cdot e_{pg}^2}{I_g} \right) (1 + .7\psi_b)$

$E_p := 2850$ $E_{ci} := 33000(.15)^{1.5} \cdot \sqrt{3} = 3.321 \times 10^3$

$A_{ps} := 12 \cdot .217 = 2.604$ $A_g := 936$

$e = 0$

$K_{id} := \frac{1}{\left[1 + \frac{E_p}{E_{ci}} \cdot \frac{A_{ps}}{A_g} (1) (1 + .7\psi_b) \right]} = 0.953$

$f_{cgp} = \frac{P_i}{A_g}$ $P_i := 202.5(.99) \cdot 12 \cdot .217 = 522.037$

$f_{cgp} := \frac{P_i}{A_g} = 0.558$

$\Delta f_{pCR} := \frac{E_p}{E_{ci}} f_{cgp} \cdot \psi_b \cdot K_{id} = 6.986$ ksi

$\varepsilon_{creep} := \frac{\Delta f_{pCR}}{E_p} = 2.451 \times 10^{-4}$